Role of Calcium Signaling in Pacemaking Activity of NRK Fibroblasts

Een wetenschappelijke proeve op het gebied van de
Natuurwetenschappen, Wiskunde en Informatica

Proefschrift

ter verkrijging van de graad van doctor
aan de Radboud Universiteit Nijmegen
op gezag van de rector magnificus prof.mr. S.C.J.J. Kortmann,
volgens besluit van het college van decanen
in het openbaar te verdedigen op dinsdag 8 november 2011
om 13.30 uur precies

door

Wadia Hassan Almirza

geboren op 6 december 1970

te Basra, Irak

Role of Calcium Signaling in Pacemaking Activity of NRK Fibroblasts

A scientific essay in Natural Sciences, Mathematics and Computer Science

Doctoral Thesis

To obtain the degree of doctor from the Radboud University Nijmegen
on the authority of the rector magnificus prof.mr. S.C.J.J. Kortmann,
according to the decision of the Council of Deans
to be defended in public on Tuesday 8 November 2011
at 1:30 p.m.

by

Wadia Hassan Almirza

born on 6 December 1970
Basra, Iraq

Supervisor: Prof.dr. E.J.J. van Zoelen

Co-supervisor: Dr. A.P.R. Theuvenet

Manuscript committee: Prof.dr. J.G.J. Hoenderop (chairman)

Prof.dr. J.W.M. Heemskerk (CARIM Maastricht)

Dr. W.J.J.M. Scheenen

ISBN: 978-90-8891-328-0

Printed & lay-out by: Proefschriftmaken.nl || Printyourthesis.com
Published by: Uitgeverij BOXPress, Oisterwijk

Abbreviations

2-APB	2-aminoethoxydiphenyl borate
ARC	arachidonate-regulated Ca^{2+} channels
AP	action potential
cADPR	cyclic adenosine diphosphate ribose
CCE	capacitative calcium entry
CICR	calcium-induced calcium release
COX	cyclooxygenase
CRAC	calcium release-activated calcium
CRACM1 (Orai1)	calcium release-activated channel molecule 1
DDGI	density-dependent growth inhibition
EGF	epidermal growth factor
ER	endoplasmic reticulum
G_{CaL}	L-type calcium conductance
$G_{Cl(Ca)}$	calcium-activated chloride conductance
G_{Kir}	inwardly rectifying potassium conductance
I_{CaL}	L-type calcium current
$I_{Cl(Ca)}$	calcium-activated chloride current
I_{Kir}	inward rectifying potassium current
Icrac	calcium release activated calcium current
IP_3	inositol-1, 4, 5 trisphosphate
NAADP	nicotinic acid adenine dinucleotide phosphate
NCX	Na^+/Ca^{2+}-exchanger
NRK	normal rat kidney
$PGF_{2\alpha}$	prostaglandin $F_{2\alpha}$
PLA2	phospholipase A_2
PLC	phospholipase C
PDGF	platelet-derived growth factor
PKC	protein kinase C
PMCA	plasma membrane Ca^{2+}-ATPase
RA	retinoic acid
RNAi	RNA interference
ROCE	receptor-operated calcium entry
RyR	ryanodine receptor
shRNA	short hairpin RNA
SERCA	sarcoplasmic/endoplasmic reticulum Ca^{2+}-ATPase
SPCA	secretory-pathway Ca^{2+}-ATPase
SOCE	store-operated calcium entry
SOAR	STIM1 Orai activating region
SR	sarcoplasmic reticulum
Stim1	stromal interaction molecule-1
TGFβ	transforming growth factor β
TRPC	transient receptor potential channel
VOC	voltage-operated calcium channels

Voor mijn ouders

Table of contents

CHAPTER 1

General Introduction

General Introduction

1. Role of intracellular calcium dynamics in the regulation of cellular physiology

Calcium signaling is a ubiquitous mechanism that controls a wide variety of cellular processes, ranging from short-term responses such as contraction and secretion, to long-term regulation of gene transcription, cell proliferation and apoptosis (Parekh and Muallem 2011). The ability of a simple cation to coordinate such a diversity of complex processes originates from the spatio-temporal nature of calcium signaling. Many extracellular signals induce a periodic transient increase in the free cytosolic Ca^{2+}concentration, whereby the amplitude and/or frequency of these calcium oscillations, as well as their localization in the cell, determine such biological responses as gene activation and release of neurotransmitter containing vesicles. In contrast, a prolonged increase in cytosolic Ca^{2+} is essential for egg fertilization and cell proliferation, whereas a sustained increase in cytosolic Ca^{2+} has been shown to trigger apoptosis (Berridge, Bootman et al. 1998; Carafoli 2002; Muallem 2005). Long-lasting and robust calcium oscillations clearly depend on two features: the release of calcium from intracellular Ca^{2+} stores and the entry of extracellular calcium, which is required to maintain an adequate Ca^{2+} concentration in these stores. This second feature often involves a process known as capacitative calcium entry (CCE) or store-operated calcium entry (SOCE). The existence of CCE is identified as a current, which is triggered by depletion of intracellular stores and is referred to as Ca^{2+} release-activated Ca^{2+} current (I_{CRAC}) (Lewis and Cahalan 1989; Hoth and Penner 1992; Cahalan 2009).

In non-excitable cells stimulation by a physiological agonist, such as hormones, cytokines or growth factors, often leads to generation of a Ca^{2+} signal (Chakrabarti and Chakrabarti 2006). This Ca^{2+} signal generally shows oscillations in time, which can be decoded by the cell with respect to its frequency and amplitude, and is subsequently translated into information for various Ca^{2+} sensitive effectors (Parekh 2011). Oscillations in cytoplasmic Ca^{2+} result from a periodic uptake and release of Ca^{2+} from intracellular stores, in combination with influx and efflux of calcium ions through the plasma membrane (see e.g. Figure 1). It has been shown that calcium oscillations underlie many physiological processes. For instance, in parotid acinar cells of the salivary gland oscillations in $[Ca^{2+}]$ form the main signaling pathway in the regulation of salivary fluid secretion. Secretion increases with higher $[Ca^{2+}]$, but prolonged elevation of $[Ca^{2+}]$ is toxic to cells; so instead $[Ca^{2+}]$ oscillations are used to maintain an average elevated $[Ca^{2+}]$. This elevation of $[Ca^{2+}]$ subsequently activates Ca^{2+}-

dependent K^+ and Cl^- channels, which in turn leads to an activation of the proteins involved in transmembrane salt and water transport. These concerted activities lead to water flow into the lumen and the resulting salivary fluid secretion (Melvin, Yule et al. 2005).

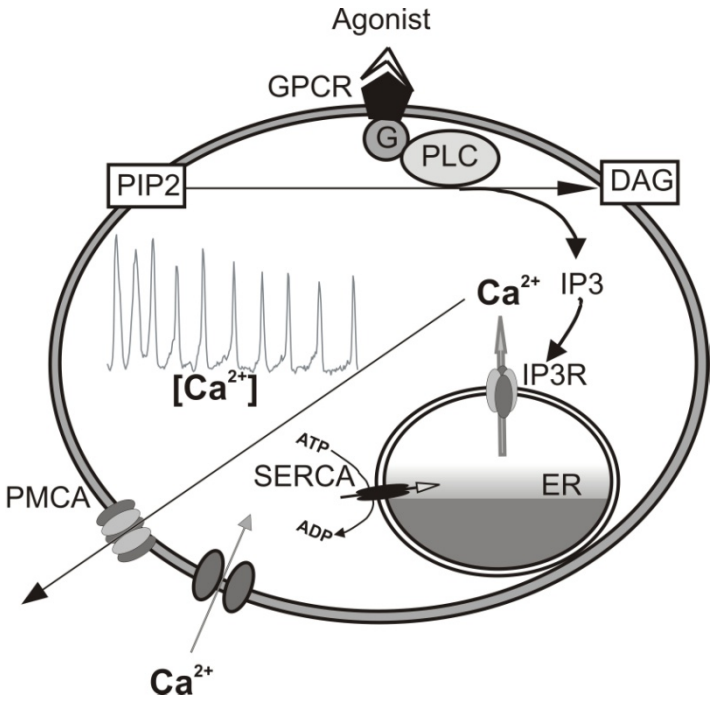

Fig. 1. Mechanism of agonist-induced Ca^{2+}oscillations. Agonist binds to a specific G protein-coupled membrane receptor (GPCR) and activates phospholipase C (PLC), which hydrolyses phosphatidylinositol 4,5-bisphosphate (PIP_2) into diacyglycerol (DAG) and inositol 1,4,5-trisphosphate (IP_3). IP_3 diffuses into the cytosol and binds to specific receptor/channels (IP_3R) on the endoplasmic reticulum (ER) membrane. Cyclic opening of this channel due to its biphasic regulation by cytosolic Ca^{2+} induces oscillations in intracellular [Ca^{2+}]. Decline of [Ca^{2+}] after each transient during the oscillations involves reuptake into the ER by the sarcoplasmic/endoplasmic reticulum Ca^{2+}-ATPase (SERCA) and the extrusion to the extracellular medium by the plasma membrane Ca^{2+} ATPase (PMCA). Depletion of the Ca^{2+} store in the ER leads to opening of store-operated Ca^{2+} channels resulting in Ca^{2+} influx, which is required for prolonged intracellular Ca^{2+} oscillations.

Another typical example of a physiological role for calcium oscillations has been described in hepatocytes; where hormone-induced waves of increased cytosolic [Ca^{2+}] originate from fixed points in the cell. These waves regulate the membrane potential of these cells through a variety of Ca^{2+}-dependent pathways that control the activity of different types of plasma membrane ion channels and transporters. These include Ca^{2+}-activated small conductance K^+ channels and Ca^{2+}-dependent non-selective cation channels, which thereby provide a pathway for Na^+ entry, and activation of Ca^{2+}-dependent Cl^- channels (Barritt, Chen et al. 2008).

Ca^{2+} oscillations have also been involved in modulating the pacemaking activity of interstitial cells of Cajal (ICCs), which play a role in gastric motility. Such oscillations are

generated by interplay between intracellular calcium stores and store-operated calcium entry, resulting in the subsequent activation of Ca^{2+}-activated Cl^- channels, which are responsible for the generation of the electrical pacemaker potentials (Huizinga, Zhu et al. 2002).

2. Calcium stores and their role in Ca^{2+} homeostasis

An increase in cytosolic Ca^{2+} concentration can result from release of calcium ions in internal stores or from influx of calcium ions into the cells through plasma membrane carriers and channels (Berridge 1993; Clapham 1995). Cells have developed specific organelles which are able to store large amounts of Ca^{2+}, from which they can be released by intracellular second messengers such as inositol-1,4,5 trisphosphate (IP_3), ATP, cyclic ADP ribose (cADPR) and nicotinic acid adenine dinucleotide phosphate (NAADP). The most important of these stores are located in the sarco/endoplasmic reticulum, mitochondria and Golgi apparatus.

2.1. Release of calcium from the sarco/endoplasmic reticulum

The endoplasmic reticulum (ER) is a tubular intracellular network that is involved in biosynthesis of proteins and other macromolecules. Furthermore it has the capacity to accumulate calcium ions, and represents the major agonist-sensitive intracellular Ca^{2+} release store in cells. The sarcoplasmic reticulum (SR) is a unique, highly specialized ER-like structure, which is characteristic for striated muscle fibers and functions exclusively as a regulator of calcium levels. The main component of the calcium storage machinery of this organelle is a unique Ca^{2+} ATPase (SERCA) which actively transports Ca^{2+} from the cytosol to the sarco(endo) plasmic reticulum against a large concentration gradient. SERCA proteins are encoded by three genes named *ATP2A1* (SERCA1), *ATP2A2* (SERCA2) and *ATP2A3* (SERCA3). Each of these genes encodes different protein isoforms as a result of alternative splicing. The calcium pumps encoded by these genes differ in their regulatory and kinetic properties, thereby allowing an optimized activity in the tissues where they are expressed. They play a central role in maintaining appropriate steady-state Ca^{2+} levels in the cytoplasm.

Release of calcium ions from the ER/SR is mediated by the inositol trisphosphate receptor (IP_3R), which is activated by the inositol phospholipid degradation product IP_3 (inositol 1,4,5 trisphosphate) in combination with Ca^{2+}. There are three different IP_3R subtypes, encoded by the genes *ITPR1*, *ITPR2* and *ITPR3*. The functional differences between these three isoforms will be described later in this chapter. Calcium release from the ER/SR can also be mediated by ryanodine receptors, which are activated by cADPR. The RYR1, RYR2 and RYR3 genes

encode the ryanodine receptors, which play a major role in so-called calcium-induced calcium release. It is anticipated that differences in the distribution and regulation mechanism of these various receptor subtypes play a key role in determining the spatiotemporal properties of the Ca^{2+} signal (see for review (Rizzuto and Pozzan 2006)).

2.2. Release of calcium from mitochondria

It has been known since the late seventies that mitochondria are able to take up Ca^{2+} from the surrounding environment and accumulate these cations in their matrix (Nicholls 1978). However, mitochondria have long been regarded as non-active Ca^{2+} stores, and until recently their contribution in the process of Ca^{2+} signaling has received less attention. The outer membrane of mitochondria contains large pores through which Ca^{2+} can diffuse freely. The inner membrane contains not only an electrogenic uniporter, which brings Ca^{2+} to electrochemical equilibrium, but also a Na^{+}/Ca^{2+} antiporter, which is driven by their ion gradients. However, details about the regulatory mechanism of these channels are still largely unknown (Giacomello, Drago et al. 2007). Studies over the last decade have shown that Ca^{2+} can shuttle between the ER and mitochondria, and thereby generate a pacemaker mechanism for Ca^{2+} waves (Hajnoczky, Csordas et al. 2000; Ishii, Hirose et al. 2006). Furthermore, it has been shown that inhibition of mitochondrial Ca^{2+} uptake is reflected by a reduction in Ca^{2+} release from the ER (Vay, Hernandez-Sanmiguel et al. 2007). This effect has been seen in many cell types, indicating that an increase or decrease of Ca^{2+} fluxes from the ER can modulate the frequency of Ca^{2+} oscillations, whereby the Ca^{2+} uptake and release from mitochondria contributes to local and global Ca^{2+} signaling.

2.3. Release of calcium from Golgi apparatus

In addition to its known function in the processing of proteins synthesized in the ER, it is well established that the Golgi apparatus is also an important Ca^{2+} store (Pinton, Pozzan et al. 1998; Wuytack, Raeymaekers et al. 2003). The Golgi apparatus possesses both thapsigargin-sensitive SERCA pumps (encoded by *ATP2A* genes) and thapsigargin-insensitive secretory-pathway SPCA pumps (encoded by *ATP2C* genes). These two types of Ca^{2+} ATPases show a differential distribution. The SERCA pumps mediate Ca^{2+} uptake in the cis-Golgi and intermediate Golgi, while the SPCA pumps are involved in the Ca^{2+} uptake in the trans-Golgi (Dolman and Tepikin 2006; Rizzuto and Pozzan 2006). The SERCA-containing cis-Golgi and intermediate Golgi also contain IP_3 receptors, and it has been shown that IP_3 is able to release

Ca^{2+} from these organelles. In contrast, the SPCA-containing trans-Golgi contains specifically ryanodine receptors, although direct evidence for cADPR or NAADP-induced Ca^{2+} release from these organelles is still lacking. A direct role for Ca^{2+} uptake by the Golgi apparatus in supporting repetitive Ca^{2+} oscillations has been suggested (Berridge 1990). Moreover, it has been reported that the Golgi can cooperate with the ER in order to elevate the cytosolic Ca^{2+} concentration in response to agonist stimulation (Missiaen, Van Acker et al. 2004), while inhibition of Ca^{2+} release from the Golgi has been shown to reduce the duration of Ca^{2+} signals upon cell stimulation (Vanoevelen, Raeymaekers et al. 2005). These data show that the Golgi apparatus is an important calcium store and may contribute significantly to the dynamics of intracellular Ca^{2+} signaling.

2.4. Release of calcium from other organelles

In addition to the above three organelles, also secretory granules, lysosomes and peroxisomes can contribute to Ca^{2+} homeostasis in the cell. These are all three single membrane-bound compartments that can accumulate and release Ca^{2+} under specific conditions. The mechanisms by which these organelles control Ca^{2+} homeostasis are less well understood than in the case of ER/SR, mitochondria and Golgi, and accordingly at the moment most hypotheses are based on indirect evidence or mere speculation.

Secretory granules are subcellular vesicles, surrounded by a membrane formed from the Golgi apparatus, which contain a high content of proteins destined for secretion. So-called insulin granules can accumulate Ca^{2+} by means of a vanadate-sensitive, SPCA-related Ca^{2+}-ATPase, while chromaffin granules and synaptic vesicles can upload Ca^{2+} through a pH-driven H^+ (Na^+)/Ca^{2+} antiporter. There is no evidence for the presence of classical IP_3R or RYR receptors in these organelles, but still experimental data show that NAADP, cADPR and IP_3 can release Ca^{2+} from secretory granules within pancreatic acinar cells. Recently, it has been shown that such granules contain so-called two-pore segment channels (encoded by *TPCN* genes), which function as voltage-dependent Ca^{2+} channels when stimulated by NAADP (Fasolato, Zottini et al. 1991; Gerasimenko, Gerasimenko et al. 1996; Nguyen, Chin et al. 1998; Yoo 2000; Quesada, Chin et al. 2001).

In addition to their function in digestion of macromolecules, lysosomes can also function as Ca^{2+} storing organelles, although they are only able to do so at very high cytosolic concentrations. The mechanism of uptake is unknown, since lysosomes do not contain a SERCA pump. Recent studies indicate that particularly NAADP is able to release Ca^{2+} from

lysosomes, which can subsequently initiate calcium-induced calcium release (CICR), a process whereby the elevation of cytosolic Ca^{2+} causes the release of Ca^{2+} from other stores (Haller, Volkl et al. 1996; Kinnear, Boittin et al. 2004; Zhang, Zhang et al. 2006; Kinnear, Wyatt et al. 2008).

Finally peroxisomes have been shown to function as Ca^{2+} stores, but again very little is known about the mechanisms of peroxisomal calcium storage and transport, as well as its impact on cellular calcium homeostasis (see for reviews (Rizzuto and Pozzan 2006); (Raychaudhury, Gupta et al. 2006)). Recently, dynamic changes in $[Ca^{2+}]$ within the peroxisomal lumen have been detected, from which it has been concluded that peroxisomes can take up Ca^{2+} following agonist-induced Ca^{2+} release from internal stores (Lasorsa, Pinton et al. 2008). However, the various calcium channels involved have not been identified yet.

2.5. Influx of calcium across the plasma membrane

The plasma membrane plays a central role in the control of Ca^{2+} homeostasis, since it is the target for extracellular stimuli that act by mobilizing intracellular Ca^{2+} (Berridge, Bootman et al. 1998; Carafoli 2002). The plasma membrane contributes to Ca^{2+} homeostasis by at least three distinct processes. First of all, binding of extracellular stimuli to their plasma membrane receptor can induce intracellular phospholipase C activity, which leads to the degradation of phosphatidyl-inositol bisphosphate (PIP_2) into diacylglycerol (DAG) and inositol trisphosphate (IP_3). The soluble IP_3 is subsequently able to activate IP_3 receptors in intracellular organelles, which results in release of Ca^{2+} (Clapham 1995; Shuttleworth, Thompson et al. 2004). Secondly, cytosolic Ca^{2+} is pumped out of the cell be means of the plasma membrane Ca^{2+}-ATPase (PMCA), which is encoded by *ATP2B* genes. This pump is particularly activated when the cytosolic Ca^{2+} concentration reaches a peak values. Also the plasma membrane Na^{+}/Ca^{2+}-exchanger (encoded by *SLC8A* genes) contributes to efflux of Ca^{2+} from the cell, since it can extrude Ca^{2+} against a large electrochemical gradient (Carafoli, Santella et al. 2001; Strehler, Filoteo et al. 2007). Thirdly, the plasma membrane contains various types of channels by which Ca^{2+} can be taken up from the extracellular medium into the cell. Particularly for sustained increase in intracellular Ca^{2+}, influx of Ca^{2+} from the extracellular medium is essential. Moreover, intracellular Ca^{2+} stores have only a limited capacity, and uptake of extracellular Ca^{2+} is essential to refill depleted stores. Three different types of plasma membrane calcium channels can be distinguished: voltage-operated Ca^{2+} channels (VOCs), store-operated Ca^{2+} channels (SOCs) and receptor-operated Ca^{2+} channels (ROCs).

VOCs can mediate Ca^{2+} influx in response to membrane depolarization and are found particularly in excitable cells such as nerve and muscle cells, but are largely excluded from non-excitable cells (Burnashev 1998; Catterall 2000). SOCs are activated when intracellular Ca^{2+} stores become depleted, by a process known as capacitative calcium entry (Parekh 2003). ROCs are activated by second messengers that are generated upon ligand-receptor interaction, including IP_3, IP_4, DAG and arachidonate (Clapham 1995; Shuttleworth, Thompson et al. 2004). There is currently great interest in the mechanisms underlying capacitative calcium entry, and therefore the proteins involved will be described in detail in the following section.

2.6. Role of TRP, ORAI and STIM proteins in the entry of extracellular calcium

In recent years it has become clear that canonical TRP channels (TRPC), which form the so-called subfamily C of the transient receptor potential (TRP) family of cation channels (see for review e.g. (Clapham 2003), play an important role in both SOC- and ROC-mediated Ca^{2+} entry (Parekh and Putney 2005; Ambudkar and Ong 2007). This subfamily comprises seven related members, designated TRPC1 to TRPC7, which can be further subdivided depending on their biochemical and functional similarity. TRPC proteins can form both homo- and heterotetramers, but the role of protein multimerization in channel activity is not yet clear. TRPC1 can form heteromers with TRPC4 and TRPC5, while the TRPC subfamily members TRPC4/5 and TRPC3/6/7 can form heteromers among themselves, and may thereby exhibit current characteristics, which are significantly different from those of homotetramers (see e.g. (Strubing, Krapivinsky et al. 2003)). Although TRPC channels are involved in the uptake of Ca^{2+} from the extracellular medium, the mechanism of activation of these channels and their potential involvement in capacitative calcium entry remain highly controversial. Using a variety of approaches (over-expression, RNAi and pharmacological agents) it has been shown that TRPC1 and TRPC4 can contribute to SOC channel activity, whereas TRPC3 and TRPC7 can also mediate SOC activity when they are in complex with TRPC1. However, these latter TRPCs mainly act as ROCs, which can be activated by receptor-stimulated PIP_2 hydrolysis, independent of internal store depletion (see for review (Salido, Sage et al. 2009)).

During the last four years, important discoveries have provided new insight into the mechanism by which Ca^{2+} stores in the ER communicate with Ca^{2+} channels in the plasma membrane. It has been shown that STIM1 (stromal interaction molecule protein 1) acts as a Ca^{2+} sensor in the ER. Upon store depletion STIM1 translocates to defined punctae in the ER, which are located close to the plasma membrane (Liou, Kim et al. 2005; Zhang, Yu et al. 2005; Soboloff, Spassova et al. 2006), and consequently activates the plasma membrane

calcium channel ORAI1 (calcium release-activated calcium modulator 1) (Mercer, Dehaven et al. 2006; Peinelt, Vig et al. 2006; Soboloff, Spassova et al. 2006). Strong evidence from different laboratories indicates that STIM1 in the ER and ORAI1 in the plasma membrane functionally interact and in combination are responsible for capacitative calcium entry. Co-expression of ORAI1 and STIM1 in cells strongly enhances calcium release-activated calcium (CRAC) currents upon depletion of intracellular Ca^{2+} stores. However, not all cells that express both ORAI1 and STIM1 are able to generate CRAC currents (DeHaven, Smyth et al. 2007; Gross, Wissenbach et al. 2007; Wissenbach, Philipp et al. 2007). A recent study by Vig et al. even shows that ORAI1 expressed in mouse T-lymphocytes is not involved in CRAC currents (Vig, DeHaven et al. 2008). This suggests that ORAI1 and STIM1 proteins serve multiple functions in the cell and that their biophysical properties may depend on the cell type and the molecular composition of the channel complexes. Interestingly, several reports have shown that STIM1 and ORAI1 also interact with TRPC1, and together form a functional SOC complex (Ong, Cheng et al. 2007; Cheng, Liu et al. 2008; Jardin, Lopez et al. 2008). Furthermore, ORAI1 has been proposed to interact with other members of TRPC subfamily, including TRPC3, TRPC6 and TRPC7, which may regulate their function and make them responsive to store depletion (Liao, Erxleben et al. 2007; Cheng, Ong et al. 2011).

Additional studies have shown that STIM1 and ORAI1 also contribute to ROC-mediated calcium uptake. A mutant form of ORAI1 (R91W) can block DAG-activated Ca^{2+} entry into cells that stably, or transiently, express DAG-responsive TRPC channels (Liao, Erxleben et al. 2008). Mignen et al. reported that STIM1 and ORAI1 also regulate arachidonic acid-activated Ca^{2+} entry channels, independent of intracellular store depletion (Mignen, Thompson et al. 2007; Mignen, Thompson et al. 2008). In combination these data indicate that ORAI1 and STIM1 can participate in both SOC- and ROC-mediated calcium uptakes. Recent overall findings suggest that the stoichiometry of STIM1, ORAI1 and TRPCs in protein complexes determine their function as SOCs or as ROCs (see for review, (Lee, Yuan et al. 2010)). At physiological expression levels, STIM1, ORAI1 and TRPCs appear to exist in molecular complexes, which function as SOCs. The channels can also function independently of each other, whereby ORAI1 mediates CRAC current when interacting with STIM1 in the absence of TRPCs. On the other hand, TRPCs function as SOCs when interacting with STIM1 directly or with the aid of other TRPCs, while they function as ROCs in the absence of STIM1. In this manner STIM1 functions by tuning the SOC activity of the TRPCs. Further studies will be required to examine how complex formation between TRPCs, ORAI1 and STIM1 controls the characteristics of calcium entry.

3. Inositol 1,4,5-triphosphates (IP_3) receptor subtypes and their role in shaping the calcium oscillations

Various extracellular stimuli can induce the production of cytoplasmic IP_3 (Berridge, Bootman et al. 2003), which as a soluble second messenger can activate the IP_3 receptor on Ca^{2+}-storing organelles such as the ER. Mammalian cells have three different IP_3R isoforms, IP_3R1, IP_3R2 and IP_3R3, which can form functional homo- and hetero-tetrameric structures. Their expression is tissue and development specific, although many cells co-express multiple isoforms. The three IP_3R isoforms display similar Ca^{2+} permeability properties; however, they differ significantly in their regulatory properties. Biochemical analysis has revealed that the affinity to IP_3 for the IP_3-binding core is similar for each of the isoforms, but that an IP_3-binding suppressor domain linked to the N-terminal side of the binding core is responsible for the isoform-specific tuning of IP_3 binding affinity (Iwai, Michikawa et al. 2007; Zhang, Fritz et al. 2011). Single-channel studies have been used to investigate the basic regulatory mechanisms of the various IP_3R isoforms, as well as their role in intracellular Ca^{2+} signals. It appears that small differences in the interaction of the endogenous regulators, including Ca^{2+} itself, with each of the receptor isoforms govern their pattern of Ca^{2+} release, thus allowing fine-tuning of intracellular signals in the whole-cell environment.

The IP_3R1 receptor, which shows both Ca^{2+}-dependent activation and inhibition, is a candidate for establishing Ca^{2+} oscillations, whereby increasing IP3 concentrations can modulate the frequency of Ca^{2+} transients. Figure 2 show the typical dynamic behavior of changes in the intracellular Ca^{2+} concentration mediated by IP_3R1 as a function of the concentration of IP_3. A stable steady increase in the Ca^{2+} concentration occurs for small values of the IP_3 concentration up to 0.2 μM. Higher concentrations give rise to dynamics following a supercritical Hopf bifurcation, whereby the system becomes a calcium oscillator in broad range of IP_3 concentrations. For concentrations of IP_3 exceeding that range the system remains stable at an intracellular Ca^{2+} concentration near 5 μM. In contrast, IP_3R2 exhibits a greater sensitivity for IP_3 in mobilizing Ca^{2+} and lacks Ca^{2+}-dependent inhibition. This results in earlier and larger calcium signals, which makes the IP_3R2 receptor a better candidate for initiation of intracellular Ca^{2+} signals at low IP_3 concentration rather than for supporting a regenerative response. IP_3R3 can be activated in the presence of high IP_3 concentrations, even when the Ca^{2+} concentration is very low. As a result the IP_3R3 receptor will be able to initiate Ca^{2+} release in cells, which have been stimulated to produce maximal levels of IP_3. These distinct features of IP_3 receptor regulation offer a wide variety of Ca^{2+} signaling profiles (Foskett, White et al. 2007), and therefore these isoforms play an important role in the shaping

of intracellular calcium oscillations.

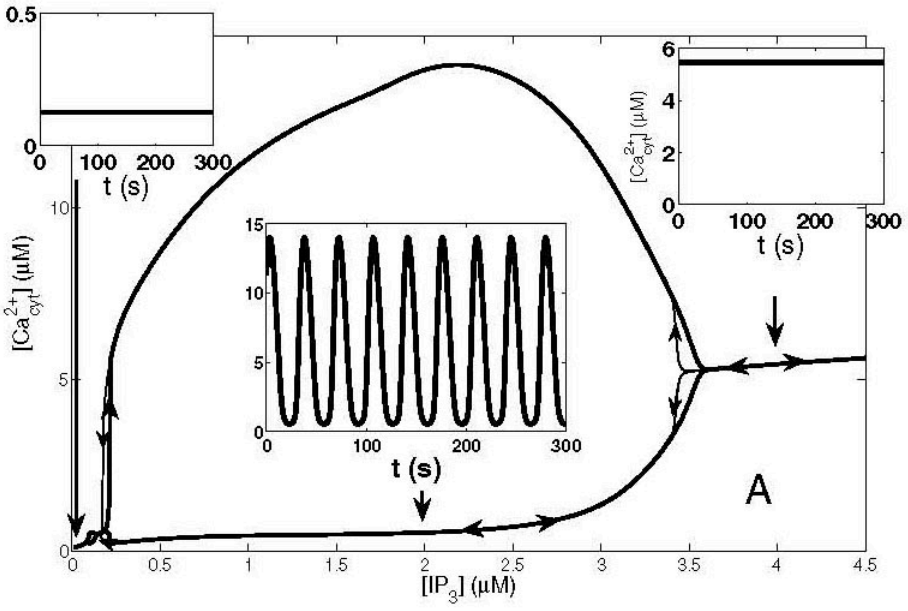

Fig. 2. The Hopf bifurcation diagram for the IP_3R1-mediated intracellular calcium oscillator in a single-NRK cell model as a function of $[IP_3]$. The thick and thin solid lines correspond to the stable states for increasing and decreasing (indicated by arrows) values for $[IP_3]$, respectively. The three insets show the Ca-concentration as a function of time for $[IP_3]$ values at 0.01; 2; and 4 μM, respectively (modified from Fig.3 in (Kusters, Cortes et al. 2007)).

4. Normal Rat Kidney fibroblasts as a model system for studying Ca^{2+} dynamics

Normal rat kidney fibroblasts (NRK) represent an excellent in vitro model system for studying the control mechanisms of cellular growth and phenotypic alterations upon cellular transformation. These cells are strictly dependent on extracellular growth factors for their proliferation, but depending on the combinations of growth factors added these cells they either show density-dependent growth inhibition or undergo phenotypic transformation concomitant with a loss of density-dependent growth control, as illustrated in Figure 3 (van Zoelen, van Oostwaard et al. 1988; van Zoelen 1991). NRK cells cultured in the presence of serum form a confluent monolayer after 3-4 days and upon subsequent addition of serum-free medium they become quiescent due to the absence of growth factors. Upon addition of epidermal growth factor (EGF) and insulin, these quiescent cells are re-stimulated to grow, but after one additional cell cycle they undergo density-dependent growth inhibition (also referred to as contact inhibition). However, if in addition to EGF also retinoic acid (RA) or transforming growth factor-beta (TGFβ) is added, these cells overcome density-dependent growth inhibition and continue to proliferate for multiple cell cycles. This process, which is

referred to as phenotypic transformation, also allows NRK cells to grow under anchorage-independent conditions. Electrophysiological studies have shown that NRK fibroblasts display distinct calcium dynamics depending on whether they are in the quiescent state, the density-arrested state or phenotypically transformed state (Harks, Peters et al. 2005).

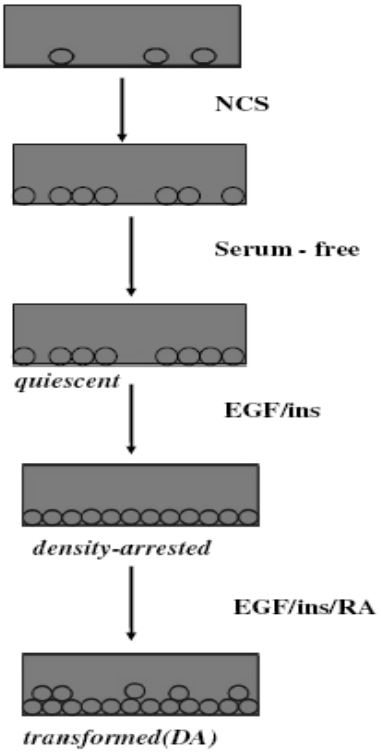

Fig. 3. Schematic overview showing how NRK fibroblasts are cultured to different growth states. In the presence of serum-containing medium (NCS; new born calf serum) NRK cells are grown to subconfluency, after which all growth factors are removed from the culture medium and NRK cells become quiescent. NRK cells can then be triggered to reenter the cell cycle by treatment with EGF and insulin (ins), but the cells are unable to proceed through more than one cell cycle and become density-arrested. Finally, upon addition of RA (retinoic acid) to these EGF- and insulin-treated density-arrested NRK monolayers, the cells undergo phenotypic transformation and start to grow in cellular multilayers.

Although fibroblasts are considered to be classical non-excitable cells, we have shown that NRK cells can exhibit excitable properties under specific growth conditions (see Figure 4). NRK cells in quiescent monolayers have a stable membrane potential of around -70 mV and a relatively low but stable intracellular calcium concentration (Harks, Torres et al. 2003). In contrast, cells in density-arrested monolayers fire repetitive action potentials (APs), which are associated with periodic calcium transients. These action potentials result from the sequential opening of an L-type calcium channel, a calcium-dependent chloride channel and an inwardly rectifying potassium channel (De Roos, Van Zoelen et al. 1997; Harks, Camina et al. 2003). Finally, phenotypically transformed NRK cells have an elevated intracellular calcium

concentration in comparison with quiescent cells and are depolarized with a membrane potential near -20 mV, caused by sustained activation of calcium-dependent chloride channels. NRK cells contain FP receptors (encoded by the *Ptgfr* gene), a Gq-coupled seven transmembrane protein which can be activated by prostaglandin (PG) $F_{2\alpha}$. $PGF_{2\alpha}$ is an arachidonic acid derivative, which is produced by the cyclooxygenase pathway. Multiple isoforms of the FP receptor have been identified, both in bovine (referred to as FPA and FPB) and human cells, all resulting from alternative splicing of the *Ptgfr* gene. As far as it has been established so far, $PGF_{2\alpha}$ can bind all these isoforms and induce the hydrolysis of PIP_2 by activation of PLCβ and the subsequent release of Ca^{2+} from intracellular stores in an oscillatory manner.

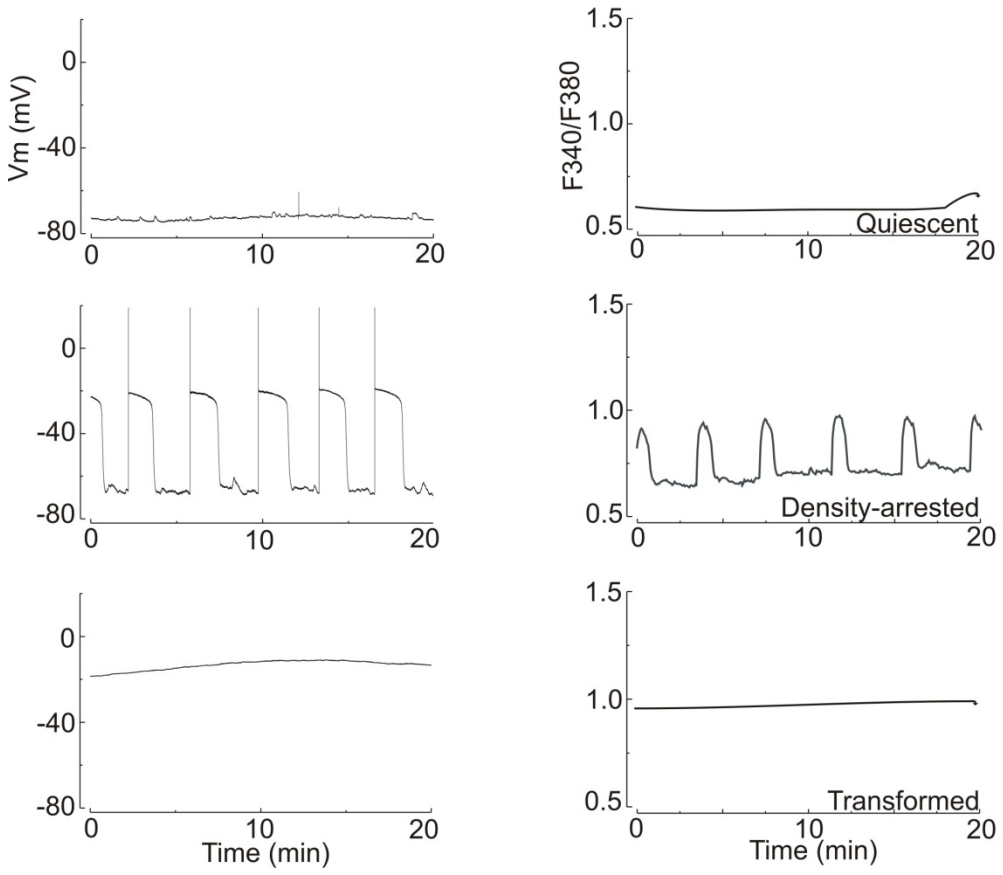

Fig. 4. Schematic overview showing the membrane potential (left panels) and cytosolic calcium (measured as Fura F340/F380 fluorescence ratio, right panels) of NRK fibroblasts monolayers in different growth states.

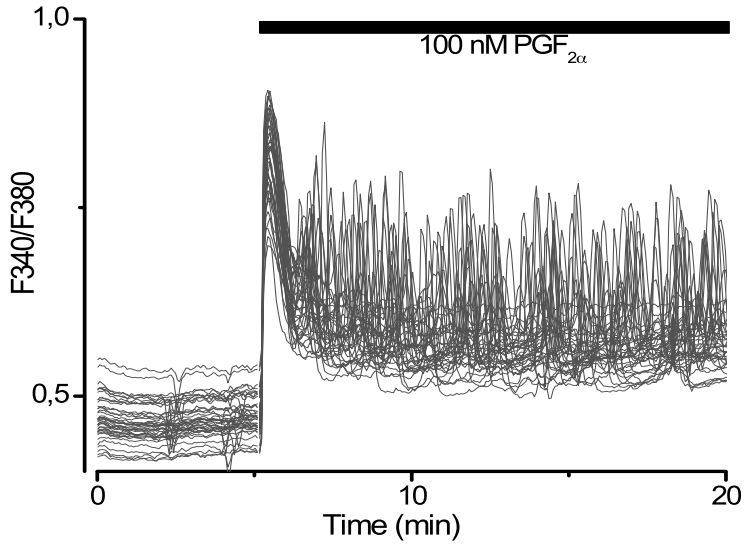

Fig. 5. Typical calcium response induced by $PGF_{2\alpha}$ in NRK fibroblasts monolayer. Al though they are electrically coupled by gap junction, $PGF_{2\alpha}$ induces unsynchronized calcium oscillations in NRK cells.

Addition of $PGF_{2\alpha}$ to quiescent NRK cells induces Ca^{2+} oscillations, which are not synchronous in the population, this in spite of the observation that all cells are electrically coupled (see Figure 5). A dose-dependent increase in $PGF_{2\alpha}$ concentration affects the frequency, but not the amplitude of these Ca^{2+} oscillations. In contrast, phenotypically transformed NRK cells are able to secrete $PGF_{2\alpha}$ in an autocrine manner, which causes a constitutive elevation in intracellular calcium and depolarization of these cells (Harks, Peters et al. 2005). The observed action potentials in density-arrested NRK cells require the presence of so-called pacemaker centers. We have hypothesized that in density-arrested monolayers groups of cells may locally secrete an enhanced concentration of $PGF_{2\alpha}$. The resulting calcium oscillations may subsequently induce the formation of pacemaker centers from which the action potentials propagate throughout the monolayer as a result of electrical coupling, thus giving rise to the periodic intracellular calcium waves shown in Figure 4 (de Roos, Willems et al. 1997; Kusters, van Meerwijk et al. 2008).

Calcium oscillations induced by $PGF_{2\alpha}$ in quiescent NRK cells are not affected by nifedipine, a blocker of L-type Ca^{2+}-channels, but become abolished when extracellular [Ca^{2+}] is removed. These findings support the prediction of a modeling study (Kusters, Dernison et al. 2005) that entry of Ca^{2+} across the plasma membrane is crucial for sustaining the $PGF_{2\alpha}$-induced Ca^{2+} oscillations in NRK cells (Harks, Scheenen et al. 2003). The above findings also show that this Ca^{2+} entry cannot be mediated by L-type Ca^{2+} channels, but must result from other types of plasma membrane Ca^{2+} channels expressed in NRK cells. In a mathematical modeling study

we have shown that uptake of extracellular calcium is essential to ensure stable long-term Ca^{2+} oscillations and to initiate calcium action potentials (Kusters, Dernison et al. 2005). This uptake of extracellular calcium ions can take place by store-operated calcium channels, or alternatively by diacylglycerol (DAG)-activated (Hofmann, Obukhov et al. 1999) and arachidonate (ARC)-regulated Ca^{2+} channels (Mignen, Thompson et al. 2003) or even by reversible SERCA pumps (MacLennan, Rice et al. 1997). Figure 6 shows all the essential components of a single-cell model that are required to produce calcium dynamics and membrane excitability in NRK fibroblasts.

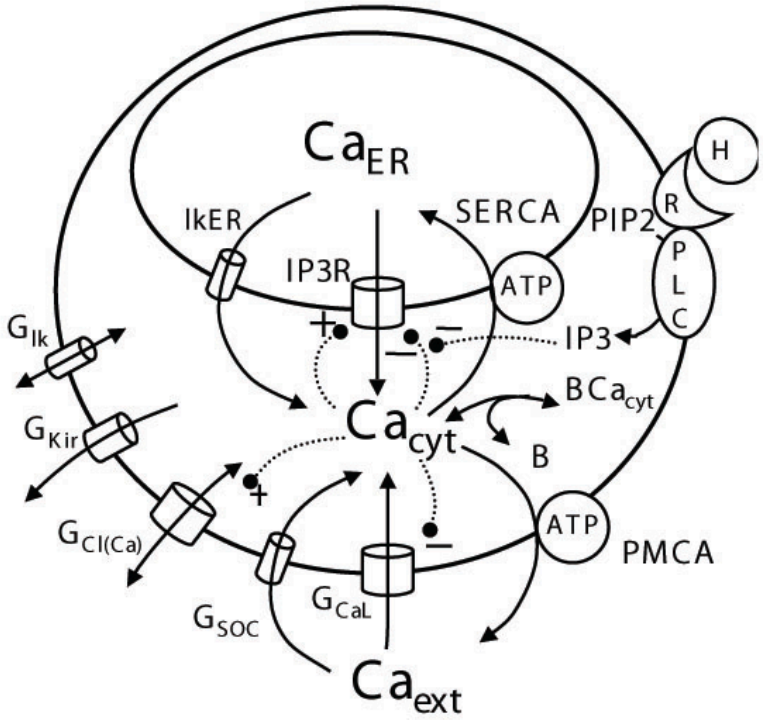

Fig. 6. Conceptual model of the processes involved in membrane excitability and intracellular calcium oscillations in NRK cells (adapted from Kusters, Dernison, et al. 2005). The model of NRK cell membrane excitability consists of leak channels (see G_{IK}), K_{IR} channels (see G_{kir}), calcium-dependent Cl-channels (see $G_{Cl(Ca)}$), SOC channels (see G_{SOC}), L-type Ca-channels (see G_{CaL}) and a PMCA pump. The model for intracellular calcium oscillations consists of a SERCA pump, leak channels through the ER membrane (see IkER) and an IP_3-receptor (see IP_3R). IP_3 is produced by phospholipase C (PLC) activity upon binding of a hormone (H) to a plasma membrane receptor (R).

5. Aim and outline of thesis

We have previously studied the role of ion channels in calcium signaling of NRK cells, by using the distinct behavior of quiescent, density-arrested and phenotypically transformed cells as a starting point. By the subsequent use of specific blockers the role of individual ion channels could be tested. This approach is limited, however, by the availability and specificity of pharmacological drugs, and does not allow a study of the role of individual receptor isoforms. It was the aim of the present study to investigate the role of specific ion channels and receptors in calcium oscillations and calcium action potentials of NRK cells, by selective knock down of their genes using an RNAi approach.

In **Chapter 2** we studied the role of the prostanoid FP receptor in action potential generation and phenotypic transformation of NRK fibroblasts by knocking down the expression of the rat *Ptgfr* gene. We demonstrate in this study that a membrane depolarization is not a prerequisite for the acquisition of a transformed phenotype and provide the first direct evidence that activity of $PGF_{2\alpha}$ by putative pacemaker cells underlies the generation of calcium action potentials in density-arrested NRK fibroblasts.

In **Chapter 3** we examined the involvement of different IP_3 receptor subtypes in $PGF_{2\alpha}$-induced calcium oscillations and pacemaking activity of NRK fibroblasts. Our results show that these cells express two IP_3R subtypes, whereby the reduced frequency of $PGF_{2\alpha}$-induced calcium oscillations in density-arrested compared to quiescent cells can be explained by differences in the expression ratio between IP_3R1 and IP_3R3 receptors. Moreover, by knock down of individual *Itpr* genes we provide the first direct evidence that the frequency of IP_3-dependent calcium oscillations determines the periodicity of action potential firing in density-arrested NRK fibroblasts.

In **Chapter 4** we investigated the mechanism of calcium entry and the channels that are involved in the growth-dependent electrophysiological behavior of NRK fibroblasts. We show that calcium store-dependent calcium entry is differentially regulated via SOCs and ROCs in quiescent and density-arrested fibroblasts.

In **Chapter 5** we investigated the molecular components that are involved in calcium entry and $PGF_{2\alpha}$-induced calcium oscillations in NRK fibroblasts. By selective gene knock down we demonstrate a role for Trpc1, Stim1 and Orai1 in mediating store-operated calcium entry, whereas Trpc6 is able to activate receptor-operated calcium entry. Finally, our data show that Stim1, Orai1 and Trpc1, but not Trpc6, are necessary for the $PGF_{2\alpha}$-induced Ca^{2+} oscillations in NRK cells.

Finally, in **Chapter 6** the results presented in this thesis are summarized, discussed and put into the broad perspective regarding the role of calcium oscillations in the regulation of pacemaking activity and the growth-dependent firing of calcium action potentials by NRK cells.

References

Ambudkar, I. S. and H. L. Ong (2007). "Organization and function of TRPC channelosomes." Pflugers Arch **455**(2): 187-200.

Barritt, G. J., J. Chen, et al. (2008). "Ca(2+) -permeable channels in the hepatocyte plasma membrane and their roles in hepatocyte physiology." Biochim Biophys Acta **1783**(5): 651-72.

Berridge, M. J. (1990). "Calcium oscillations." J Biol Chem **265**(17): 9583-6.

Berridge, M. J. (1993). "Inositol trisphosphate and calcium signalling." Nature **361**(6410): 315-25.

Berridge, M. J., M. D. Bootman, et al. (1998). "Calcium--a life and death signal." Nature **395**(6703): 645-8.

Berridge, M. J., M. D. Bootman, et al. (2003). "Calcium signalling: dynamics, homeostasis and remodelling." Nat Rev Mol Cell Biol **4**(7): 517-29.

Burnashev, N. (1998). "Calcium permeability of ligand-gated channels." Cell Calcium **24**(5-6): 325-32.

Cahalan, M. D. (2009). "STIMulating store-operated Ca(2+) entry." Nat Cell Biol **11**(6): 669-77.

Carafoli, E. (2002). "Calcium signaling: a tale for all seasons." Proc Natl Acad Sci U S A **99**(3): 1115-22.

Carafoli, E., L. Santella, et al. (2001). "Generation, control, and processing of cellular calcium signals." Crit Rev Biochem Mol Biol **36**(2): 107-260.

Catterall, W. A. (2000). "Structure and regulation of voltage-gated Ca^{2+} channels." Annu Rev Cell Dev Biol **16**: 521-55.

Chakrabarti, R. and R. Chakrabarti (2006). "Calcium signaling in non-excitable cells: Ca^{2+} release and influx are independent events linked to two plasma membrane Ca^{2+} entry channels." J Cell Biochem **99**(6): 1503-16.

Cheng, K. T., X. Liu, et al. (2008). "Functional requirement for Orai1 in store-operated TRPC1-STIM1 channels." J Biol Chem **283**(19): 12935-40.

Cheng, K. T., H. L. Ong, et al. (2011). "Contribution of TRPC1 and Orai1 to Ca(2+) entry activated by store depletion." Advances in experimental medicine and biology **704**: 435-449.

Clapham, D. E. (1995). "Calcium signaling." Cell **80**(2): 259-68.

Clapham, D. E. (2003). "TRP channels as cellular sensors." Nature **426**(6966): 517-24.

De Roos, A. D., E. J. Van Zoelen, et al. (1997). "Membrane depolarization in NRK fibroblasts by bradykinin is mediated by a calcium-dependent chloride conductance." J Cell Physiol **170**(2): 166-73.

de Roos, A. D., P. H. Willems, et al. (1997). "Synchronized calcium spiking resulting from spontaneous calcium action potentials in monolayers of NRK fibroblasts." Cell Calcium **22**(3): 195-207.

DeHaven, W. I., J. T. Smyth, et al. (2007). "Calcium inhibition and calcium potentiation of Orai1, Orai2, and Orai3 calcium release-activated calcium channels." J Biol Chem **282**(24): 17548-56.

Dolman, N. J. and A. V. Tepikin (2006). "Calcium gradients and the Golgi." Cell Calcium **40**(5-6): 505-12.

Fasolato, C., M. Zottini, et al. (1991). "Intracellular Ca_{2+} pools in PC12 cells. Three intracellular pools are distinguished by their turnover and mechanisms of Ca^{2+} accumulation, storage, and release." J Biol Chem **266**(30): 20159-67.

Foskett, J. K., C. White, et al. (2007). "Inositol trisphosphate receptor Ca^{2+} release channels." Physiol Rev **87**(2): 593-658.

Gerasimenko, O. V., J. V. Gerasimenko, et al. (1996). "Inositol trisphosphate and cyclic ADP-ribose-mediated release of Ca^{2+} from single isolated pancreatic zymogen granules." Cell **84**(3): 473-80.

Giacomello, M., I. Drago, et al. (2007). "Mitochondrial Ca^{2+} as a key regulator of cell life and death." Cell Death Differ **14**(7): 1267-74.

Gross, S. A., U. Wissenbach, et al. (2007). "Murine ORAI2 splice variants form functional Ca^{2+} release-activated Ca^{2+} (CRAC) channels." J Biol Chem **282**(27): 19375-84.

Hajnoczky, G., G. Csordas, et al. (2000). "The machinery of local Ca^{2+} signalling between sarco-endoplasmic reticulum and mitochondria." J Physiol **529 Pt 1**: 69-81.

Haller, T., H. Volkl, et al. (1996). "The lysosomal Ca^{2+} pool in MDCK cells can be released by ins(1,4,5)P3-dependent hormones or thapsigargin but does not activate store-operated Ca^{2+} entry." Biochem J **319 (Pt 3)**: 909-12.

Harks, E. G., J. P. Camina, et al. (2003). "Besides affecting intracellular calcium signaling, 2-APB reversibly blocks gap junctional coupling in confluent monolayers, thereby allowing measurement of single-cell membrane currents in undissociated cells." Faseb J **17**(8): 941-3.

Harks, E. G., P. H. Peters, et al. (2005). "Autocrine production of prostaglandin F2alpha enhances phenotypic transformation of normal rat kidney fibroblasts." Am J Physiol Cell Physiol **289**(1): C130-7.

Harks, E. G., W. J. Scheenen, et al. (2003). "Prostaglandin F2 alpha induces unsynchronized intracellular calcium oscillations in monolayers of gap junctionally coupled NRK fibroblasts." Pflugers Arch **447**(1): 78-86.

Harks, E. G., J. J. Torres, et al. (2003). "Ionic basis for excitability of normal rat kidney (NRK) fibroblasts." J Cell Physiol **196**(3): 493-503.

Hofmann, T., A. G. Obukhov, et al. (1999). "Direct activation of human TRPC6 and TRPC3 channels by diacylglycerol." Nature **397**(6716): 259-63.

Hoth, M. and R. Penner (1992). "Depletion of intracellular calcium stores activates a calcium current in mast cells." Nature **355**(6358): 353-6.
Huizinga, J. D., Y. Zhu, et al. (2002). "High-conductance chloride channels generate pacemaker currents in interstitial cells of Cajal." Gastroenterology **123**(5): 1627-36.
Ishii, K., K. Hirose, et al. (2006). "Ca^{2+} shuttling between endoplasmic reticulum and mitochondria underlying Ca^{2+} oscillations." EMBO Rep **7**(4): 390-6.
Iwai, M., T. Michikawa, et al. (2007). "Molecular basis of the isoform-specific ligand-binding affinity of inositol 1,4,5-trisphosphate receptors." J Biol Chem **282**(17): 12755-64.
Jardin, I., J. J. Lopez, et al. (2008). "Orai1 mediates the interaction between STIM1 and hTRPC1 and regulates the mode of activation of hTRPC1-forming Ca^{2+} channels." J Biol Chem **283**(37): 25296-304.
Kinnear, N. P., F. X. Boittin, et al. (2004). "Lysosome-sarcoplasmic reticulum junctions. A trigger zone for calcium signaling by nicotinic acid adenine dinucleotide phosphate and endothelin-1." J Biol Chem **279**(52): 54319-26.
Kinnear, N. P., C. N. Wyatt, et al. (2008). "Lysosomes co-localize with ryanodine receptor subtype 3 to form a trigger zone for calcium signalling by NAADP in rat pulmonary arterial smooth muscle." Cell Calcium **44**(2): 190-201.
Kusters, J. M., J. M. Cortes, et al. (2007). "Hysteresis and bistability in a realistic cell model for calcium oscillations and action potential firing." Phys Rev Lett **98**(9): 098107.
Kusters, J. M., M. M. Dernison, et al. (2005). "Stabilizing role of calcium store-dependent plasma membrane calcium channels in action-potential firing and intracellular calcium oscillations." Biophys J **89**(6): 3741-56.
Kusters, J. M., W. P. van Meerwijk, et al. (2008). "Fast calcium wave propagation mediated by electrically conducted excitation and boosted by CICR." Am J Physiol Cell Physiol **294**(4): C917-30.
Lasorsa, F. M., P. Pinton, et al. (2008). "Peroxisomes as novel players in cell calcium homeostasis." J Biol Chem **283**(22): 15300-8.
Lee, K. P., J. P. Yuan, et al. "An endoplasmic reticulum/plasma membrane junction: STIM1/Orai1/TRPCs." FEBS Lett **584**(10): 2022-7.
Lewis, R. S. and M. D. Cahalan (1989). "Mitogen-induced oscillations of cytosolic Ca^{2+} and transmembrane Ca2+ current in human leukemic T cells." Cell Regul **1**(1): 99-112.
Liao, Y., C. Erxleben, et al. (2008). "Functional interactions among Orai1, TRPCs, and STIM1 suggest a STIM-regulated heteromeric Orai/TRPC model for SOCE/Icrac channels." Proc Natl Acad Sci U S A **105**(8): 2895-900.
Liao, Y., C. Erxleben, et al. (2007). "Orai proteins interact with TRPC channels and confer responsiveness to store depletion." Proc Natl Acad Sci U S A **104**(11): 4682-7.
Liou, J., M. L. Kim, et al. (2005). "STIM is a Ca2+ sensor essential for Ca^{2+}-store-depletion-triggered Ca2+ influx." Curr Biol **15**(13): 1235-41.
MacLennan, D. H., W. J. Rice, et al. (1997). "The mechanism of Ca^{2+} transport by sarco(endo)plasmic reticulum Ca^{2+}-ATPases." J Biol Chem **272**(46): 28815-8.
Melvin, J. E., D. Yule, et al. (2005). "Regulation of fluid and electrolyte secretion in salivary gland acinar cells." Annu Rev Physiol **67**: 445-69.
Mercer, J. C., W. I. Dehaven, et al. (2006). "Large store-operated calcium selective currents due to co-expression of Orai1 or Orai2 with the intracellular calcium sensor, Stim1." J Biol Chem **281**(34): 24979-90.
Mignen, O., J. L. Thompson, et al. (2003). "Calcineurin directs the reciprocal regulation of calcium entry pathways in nonexcitable cells." J Biol Chem **278**(41): 40088-96.
Mignen, O., J. L. Thompson, et al. (2007). "STIM1 regulates Ca^{2+} entry via arachidonate-regulated Ca2+-selective (ARC) channels without store depletion or translocation to the plasma membrane." J Physiol **579**(Pt 3): 703-15.
Mignen, O., J. L. Thompson, et al. (2008). "Both Orai1 and Orai3 are essential components of the arachidonate-regulated Ca^{2+}-selective (ARC) channels." J Physiol **586**(1): 185-95.
Missiaen, L., K. Van Acker, et al. (2004). "Calcium release from the Golgi apparatus and the endoplasmic reticulum in HeLa cells stably expressing targeted aequorin to these compartments." Cell Calcium **36**(6): 479-87.
Muallem, S. (2005). "Decoding Ca^{2+} signals: a question of timing." J Cell Biol **170**(2): 173-5.
Nguyen, T., W. C. Chin, et al. (1998). "Role of Ca2+/K+ ion exchange in intracellular storage and release of Ca^{2+}." Nature **395**(6705): 908-12.
Nicholls, D. G. (1978). "The regulation of extramitochondrial free calcium ion concentration by rat liver mitochondria." Biochem J **176**(2): 463-74.
Ong, H. L., K. T. Cheng, et al. (2007). "Dynamic assembly of TRPC1-STIM1-Orai1 ternary complex is involved in store-operated calcium influx. Evidence for similarities in store-operated and calcium release-activated calcium channel components." J Biol Chem **282**(12): 9105-16.

Parekh, A. B. (2003). "Store-operated Ca^{2+} entry: dynamic interplay between endoplasmic reticulum, mitochondria and plasma membrane." J Physiol **547**(Pt 2): 333-48.
Parekh, A. B. and J. W. Putney, Jr. (2005). "Store-operated calcium channels." Physiol Rev **85**(2): 757-810.
Parekh, A. B. (2011). "Decoding cytosolic Ca2+ oscillations." Trends in biochemical sciences **36**(2): 78-87.
Parekh, A. B. and S. Muallem (2011). "Ca(2+) signalling and gene regulation." Cell Calcium **49**(5): 279.
Peinelt, C., M. Vig, et al. (2006). "Amplification of CRAC current by STIM1 and CRACM1 (Orai1)." Nat Cell Biol **8**(7): 771-3.
Pinton, P., T. Pozzan, et al. (1998). "The Golgi apparatus is an inositol 1,4,5-trisphosphate-sensitive Ca^{2+} store, with functional properties distinct from those of the endoplasmic reticulum." Embo J **17**(18): 5298-308.
Quesada, I., W. C. Chin, et al. (2001). "Mouse mast cell secretory granules can function as intracellular ionic oscillators." Biophys J **80**(5): 2133-9.
Raychaudhury, B., S. Gupta, et al. (2006). "Peroxisome is a reservoir of intracellular calcium." Biochim Biophys Acta **1760**(7): 989-92.
Rizzuto, R. and T. Pozzan (2006). "Microdomains of intracellular Ca^{2+}: molecular determinants and functional consequences." Physiol Rev **86**(1): 369-408.
Salido, G. M., S. O. Sage, et al. (2009). "TRPC channels and store-operated Ca(2+) entry." Biochim Biophys Acta **1793**(2): 223-30.
Shuttleworth, T. J., J. L. Thompson, et al. (2004). "ARC channels: a novel pathway for receptor-activated calcium entry." Physiology (Bethesda) **19**: 355-61.
Soboloff, J., M. A. Spassova, et al. (2006). "Orai1 and STIM reconstitute store-operated calcium channel function." J Biol Chem **281**(30): 20661-5.
Strehler, E. E., A. G. Filoteo, et al. (2007). "Plasma-membrane Ca(2+) pumps: structural diversity as the basis for functional versatility." Biochem Soc Trans **35**(Pt 5): 919-22.
Strubing, C., G. Krapivinsky, et al. (2003). "Formation of novel TRPC channels by complex subunit interactions in embryonic brain." J Biol Chem **278**(40): 39014-9.
van Zoelen, E. J. (1991). "Phenotypic transformation of normal rat kidney cells: a model for studying cellular alterations in oncogenesis." Crit Rev Oncog **2**(4): 311-33.
van Zoelen, E. J., T. M. van Oostwaard, et al. (1988). "The role of polypeptide growth factors in phenotypic transformation of normal rat kidney cells." J Biol Chem **263**(1): 64-8.
Vanoevelen, J., L. Raeymaekers, et al. (2005). "Cytosolic Ca^{2+} signals depending on the functional state of the Golgi in HeLa cells." Cell Calcium **38**(5): 489-95.
Vay, L., E. Hernandez-Sanmiguel, et al. (2007). "Modulation of Ca(2+) release and Ca(2+) oscillations in HeLa cells and fibroblasts by mitochondrial Ca(2+) uniporter stimulation." J Physiol **580**(Pt 1): 39-49.
Vig, M., W. I. DeHaven, et al. (2008). "Defective mast cell effector functions in mice lacking the CRACM1 pore subunit of store-operated calcium release-activated calcium channels." Nat Immunol **9**(1): 89-96.
Wissenbach, U., S. E. Philipp, et al. (2007). "Primary structure, chromosomal localization and expression in immune cells of the murine ORAI and STIM genes." Cell Calcium **42**(4-5): 439-46.
Wuytack, F., L. Raeymaekers, et al. (2003). "PMR1/SPCA Ca2+ pumps and the role of the Golgi apparatus as a Ca^{2+} store." Pflugers Arch **446**(2): 148-53.
Yoo, S. H. (2000). "Coupling of the IP3 receptor/Ca^{2+} channel with Ca^{2+} storage proteins chromogranins A and B in secretory granules." Trends Neurosci **23**(9): 424-8.
Zhang, F., G. Zhang, et al. (2006). "Production of NAADP and its role in Ca^{2+} mobilization associated with lysosomes in coronary arterial myocytes." Am J Physiol Heart Circ Physiol **291**(1): H274-82.
Zhang, S. L., Y. Yu, et al. (2005). "STIM1 is a Ca^{2+} sensor that activates CRAC channels and migrates from the Ca^{2+} store to the plasma membrane." Nature 437(7060): 902-5.
Zhang, S., N. Fritz, et al. (2011). "Inositol 1,4,5-trisphosphate receptor subtype-specific regulation of calcium oscillations." Neurochemical research **36**(7): 1175-1185.

CHAPTER 2

Role of Prostanoid FP Receptor in Action Potential Generation and Phenotypic transformation of NRK Fibroblasts

Almirza WH, Dernison MM, Peters PH, van Zoelen EJ, Theuvenet AP

Cell Signal. 2008 Nov; 20 (11): 2022-9

Abstract

By using an shRNA approach to knock down the expression of the prostaglandin (PG)- $F_{2\alpha}$ receptor (FP-R), the role of $PGF_{2\alpha}$ in the process of phenotypic transformation of normal rat kidney (NRK) fibroblasts has been studied. Our data show that $PGF_{2\alpha}$ up-regulates Cox-2 expression both at the mRNA and protein level, indicating that activation of FP-R in NRK fibroblasts induces a positive feedback loop in the production $PGF_{2\alpha}$. Knock down of FP-R expression fully impaired the ability of $PGF_{2\alpha}$ to induce a calcium response and subsequent depolarization in NRK cells. However, these cells could still undergo phenotypic transformation when treated with a combination of EGF and retinoic acid, but in contrast to the wild-type cells, this process was not accompanied by a membrane depolarization to –20 mV. Knock down of FP-R expression also impaired the spontaneous firing of calcium action potentials by density-arrested NRK cells. These data show that a membrane depolarization is not a prerequisite for the acquisition of a transformed phenotype. Furthermore, our data provide the first direct evidence that activity of $PGF_{2\alpha}$ by putative pacemaker cells underlies the generation of calcium action potentials in NRK monolayers.

GF growth factor; RA, retinoic acid; TGF_{β}, transforming growth factor beta; FP-R, prostanoid

The abbreviations used are: $[Ca^{2+}]_i$, intracellular Ca^{2+} concentration; EGF, epidermal FP receptor; COX, cyclo-oxygenase; Ptfgr, gene encoding FP-R.

Introduction

There is currently great interest in the role of cyclooxygenases (COXs) and their derived products (prostaglandins) in tumorigenesis. It has been shown that COX activity in general, and that of the isoform COX-2 in particular, is significantly enhanced in tumor tissue (see (Trifan and Hla 2003; Dannenberg, Lippman et al. 2005) for reviews). In particular, prostaglandin E_2 (PGE_2) and its receptor (EP_2) have been shown to be involved in colon cancer, while prostaglandin $F_{2\alpha}$ ($PGF_{2\alpha}$) plays an important role in cervical cancer (DuBois, Radhika et al. 1996; Kulkarni, Rader et al. 2001). A further understanding of the role of COX enzymes and their products in tumorigenesis is of great importance for the further development of COX-2 directed anti-cancer therapies.

Normal rat kidney (NRK) fibroblasts provide an interesting in vitro model system for studying the role of COX enzymes and their products in tumorigenic transformation, since depending on the addition of specific combinations of growth factors these cells either show density-dependent growth inhibition or undergo phenotypic transformation (van Zoelen 1991). Such transformed NRK cells are able to proliferate under anchorage-independent conditions (van Zoelen, van Oostwaard et al. 1988) which is considered to be the best in vitro correlate of tumorigenesis (Cifone and Fidler 1980). Our previous study has indicated that phenotypic transformation of NRK cells is associated with depolarization of the plasma membrane and enhanced cyclooxygenases activity, both important characteristics of a variety of human and animal cancer cells (Harks, Peters et al. 2005).

The membrane potential of NRK cells strongly depends on the growth state of these cells. Confluent cultures made quiescent by serum deprivation show a stable membrane potential of –70 mV, while cells, which have become density-arrested in the presence of epidermal growth factor (EGF) and insulin show spontaneous calcium action potentials. During such action potentials the cell depolarizes transiently from –70 mV to positive values (De Roos, Van Zoelen et al. 1997; de Roos, Willems et al. 1997; Harks, Torres et al. 2003). Upon subsequent addition of retinoic acid (RA) or transforming growth factor-beta (TGF_β) these density-arrested cells resume their proliferation, which after 1-2 days is accompanied by a depolarization of the plasma membrane to –20 mV and the formation of cellular multilayer's with a transformed morphology. Upon wash-out of the culture medium of these phenotypically transformed cells by perfusion with fresh growth factor-deficient medium, the membrane repolarizes to -70 mV within a period of 10-30 min,

indicating that a soluble factor in the conditioned medium is responsible for the observed depolarization of these cells. This factor was identified as $PGF_{2\alpha}$. In previous studies we have shown that externally added $PGF_{2\alpha}$ induces asynchronous calcium oscillations in quiescent NRK cells, resulting in a depolarization to –20 mV (Harks, Scheenen et al. 2003). Furthermore we have shown that particularly phenotypically transformed NRK cells secrete high levels of $PGF_{2\alpha}$ whereas the two other calcium-mobilizing prostaglandins PGD_2 and PGE_2 could not be detected in the growth media conditioned by the transformed cells (Harks, Peters et al. 2005). In the present study we have investigated the causal relation between the productions of $PGF_{2\alpha}$ by phenotypically transformed NRK cells and their acquisition of a transformed phenotype, including depolarization to –20 mV, loss of density-dependent growth arrest and anchorage-independent proliferation. $PGF_{2\alpha}$ exerts its activity by binding to the FP receptor (FP-R), a G_q-protein coupled transmembrane protein (Narumiya, Sugimoto et al. 1999). In order to understand the role of $PGF_{2\alpha}$ in phenotypic transformation of NRK cells in more detail, we have used an shRNA approach to knock down the expression the FP-R in NRK cells. Our results show that the membrane depolarization of phenotypically transformed NRK cells is a consequence of FP-R activation, indicating that in these cells $PGF_{2\alpha}$ acts in an autocrine manner. However, activation of FP-R was not essential for cellular transformation induced by RA of TGF_{β}. Furthermore, our data show that FP-R activation establishes a positive feedback loop by up regulating COX-2 expression and $PGF_{2\alpha}$ synthesis, thereby enhancing the phenotypic transformation process of NRK fibroblasts.

Material and Methods

Cell culturing

NRK fibroblasts (clone 49F) were cultured in bicarbonate- buffered Dulbecco's modified Eagle's medium (DMEM; Invitrogen, Paisley, UK) supplemented with 10% newborn calf serum (NCS; HyClone Laboratories, Logan, UT). Confluent cultures were made quiescent by subsequent incubation for 1-3 days in serum-free DF medium (1:1 mixture of DMEM-Ham's F-12 medium; Invitrogen, UK) supplemented with 30 nM Na_2SeO_3 and 10 mg/ml human transferrin. Density-arrested monolayers were obtained by a subsequent 2-days incubation with 5 ng/ml EGF (Collaborative Biomedical Products, Bedford, MA) in combination with 5 mg/ml insulin (Sigma, St. Louis, MO). Phenotypically transformed NRK cells were obtained by a 2-3 days treatment of density-arrested monolayers with 50 ng/ml RA or 2 ng/ml TGF_{β}.

shRNA constructs

In order to knock down expression of the rat *Ptgfr* gene, two different sets of siRNAs sequences were chosen by entering the nucleotide sequence of rat *Ptgfr* (NM-013115) into the web-based design tool from Dharmacon (http://design.dharmacon.com). The first identified 19-nucleotides target sequence (siRNA-1 bases 390–409) was 5'-ggatagctgtcttcgtata-3', while the second one (siRNA-2 bases 564–583) consisted of sequence 5'-ctacaaagatcacgtctaa-3'. Verification of these siRNA sequences for their specificity by BLAST database search did not show significant homology to any other known gene sequence in the human, mouse and rat genome. Specific and scrambled short hairpin (shRNA) template oligonucleoties were designed by entering the siRNA target sequences into the siRNA Wizard web-based design tool (http://www.sirnawizard.com/construct.php). The derived complementary oligonucleotides were synthesized by Sigma-Aldrich (UK), annealed, and ligated into the linearized pSUPER.retro puro vector (Oligo Engine, Seattle WA, USA) according to pSUPER RNAi system protocol.

Virus production and cell infections

The resulting constructs, shRNA-FP-R1 from siRNA-1, shRNA-FP-R2 from siRNA-2, scrambled shRNA and a control construct (pSUPER-empty vector not expressing shRNA, further denoted control cells), were transfected into Phoenix packaging cell line (Nolan Lab, Stanford, USA) in order to produce ecotropic retroviral supernatants. Phoenix cells were seeded in tissue culture dishes in DMEM supplemented with 10% NCS and pretreated with chloroquine at a final concentration of 25 mM. One day before transfection, Phoenix cells were seeded in culture dishes at a density of $4.0x10^4$ cells/cm^2 in order to reach 60% confluence at the time of transfection. Cells were then transfected with 20 µg of viral vector DNA using the calcium–phosphate precipitation method (Wigler, Silverstein et al. 1977; Chen and Okayama 1987). After 48 h transfection, the

culture medium was filtered through a 0.45 mm filter and the viral supernatant was used for infection of NRK cells pretreated with 4 mg/ml of polybrene (Sigma, USA). After infection, NRK cells were incubated for 24 h at 37 ^{0}C. Subsequently, medium was replaced by fresh virus-free medium and NRK cells were allowed to recover for 48 h at 37 ^{0}C. Infected cells were selected by culturing them in the presence of puromycin (6 mg/ml) for 5 days. *Ptgfr* expression in NRK wild-type cells, empty vector cells and shRNA producing cells was analyzed by quantitative real-time polymerase chain reaction (RT-PCR) and Western blot analysis, as described in detail below.

RNA extraction and quantitative RT-PCR

Total RNA was purified by applying Trizol reagent (Invitrogen, Paisley, UK) to NRK monolayer cells according to the manufacturer's instructions. Total RNA was quantified at 260 nm and analyzed by electrophoresis on 1% agarose/formaldehyde denaturing gels in order to exclude the presence of RNA degradation. mRNA levels for genes of interest were analyzed by using quantitative RT-PCR (Detection System 5700 ABI Prism, Applied Biosystems, USA).

For rat *Ptfgr* the forward primer 5'-gctctcggcatctcattctc-3' and reverse primer 5'-gtcaccagaaagggactcca-3' were used. For cyclooxygenase-1 (*Ptgs1*) forward primer 5-ggccatggagtggacttaaa-3 and reverse primer 5-ctctccaccgatgacctgat-3 was used. For cyclooxygenase-2 (*Ptgs2*) the forward primer 5-gctgacacacggatactggat-3 and reverse primer 5-tgggacagtctttgggtacag-3 and for 18S rat rRNA the forward primer 5'-cggctaccacatccaaggaa-3' and reverse primer 5'-gctggaattaccgcggct-3', giving rise to amplicons of 100–125 base pairs with a melting temperature between 58 and 60 ^{0}C. For complementary DNA (cDNA) synthesis, 2 mg of total RNA were reverse transcribed from random hexamer primers using the SUPER SCRIPT II reverse transcriptase kit (Invitrogene, Paisley, UK). Subsequently, 0.2 mg of total cDNA was amplified using SYBR Green PCR Mastermix (Applied Biosystems, USA) under the following conditions: initial denaturation for 10 min at 95 ^{0}C, followed by 40 cycles consisting of 15 s at 94 ^{0}C and 1 min at 60 ^{0}C. Expression values were calculated from threshold cycles at which an increase in reporter fluorescence above the baseline signal was first detected.

Western blot analysis

NRK cells were plated on dishes at a density of $1.4x10^4$ cells/cm^2 under the conditions described above. Cells were then lysed in lysis buffer (50 mM Tris-HCl, pH 7.5, 2 mM EDTA, 100 mM NaCl, 1% Triton X-100 and protease inhibitors mixture), supplemented with 50 mM NaF, 1 mM Na_3VO_4, and 10 mM β-glycerol phosphate. Cell lysates were incubated for 1 h on ice and centrifuged at 12000xg to collect supernatants. Protein concentration in the supernatants was evaluated by the Bradford method (Bradford 1976). After addition of sample buffer and boiling, 50 mg of the denatured proteins were separated on 12% SDS–PAGE gels and subsequently transferred

to nitrocellulose papers. After a 1 h blocking period, nitrocellulose papers were incubated with specific antibodies. The primary antibodies used were: polyclonal anti-FP receptor, anti- COX-1 and anti-COX-2 antibodies (Cayman Chemicals, USA), and anti-GAPDH antibodies (Sigma, USA). HRP-conjugated secondary antibodies were purchased from Santa Cruz Biotechnology, USA. Immunolabelling was visualized using the ECL procedure (Amersham Biosciences, USA). Bands were quantified by densitometric image analysis software (Image Master VDS, Pharmacia Biotech, Uppsala, Sweden). Results were normalized on the basis of GAPDH expression.

Patch-clamp measurement

NRK cell lines were seeded at a density of $1.4x10^4$ cells/cm^2 in culture dishes as described above to obtain quiescent, density-arrested and phenotypically transformed cells. Whole cell current-clamp experiments were performed with quiescent and phenotypically transformed NRK cells that were perfused at room temperature with serum-free DF medium equilibrated with 7.5% CO_2 to pH 7.4. In order to study the spontaneous calcium action potentials in NRK monolayers, density-arrested cells were perfused with Sr^{2+} -containing HEPES-buffered saline (Sr-HBS; 135.5 mM NaCl, 5.0 mM KCl, 5.0 mM $SrCl_2$, 10 mM glucose, 1.0 mM $MgCl_2$, 10 mM HEPES, pH 7.4). Borosilicate patch pipettes (GC 150-15; Clark, Reading, UK) with resistances of 4-6 MΩ were used, filled with an intracellular pipette solution containing 25 mM NaCl, 120 mM KCl, 1.0 mM $CaCl_2$, 1.0 mM $MgCl_2$, 3.5 mM EGTA, and 10 mM HEPES-KOH (pH 7.4). Data were acquired with an EPC-10 patch-clamp amplifier in conjugation with Pulse/Pulsefit v8.74 software (HEKA Elektronik, Lambrecht, Germany) at a sampling frequency of 0.1 kHz. Data analysis was performed offline using Microcal Origin software version 6.0 (Microcal Software, Northampton, MA).

Intracellular Ca^{2+} measurements

NRK cell lines were plated on glass cover slips coated with 0.1% gelatin at a density of $1.4x10^4$ cells/cm^2, as described above, and then were placed in a Leiden cell chamber and loaded with 4 mM Fura-2 AM (Invitrogen, Eugene, OR) for 30 min at room temperature in serum-free DF medium. Prior to measuring, the loading medium was replaced by Ca^{2+} containing HEPES-buffered saline (Ca-HBS; 141.5 mM NaCl, 5.0 mM KCl, 1.0 mM $CaCl_2$, 10 mM glucose, 1.0 mM $MgCl_2$, 10 mM HEPES, pH 7.4). Dynamic calcium video imaging was performed as described elsewhere (12). Excitation wavelengths of 340 and 380 nm (bandwidth 8-15 nm) were provided by a 150-W xenon lamp (UXL S150 MO; Ushio, Tokyo, Japan), while fluorescence emission was monitored above 440 nm, using a 440 nm DCLP dichroic mirror in front of the camera. Image acquisition, using camera pixel binning of 4, and computation of ratio images (F340/F380) was performed every 4 s using MetaFluor software v.6.2 (Universal Imaging Corporation, Downingtown, PA, US). Camera acquisition time was 100 ms per excitation wavelength.

Growth stimulation assays

Transfected and untransfected NRK cells lines were grown to confluency in serum-containing medium and subsequently made quiescent by incubation with serum-free medium for 1-3 days. These cells were then grown to density-arrest by incubation with 5 ng/ml EGF and 5 mg/ml insulin for an additional 48 h. Density-arrested cell were subsequently restimulated to proliferate by treatment with indicated factors to induce phenotypic transformation. Cumulative incorporation of [^{3}H] thymidine (0.5 mCi/ml added; Amersham International) was measured between 24-48 h after addition of serum-free medium, which contained in addition to EGF and insulin also the transforming factors RA, $PGF_{2\alpha}$ or TGF_{β} (van Zoelen, van Oostwaard et al. 1986).

Soft agar assay for anchorage-independent growth

Anchorage-independent growth of NRK cells was assayed under growth factor-defined conditions as described by Van Zoelen et al. (van Zoelen, Twardzik et al. 1984). To 60-mm culture dishes first 2 ml of DF medium containing 10% growth factor-inactivated serum (SH-FCS) were added in the presence of 0.5 % agar noble (Difco). After solidification of the underlayer, $1.0x10^4$ freshly trypsinized NRK cells were added in DF medium containing 10% SH-FCS in the presence of 0.5% agar noble, supplemented with 10 ng/ml EGF, 5 μg/ml insulin and as transforming factors either 50 ng/ml RA or 100 nM PGF_{2a}. After solidification of the upper layer, the cultures were incubated for 14 days without further addition under standard culture conditions. Colony formation was assessed in unfixed and unstained cultures by use of a light microscope Olympus CK2 (Japan). Colonies larger than 8 cells were counted in 20 random 2.3 mm^2 microscopic fields from two replicate culture dishes. Data are expressed as the number of colonies relative to the number of inoculated cells.

Statistics

Student's *t*-test was used for statistical comparisons. Numeric data are represented as ±SEM throughout this article, *n* representing the number of replicates of each experiment.

Results

Induction of COX enzymes by RA, TGFβ and $PGF_{2\alpha}$

In a previous study we have shown that NRK fibroblasts, which had been grown to density arrest in the presence of insulin and EGF, become phenotypically transformed upon treatment with $PGF_{2\alpha}$ (Lahaye, Walboomers et al. 1999). Furthermore we have shown that NRK fibroblasts that are phenotypically transformed upon addition of RA or TGFβ secrete elevated levels of $PGF_{2\alpha}$ in their culture medium (Harks, Peters et al. 2005). These observations prompted us first to examine the mRNA levels of genes encoding COX-1 and COX-2, the two enzymes that mediate the production of prostaglandins, in NRK cells at the different growth states. Figure 1A (black bar) shows that COX-1 expression by quiescent, density-arrested and phenotypically transformed NRK cells, respectively, did not differ significantly. In striking contrast to that, great growth state-dependent differences in COX-2 expression were observed; the level of mRNA expression of Cox-2 in density-arrested cells was 8-fold higher than in the quiescent cells, and strongly further up-regulated (16-fold) in the RA-induced transformed cells. (Fig.1A white bar). Also on the protein level, similar results were obtained for the growth state-dependent expression of COX-1 and COX-2 (Fig.1B and 1C). These findings indicate that the elevation of the concentration of $PGF_{2\alpha}$ secreted by NRK fibroblasts into their growth medium upon phenotypic transformation is related to an up-regulation of COX-2 activity in the transformed cells.

We subsequently investigated how external growth modulating stimuli affect the expression of the COX-1 and COX-2 genes in NRK fibroblasts. Figure 1D (white bar) shows that 4 h after addition of growth modulating stimuli to quiescent NRK cells, mRNA levels for the Cox-2 gene (*Ptgs2*) are strongly up regulated, while that for Cox-1 (*Ptgs1*) are not (Fig.1D (black bar)). $PGF_{2\alpha}$ induced a nearly 30-fold increase in the Cox-2 gene mRNA levels in these cells, while EGF, RA and TGFβ induced only a 9, 5 and 14 - fold increase, respectively. Also at the protein level $PGF_{2\alpha}$ was particularly potent in inducing Cox-2 (Fig. 1F), while the expression of COX-1 was hardly affected by the four growth modulating agents applied in this study (Fig. 1E). Since activation of Cox enzymes is considered to be the rate-limiting step in prostaglandin synthesis, these data indicate that $PGF_{2\alpha}$ may stimulate its own production. The observed production of $PGF_{2\alpha}$ upon phenotypic transformation of NRK cells by RA or TGFβ may therefore have been initiated

by these transforming agents, but are most likely further enhanced by this positive feedback loop.

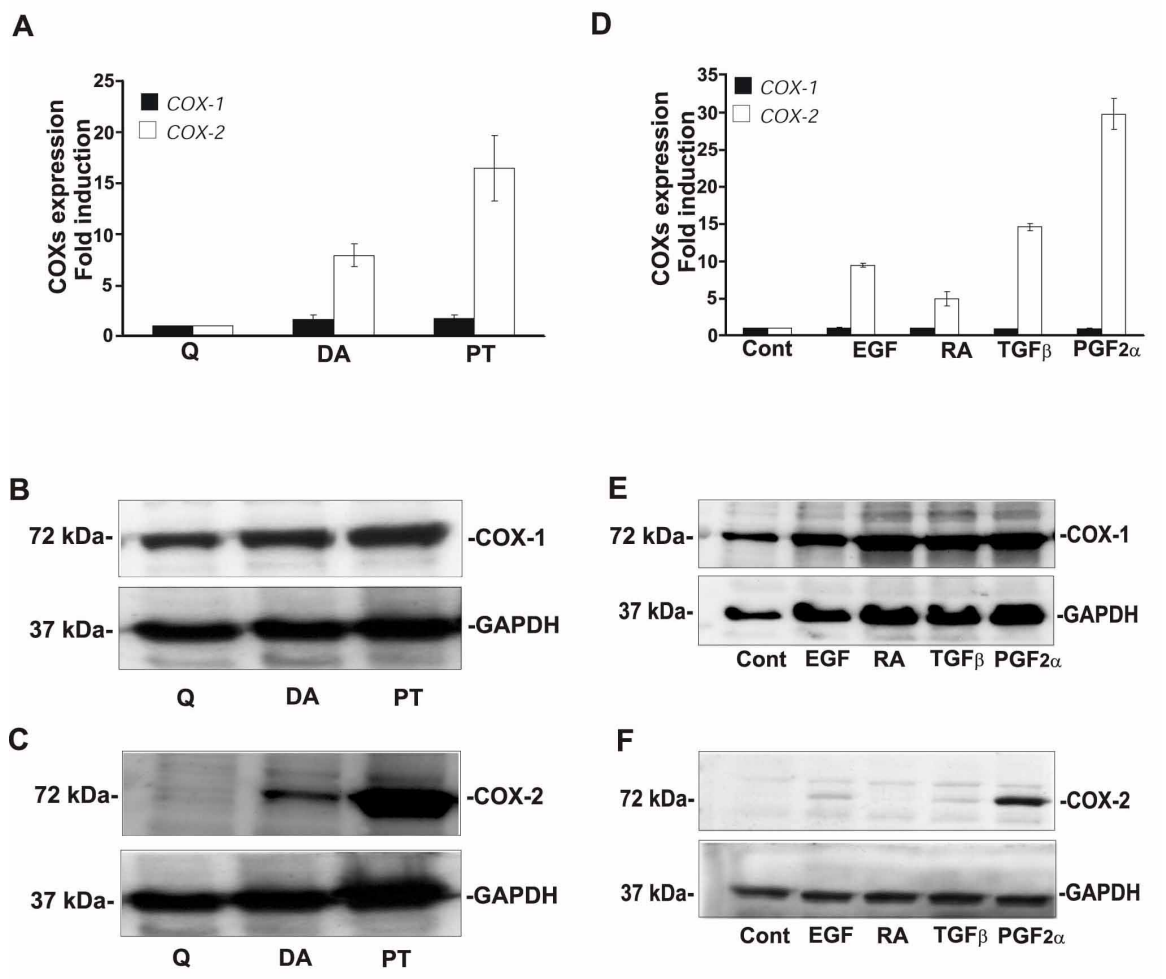

Fig. 1. Growth state-dependent expression of COX-1 and COX-2 in NRK fibroblasts and the effect of EGF, RA, TGFβ and $PGF_{2\alpha}$ on COXs expression in quiescent NRK cells.

(A) mRNA expression levels of COX-1 (black bar) and COX-2 (white bar) in quiescent (Q), density-arrested (DA) and RA-induced phenotypically transformed (PT) NRK fibroblasts, and (B) and (C) the corresponding Western blots of the COX-1 and COX-2 proteins, respectively. (D) Effect of EGF, RA, TGFβ and $PGF_{2\alpha}$ on mRNA expression levels of COX-1 and COX-2 in quiescent NRK fibroblasts, and (E) and (F) the corresponding Western blots of the COX-1 and COX-2 proteins, respectively. Quiescent NRK fibroblasts cells were treated with 5 ng/ml EGF, 50 ng/ml RA, 2 ng/ml TGFβ and 100 nM PGF_{2a} for 4 h. Data in (A) and (D) are represented as mean ± SEM (n=3). mRNA levels were measured by quantitative PCR analysis as described under Materials and Methods, and expressed relative to the amount of 18S rRNA . For Western blot analysis specific antibodies against Rat COX-2 (C, F) and COX-1 (B,E) were used, and antibodies against glyceraldehyde-3-phosphate dehydrogenase (GAPDH) as a loading control.

Suppression of $PGF_{2\alpha}$ receptor expression in NRK fibroblasts by shRNA

$PGF_{2\alpha}$ mediates its action by binding to the G_q-protein coupled receptor FP-R, which is encoded by the *Ptgfr* gene. Quiescent and density-arrested NRK cells respond to externally added $PGF_{2\alpha}$ by intracellular Ca^{2+} oscillations, concomitant with a depolarization of the cell to –20 mV, indicating that these cells have functional FP receptors (Harks, Scheenen et al. 2003). Autocrine activity of $PGF_{2\alpha}$ in phenotypically NRK cells requires sufficient expression of its receptor in these cells. In order to investigate a possible modulation of *Ptgfr* expression in NRK cells, we studied its mRNA levels by quantitative real-time PCR (qRT-PCR) analysis as a function of the NRK growth status. Figure 2A and 2B shows that quiescent and density-arrested NRK cells have significantly higher *Ptgfr* mRNA and protein levels than phenotypically transformed cells. The cause of this reduced *Ptgfra* expression in transformed cells is unknown, but may reflect a downregulation of expression as a result of autocrine receptor activation.

Figure 2C shows that quiescent NRK cells transfected with a *Ptgfr* specific shRNA encoding vector (dFPR1) exhibit an 83% reduction in steady state *Ptgfr* mRNA level. No such knockdown of *Ptgfr* expression was observed in the control cells (not expressing shRNA) or cells transfected with the scrambled shRNA nucleotide sequence (scr1) (see Material and Methods). At the protein level, a similar reduction in FP-R expression levels was induced by the shRNA vector, as shown by immunoblotting with anti-FP-R antibodies (Fig. 2D). These data combined show that *Ptgfr* expression in NRK cells is modulated during different proliferation states, while expression can be strongly suppressed by RNA interference approaches.

Suppression of Ptgfr expression by shRNA prevents membrane depolarization of quiescent NRK fibroblasts by $PGF_{2\alpha}$

In order to study the effect of *Ptgfr* knockdown on the sensitivity of NRK cells for PGF_{2a}, we measured the effect of $PGF_{2\alpha}$ (0.1 μM) and bradykinin (1 μM) on the membrane potential of quiescent NRK cells. Figure 3A shows that addition of $PGF_{2\alpha}$ to quiescent control cells results in a depolarization from –69 ± 3.3 mV (mean ± SEM; n=5) to –19 ± 2.4 mV (mean ± SEM; n=5). Subsequent removal of $PGF_{2\alpha}$ from the perfusion medium resulted in a complete hyperpolarization, after an intermediate stage in which the membrane potential showed transient oscillations. In contrast, no depolarization was observed upon addition of $PGF_{2\alpha}$ to the shRNA transfected NRK cells (dFPR1) cells in

which *Ptgfr* was knocked down (Fig. 3B), indicating that these cells have a strongly reduced sensitivity to $PGF_{2\alpha}$. In contrast, both cell types remained sensitive to the transiently depolarizing activity of bradykinin.

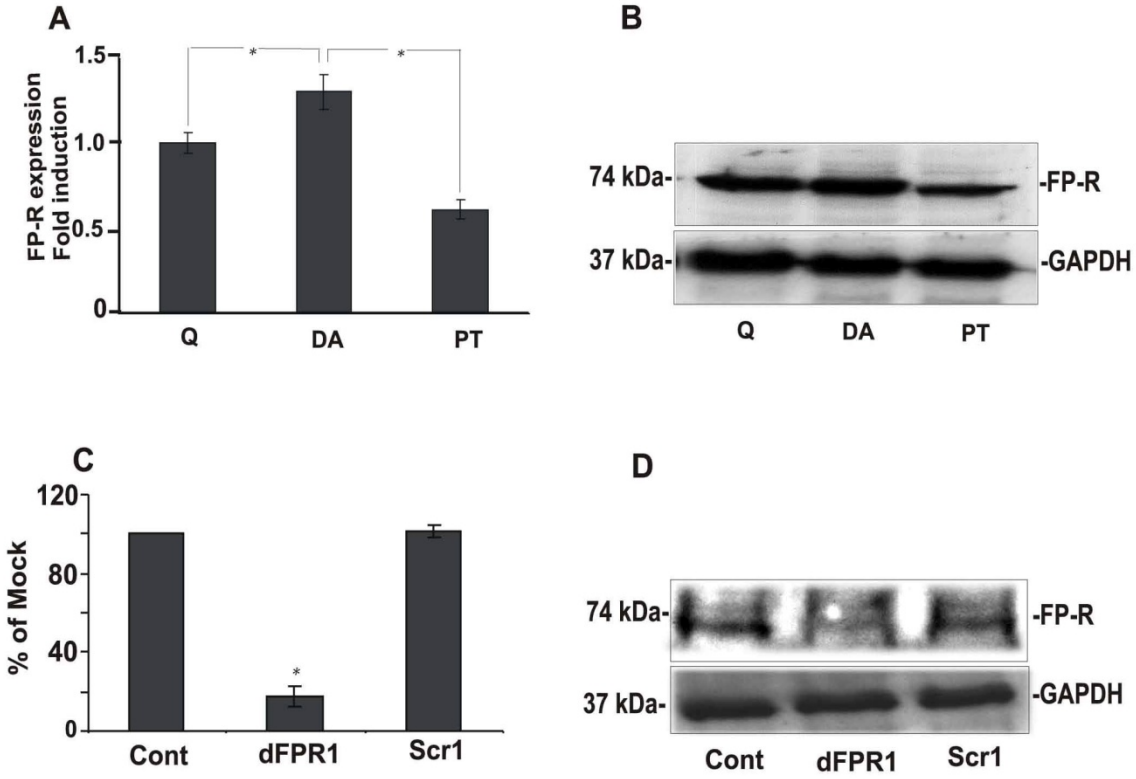

Fig. 2. Expression level of FP receptor in NRK fibroblasts and dFPR1 cells.

(A) Expression level of FP receptor in quiescent (Q), density-arrested (DA) and phenotypically transformed (PT) NRK fibroblasts as determined by Quantitative PCR analysis. (B) Western blot analysis of FP receptor protein in quiescent (Q), density-arrested (DA) and phenotypically transformed (PT) NRK cells using antibodies against FP-R; antibodies against glyceraldehyde-3-phosphate dehydrogenase (GAPDH) were used as a loading control (C) Quantitative PCR analysis of RNAi-mediated reduction of FP receptor mRNA level in control cells, stable cell line expressing shRNA against FP receptor (dFPR1) cells and cells expressing scrambled FP receptor shRNA (scr-1). Values are represented as mean ± SEM (n=3), whereby ***** indicates $p<0.05$ vs. control. (D) Western blot analysis of FP receptor protein in control cells, shRNA expressing dFPR1 cells and scrambled FP receptor shRNA expressing cells (scr-1), using antibodies against FP-R; antibodies against glyceraldehyde-3-phosphate dehydrogenase (GAPDH) were used as a loading control.

Activation of FP-R by $PGF_{2\alpha}$ induces the degradation of inositol-containing phospholipids resulting in intracellular Ca^{2+} oscillations. Ratiometric Fura-2 Ca^{2+} imaging showed that addition of $PGF_{2\alpha}$ (0.1 μM) to control cells resulted in a rapid and pronounced increase in intracellular Ca^{2+} concentration, which was fully absent in dFPR1 cells (average of 40 cells shown in Fig.3C). At the level of individual cells, 36 out of 40 (90%) of the control cells responded with a more than 10% increase in the Fura-2 fluorescence ratio upon treatment with $PGF_{2\alpha}$, while in the case of the dFPR1 cells only 2 out of 40 (5%) gave such a positive response. In combination, these data show that $PGF_{2\alpha}$ is unable to induce functional second messengers in NRK cells in which *Ptgfr* has been knocked down.

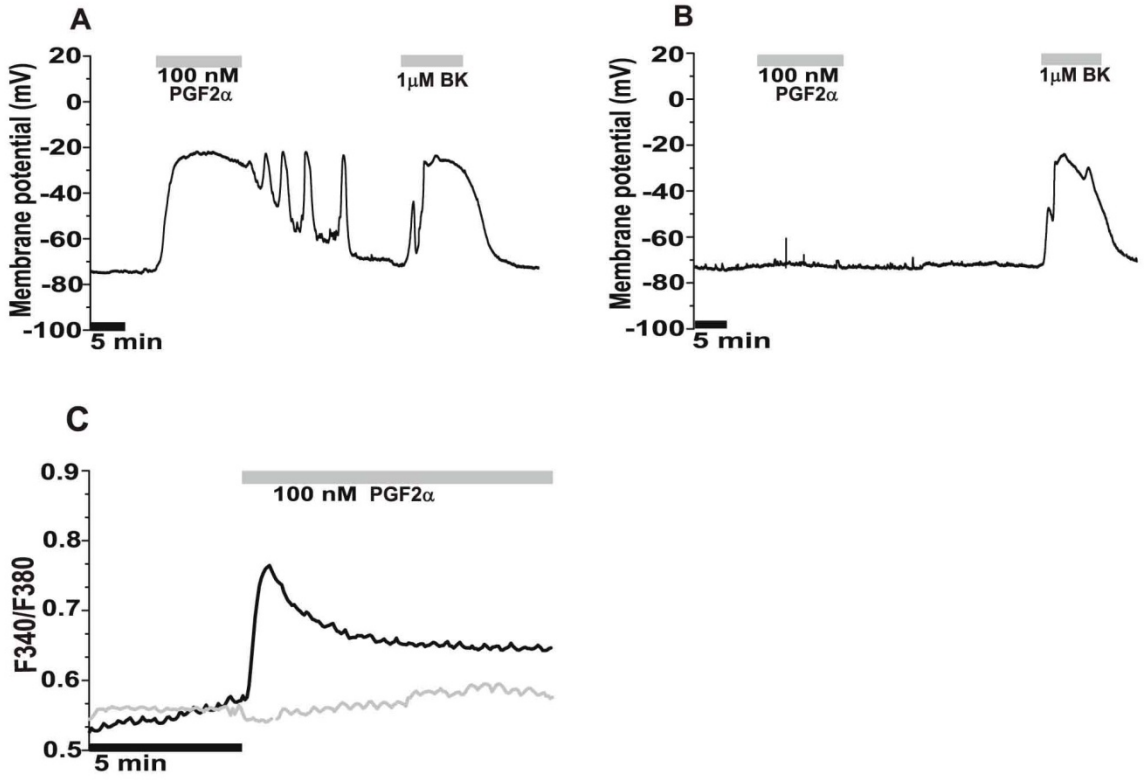

Fig. 3. Downregulation of FP receptor by shRNA prevents membrane depolarization evoked by $PGF_{2\alpha}$ in quiescent NRK fibroblasts. Cells were continuously perfused and the agonists were included in the perfusion medium during the indicated time. Typical responses to exposure to 100 nM $PGF_{2\alpha}$ or 1 mM bradykinin (BK), indicated by the bars, measured in the current clamp mode of whole cell patch clamp configuration of (A) control cells and (B) dFPR1 cells. (C) Effect of 100 nM $PGF_{2\alpha}$ on the intracellular calcium response of control cells (black trace) and dFPR1 cells (gray trace). Each trace represents an average response of 40 cells from at least three independent experiments.

Ptgfr knockdown abolishes action potential firing in density-arrested NRK fibroblasts

Density-arrested NRK cells show spontaneous periodic calcium action potentials, which result from the concerted activity of an L-type calcium channel, a calcium-activated chloride channel and an inward rectifying potassium channel. Instantaneous depolarization occurs upon opening of the L-type calcium channel, a process that is enforced in the presence of strontium ions (De Roos, Van Zoelen et al. 1997; de Roos, Willems et al. 1997; Harks, Torres et al. 2003). We have previously hypothesized that locally enhanced production of $PGF_{2\alpha}$ by density-arrested NRK fibroblasts induces calcium oscillations in these cells and thereby generates the pacemaker activity that is required for the induction of propagating action potentials [34]. In order to study the role of $PGF_{2\alpha}$ in this process, we investigated the effect of *Ptgfr* knockdown on the occurrence of such calcium action potentials. Figure 4A shows that spontaneous calcium action potentials are readily observed in density-arrested control cells, but not in dFPR1 cells (Figure 4B). Similarly as shown in Fig. 3A, subsequent addition of $PGF_{2\alpha}$ to the control cells resulted in constitutive depolarization, which was not observed in the dFPR1 cells. Previously we have shown that a single propagating calcium action potential can be generated in NRK monolayers upon local treatment with a depolarizing agent, such as K^+ or bradykinin (De Roos, Van Zoelen et al. 1997). Such a single calcium action potential, which is generated independently of $PGF_{2\alpha}$ activity, could be induced in both the control and the dFPR1 cells (data not shown). These observations support the hypothesis that activation of FP-R is essential for the generation of pacemaking activity in NRK monolayers, but are not required for propagation of the resulting action potentials.

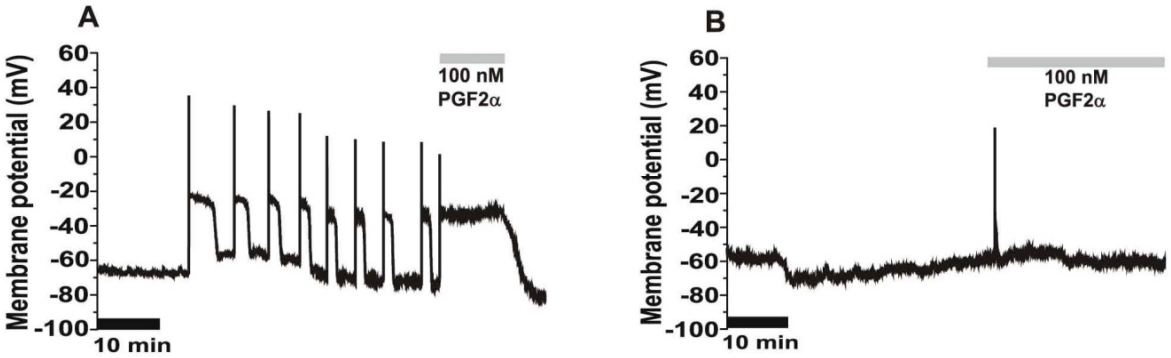

Fig. 4. Effect of FP receptor downregulation on calcium action potential firing of density-arrested NRK fibroblasts. (A) Membrane potential registration of density-arrested control cells. Cells fired spontaneously repetitive calcium action potentials. Addition of $PGF_{2\alpha}$ (100 nM) instantly depolarized the cells. (B) Membrane potential registration of density-arrested dFPR1. These cells showed no firing of

repetitive action potentials. The addition of 100 nM $PGF_{2\alpha}$ to dFPR1 cells did not depolarize the cells. Shown are typical experiments that were repeated at least three times with similar results.

Ptgfr knockdown prevents membrane depolarization of phenotypically transformed NRK fibroblasts

Addition of RA or $TGF\beta$ to density-arrested NRK cells results in restimulation of cellular growth and the acquisition of a transformed phenotype (Anzano, Roberts et al. 1982; van Zoelen, van Oostwaard et al. 1988). This process is accompanied by a gradual depolarization of the cells, concomitant with enhanced secretion levels of $PGF_{2\alpha}$. In order to study the role of $PGF_{2\alpha}$ in this process in more detail, we measured the effect of *Ptgfr* knockdown on the membrane potential of phenotypically transformed NRK cells. Table 1 shows that, 48 h after addition of RA, control cells and the wild type are depolarized with a membrane potential of –21 ± 1.2 mV (mean ± SEM; n=5), while dFPR1 cells remained hyperpolarized with a membrane potential of –57 ± 6.4 mV (mean ± SEM; n=6). In combination with the observation that perfusion of phenotypically transformed NRK cells with fresh medium results in a gradual hyperpolarization, these data underline the hypothesis that depolarization of NRK cells upon phenotypic transformation is mediated by autocrine activation of the FP receptor by $PGF_{2\alpha}$.

Cell name	transforming factor	No. of experiments	Membrane potential mV
wild type	RA	4	- 22.0 ±1.8
	TGF_β	4	- 16.7 ±2.3
	$PGF_{2\alpha}$	4	- 20.1 ±3.3
control	RA	5	- 21.1 ±1.2
	TGF_β	4	- 19.7 ±2.1
	$PGF_{2\alpha}$	5	- 20.2 ±2.1
dFPR1	RA	6	- 57.5 ±4.6
	TGF_β	6	- 55.9 ±1.2
	$PGF_{2\alpha}$	6	- 63.1 ±2.3

Table 1. FP receptor downregulation prevents the membrane depolarization of NRK fibroblasts upon phenotypic transformation. Membrane potential values of phenotypically transformed NRK (wild type, control and dFPR1 cells), measured by the current-clamp patch-clamp technique as described in Materials and Methods. Values are represented as mean ± SEM.

Ptgfr knockdown does not affect the ability of NRK cells to undergo phenotypic transformation

Phenotypic transformation of NRK cells is associated with loss of density-dependent growth inhibition and induction of anchorage-independent proliferation. The observation that density-arrested dFPR1 cells do not depolarize upon treatment with RA or TGF_{β} could either indicate that these cells have lost the ability to undergo phenotypic transformation or that membrane depolarization is not essential for the acquisition of a transformed phenotype. In order to discriminate between these two possibilities, we investigated to what extent dFPR1 cells could still be induced to undergo loss of density-dependent growth inhibition and induction of anchorage-independent proliferation upon addition of RA.

Figure 5A compares the rate of thymidine incorporation into quiescent, density-arrested and phenotypically transformed NRK cells, wild type and transfected or not with *Ptgfr* shRNA. In all cell types, low thymidine incorporation levels were observed in non-stimulated quiescent cells and in cells that had become density-arrested after stimulation with EGF and insulin. Upon subsequent addition of RA to density-arrested cells, 7-fold stimulation was observed for the wild type and control cells, while for dFPR1 cells 4.5-fold stimulation was observed. This indicates that upon reduction of *Ptgfr* expression, NRK cells retain the ability to undergo loss of density-dependent growth arrest, although to a lesser extent than control cells. Figure 5A also shows that $PGF_{2\alpha}$ itself is able to induce a 4- to 5-fold increase in thymidine incorporation in wild type and control cells, compared to a 2-fold increase in dFPR1 cells. These data agree with previous observations, which showed that $PGF_{2\alpha}$ is a much poorer inducer of phenotypic transformation than RA (Lahaye, Walboomers et al. 1999). Moreover, these data show that with respect to induction of cell proliferation dFPR1 cells are not fully insensitive to $PGF_{2\alpha}$

The observation that in mitogenic assays dFPR1 cells still respond to $PGF_{2\alpha}$ could potentially result from heterogeneity in the extent of *Ptgfr* knock down between cells in the monolayer. In order to test the ability of dFPR1 cells to undergo phenotypic transformation at the cellular level, we examined their ability to form progressively growing colonies in soft agar (Fig. 5B). Figure 5C shows that under growth factor-defined assay conditions RA induced a 4-fold increase in the number of EGF-treated NRK cells that were able to form colonies larger than 100 μm in soft agar, both for the control and the dFPR1 cells. This observation indicates that dFPR1 and control cells show a similar efficiency in soft

agar colony formation (Fig. 5B). Moreover, $PGF_{2\alpha}$ induced a 2-fold increase in colony forming ability of both the control and the dFPR1 cells. The observation that with respect to the induction of cell proliferation in control and dFPR1 cells is similarly responsive to $PGF_{2\alpha}$ argues against the possibility that only a subset of cells, which have retained substantial FP-R expression, respond mitogenically to $PGF_{2\alpha}$.

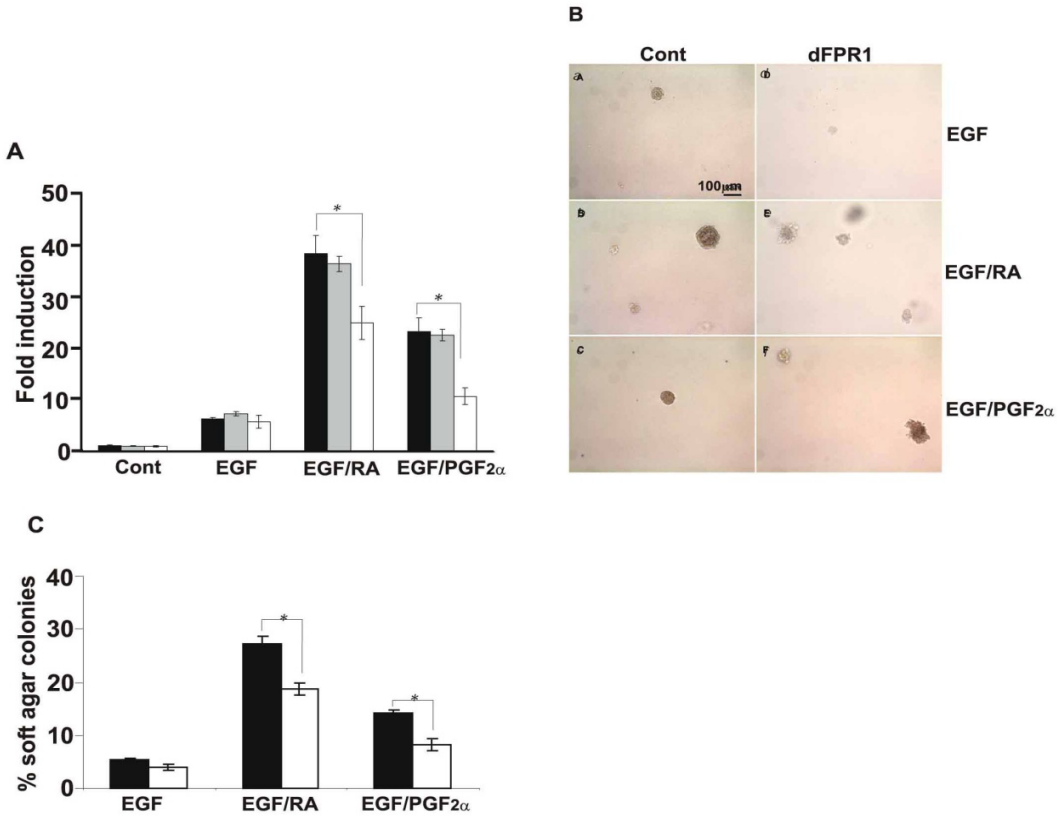

Fig. 5. Effect of FP receptor downregulation by shRNA on RA and $PGF_{2\alpha}$-induced phenotypic transformation of NRK fibroblasts. (A) [^{3}H]-Thymidine incorporation assay for wild type NRK cells (black bar), control cells (gray bar) and dFPR1 cells (white bar). The cells were grown to density arrest in the presence of 5 ng/ml EGF, and thereafter restimulated to proliferate by the addition of RA (50 ng/ml) or $PGF_{2\alpha}$ (100 nM). Cumulative incorporation of [^{3}H]-thymidine was measured between 24 and 48 h after the addition of serum-free medium, which contained in addition to EGF also the transformation-inducing agents. The control represents [^{3}H]-thymidine incorporation values of the cells in the absence of EGF and transformation-inducing agents. Values are represented as mean ± SEM (n=3) whereby * indicates $p<0.05$ vs. response of control cells. (B) Anchorage-independent growth of control and dFPR1 cells was assayed as described in Materials and Methods. Phase contrast micrographs of colonies formed in soft agar were taken at 20x magnification. Control cells and dFPR1 cells were cultured in soft agar in the presence of 10 ng/ml EGF (a,d), and in the additional presence of either 50 ng/ml RA (b,e) or 100 nM $PGF_{2\alpha}$ (c,f) as transformation-inducing agents. (C) Quantitative analysis of anchorage-independent growth. Data are expressed as the number of colonies relative to the number of inocculated cells of the average of two replicate cultures.

Discussion

In this study we have examined the role of prostanoid FP receptor (FP-R) activation in phenotypic transformation of NRK fibroblasts. Emphasis was laid on three aspects of the transformation process, i.e. membrane depolarization to –20 mV, loss of density-dependent growth arrest and the induction of anchorage-independent proliferation. In addition, we have investigated the role of the FP-R in modulating the membrane potential of these fibroblasts during their different proliferative states. The present results show that dFPR1 cells, in which the mRNA levels for the FP-R encoding gene *Ptgfr* have been reduced by 83% following introduction of a specific shRNA, are unresponsive to $PGF_{2\alpha}$, both with respect to the enhancement of the intracellular calcium concentration and the ability to depolarize the cells to –20 mV. Furthermore, density-arrested dFPR1 cells are unable to generate spontaneous calcium action potentials. However, these dFPR1 cells can still undergo phenotypic transformation, as measured by the loss of density-dependent growth arrest and induction of soft agar growth in the presence of RA, indicating that membrane depolarization is not essential for the acquisition of a transformed phenotype. Furthermore, we observed that in proliferation assays dFPR1 cells are still weakly responsive to $PGF_{2\alpha}$, indicating that for a proliferative effect of this prostaglandin much less FP receptors have to be activated than for the generation of a calcium response and subsequent depolarization. Finally our results show that FP-R activation establishes a positive feedback loop that up-regulates COX-2 expression and $PGF_{2\alpha}$ synthesis, thus enhancing phenotypic transformation of NRK fibroblasts.

There is presently substantial evidence for the involvement of COX enzymes in cell proliferation and tumor progression (Trifan and Hla 2003). In most cell types, including fibroblasts, particularly COX-2 is up-regulated upon cell transformation (Eberhart, Coffey et al. 1994; Gilroy, Saunders et al. 2001; Schenning, van Tiel et al. 2007), but up-regulation of COX-1 expression has also been reported in e.g. human prostate cancer (Narko, Ristimaki et al. 1997) and murine lung tumors (Bauer, Dwyer-Nield et al. 2000). In addition, recent studies have indicated that increased prostaglandin levels may play an important role in mediating the up-regulation of COX-2 expression and activity (Vichai, Suyarnsesthakorn et al. 2005). In this study, we report that an elevated cellular secretion of $PGF_{2\alpha}$ is accompanied with an up-regulation of the expression of COX-2 and not of COX-1, and notably also an up-regulation of functional FP receptors in NRK fibroblasts (Fig 1A-C and 2A). Furthermore, we have shown that in these cells $PGF_{2\alpha}$ is a stronger inducer

of COX-2 expression than growth factors such as EGF or transformation-inducing agents such as RA or TGFβ. Hence, these results underline the role of the FP receptor in phenotypic transformation of NRK cells and indicate that the excessive increase of $PGF_{2\alpha}$ secretion following cell transformation most likely results from a positive feedback regulation of COX-2 expression and activity.

Pierce et al. (Pierce, Bailey et al. 1997) have reported the existence of two FP-R isoforms named FP_A and FP_B, whereby FP_B is a truncated form of FP_A due to a lack of the 46 carboxy-terminal amino acids. These two isoforms have been shown to differ in their activation of second messenger pathways (Fujino, Pierce et al. 2000). In addition, a splice variant of human *PTGFR* has been identified in a variety of cell types, which leads to a 71 bp insert and a concomitant frame shift, resulting in a truncated receptor that lacks the 7^{th} transmembrane segment and the intracellular carboxy-terminal tail (Vielhauer, Fujino et al. 2004). In the present study, we designed the shRNA oligonucleotides against the third transmembrane segment, to make sure that all reported isoforms of FP-R will be targeted by the RNAi machinery. As Western blotting of whole cell lysates of NRK fibroblasts with the anti-FP-R antibody generated only one single band, it is highly unlikely that these cells express more than one form of the FP receptor.

Recently we have shown that the amount of $PGF_{2\alpha}$ produced by NRK fibroblasts in their culture medium depends on their growth status and directly influences the membrane potential of these cells (8). Quiescent cells secrete hardly detectable amounts of $PGF_{2\alpha}$ in their growth medium and display a stable membrane potential of around –70 mV. Density-arrested cells reach a concentration of 1.5 nM $PGF_{2\alpha}$ in their growth medium, which is accompanied by periodic firing of action potentials, while phenotypically transformed cells secrete $PGF_{2\alpha}$ up to concentrations of 20 nM, which is sufficient to induce constitutive depolarization of the cells to –20 mV (Harks, Peters et al. 2005). Our current results provide the first direct evidence for an exclusive role of the FP receptor in modulating the membrane potential of NRK fibroblasts during these different proliferate states, as outlined in the following paragraphs.

Firstly, we have shown that the suppression of *Ptgfr* expression by shRNA prevents the membrane depolarization of quiescent NRK cells by $PGF_{2\alpha}$. Furthermore, single-cell calcium imaging analysis of quiescent *Ptgfr* knocked-down NRK cells (dFPR1) cells revealed that almost all dFPR1 cells had become unresponsive to exposure to $PGF_{2\alpha}$. In particular, these cells did no longer show the typical intracellular calcium response of

control cells, which is characterized by an initial large calcium transient followed by repetitive oscillations (Harks, Scheenen et al. 2003). However, approximately 5% of the dFPR1 cells still showed a wild-type calcium response. This could be indicative for the possibility that these cultures still contain a small percentage of cells with functional FP-Rs, although this small number of wild-type like cells is obviously not sufficient to cause a depolarization of all cells in $PGF_{2\alpha}$- treated monolayers. All together these findings demonstrate that membrane depolarization of quiescent NRK fibroblasts by $PGF_{2\alpha}$ is mediated by activation of their FP receptors. In contrast, activation of the FP receptor by $PGF_{2\alpha}$ in cell types such as Swiss 3T3 cells and rabbit cerebral smooth muscle cells has been shown to cause hyperpolarization instead of depolarization of the cells. In these cells the induced increase in intracellular calcium concentration results in the activation of calcium-dependent potassium channels (Kusano and Gainer 1991; Woodward and Lawrence 1994; Kim, Han et al. 2003), which are absent in NRK fibroblasts.

Secondly, our present findings show that in dFPR1 cells, grown to density arrest in the presence of EGF, no spontaneous firing of periodic calcium action potentials occurs. This supports our hypothesis that activation of the FP-R by $PGF_{2\alpha}$ is essential for the generation of periodic firing activity by density-arrested NRK fibroblasts. However, dFPR1 cells are still able to undergo density-arrest to a comparable level as in control cells (Fig. 5A), which shows that periodic firing of action potentials is not a requirement for NRK cells to undergo density-dependent growth inhibition.

Thirdly, we have shown that although dFPR1 cells can still become phenotypically transformed by RA, $TGF\beta$ and surprisingly also still substantially by $PGF_{2\alpha}$, such transformation is not accompanied by a membrane depolarization. The transformed dFPR1 cells maintain a membrane potential around –60 mV, not much different from that of quiescent control cells (Table 1). This observation shows that the expression of functional FP receptors by NRK fibroblasts is required for their depolarization upon transformation by these agents. On the other hand, the above findings also show that phenotypic transformation of NRK fibroblasts does not require a depolarization of the cells.

Some of our findings suggest that dFPR1 cells are heterogeneous with respect to their expression level of functional FP receptors. Results of qPCR and Western blot analysis (Fig.2) indicated that a 83% down-regulation of the FP-R had been achieved in the dFPR1 cells. This might mean that in 83% of these cells a complete knockdown of FP-R was achieved, and that the remainder 17% of cells still retained wild-type FP-R levels in spite

of the continuous antibiotics pressure on the cells. However, the observation that dFPR1 cells treated with either RA or $PGF_{2\alpha}$, have a similar cloning efficiency in soft agar as wild-type NRK cells, indicates that under those conditions the dFPR1 cells behave as a homogeneous population. Since this population is still weakly responsive to $PGF_{2\alpha}$, this suggests that all cells have similarly low FP-R levels. Obviously these receptors levels are too low to allow a calcium response, but apparently sufficient to generate the growth response.

We have previously postulated that the induction of phenotypic transformation of NRK cells by RA and $TGF\beta$ is mediated by the ability of these growth modulators to up-regulate expression of the EGF receptor. Density-arrested cells become quiescent in spite of the presence of EGF, because at high cell density the number of EGF receptors has become too low to mediate an EGF growth response (Lahaye, Camps et al. 1998). As a result of the up-regulation of the EGF receptor density by RA or $TGF\beta$, density-arrested cells become responsive again to the growth stimulating activity of EGF. Since FP-R is not involved in this process, this explains why dFPR1 cells can still undergo phenotypic transformation upon treatment with RA or $TGF\beta$. However, the induction of COX-2 by these growth modulators, resulting in enhanced secretion of $PGF_{2\alpha}$, will only result in a depolarization of wild type and control cells but not of dFPR1 cells, since this aspect of the transformation process requires FP-R activation. $PGF_{2\alpha}$ itself is also a weak activator of phenotypic transformation (Lahaye, Walboomers et al. 1999), in agreement with the observation that it is able to weakly up-regulate EGF receptor expression, although with delayed kinetics. Preliminary results show that phenotypically transformed dFPR1 cells secrete approximately 3-fold less $PGF_{2\alpha}$ in their growth medium than transformed control NRK fibroblasts under similar conditions (W.H. Almirza; unpublished), indicating that the levels of FP-R expression control the positive feedback on $PGF_{2\alpha}$ production.

We realize that up-regulation of COX-2 activity might also lead to enhanced production of prostanoids other than $PGF_{2\alpha}$ and that these might elicit biological effects on NRK fibroblasts as well. However, although commercially produced PGE_2 and PGD_2 have been shown to be calcium-mobilizing prostaglandins for NRK fibroblasts, whereas PGI_2, PGJ_2 and PGA_2 not, the presence of none of these five prostaglandins could be detected in growth media conditioned by RA-transformed NRK cells [8]. Moreover, PGE_2 and PGD_2 appeared not able to induce phenotypic transformation of NRK fibroblasts in the presence of EGF (W.H.M.A. Almirza; unpublished). Taken together, our findings strongly suggest

that the main product of up-regulated COX-2 activity in NRK fibroblasts involved in their phenotypic transformation and growth state-dependent modulation of the membrane potential is $PGF_{2\alpha}$ and that these cellular responses are mediated by activation of their FP receptors.

In summary, our findings indicate that the extent of $PGF_{2\alpha}$–FP receptor interaction is responsible for the growth state-dependent modulation of the membrane potential of NRK fibroblasts and that this interaction enhances phenotypic transformation of the cells by RA or $TGF\beta$.

Acknowledgements

We gratefully thank Dr. Jeroen van Leeuwen (Dept. of Cell Biology, Radboud University Nijmegen) for support in the preparation of the manuscript and Walter van Rotterdam (Dept. of Cell Biology, Radboud University Nijmegen) for technical assistance. This research project was funded in part by the Netherlands Organization for Scientific Research (NWO; project 805.47.066).

References

Anzano, M. A., A. B. Roberts, et al. (1982). "Synergistic interaction of two classes of transforming growth factors from murine sarcoma cells." Cancer Res **42**(11): 4776-4778.

Bauer, A. K., L. D. Dwyer-Nield, et al. (2000). "High cyclooxygenase 1 (COX-1) and cyclooxygenase 2 (COX-2) contents in mouse lung tumors." Carcinogenesis **21**(4): 543-550.

Bradford, M. M. (1976). "A rapid and sensitive method for the quantitation of microgram quantities of protein utilizing the principle of protein-dye binding." Anal Biochem **72**: 248-254.

Chen, C. and H. Okayama (1987). "High-efficiency transformation of mammalian cells by plasmid DNA." Mol Cell Biol **7**(8): 2745-2752.

Cifone, M. A. and I. J. Fidler (1980). "Correlation of patterns of anchorage-independent growth with in vivo behavior of cells from a murine fibrosarcoma." Proc Natl Acad Sci U S A **77**(2): 1039-1043.

Dannenberg, A. J., S. M. Lippman, et al. (2005). "Cyclooxygenase-2 and epidermal growth factor receptor: pharmacologic targets for chemoprevention." J Clin Oncol **23**(2): 254-266.

De Roos, A. D., E. J. Van Zoelen, et al. (1997). "Membrane depolarization in NRK fibroblasts by bradykinin is mediated by a calcium-dependent chloride conductance." J Cell Physiol **170**(2): 166-173.

de Roos, A. D., P. H. Willems, et al. (1997). "Synchronized calcium spiking resulting from spontaneous calcium action potentials in monolayers of NRK fibroblasts." Cell Calcium **22**(3): 195-207.

DuBois, R. N., A. Radhika, et al. (1996). "Increased cyclooxygenase-2 levels in carcinogen-induced rat colonic tumors." Gastroenterology **110**(4): 1259-1262.

Eberhart, C. E., R. J. Coffey, et al. (1994). "Up-regulation of cyclooxygenase 2 gene expression in human colorectal adenomas and adenocarcinomas." Gastroenterology **107**(4): 1183-1188.

Fujino, H., K. L. Pierce, et al. (2000). "Delayed reversal of shape change in cells expressing FP(B) prostanoid receptors. Possible role of receptor resensitization." J Biol Chem **275**(38): 29907-29914.

Gilroy, D. W., M. A. Saunders, et al. (2001). "COX-2 expression and cell cycle progression in human fibroblasts." Am J Physiol Cell Physiol **281**(1): C188-194.

Harks, E. G., P. H. Peters, et al. (2005). "Autocrine production of prostaglandin F2alpha enhances phenotypic transformation of normal rat kidney fibroblasts." Am J Physiol Cell Physiol **289**(1): C130-137.

Harks, E. G., W. J. Scheenen, et al. (2003). "Prostaglandin F2 alpha induces unsynchronized intracellular calcium oscillations in monolayers of gap junctionally coupled NRK fibroblasts." Pflugers Arch **447**(1): 78-86.

Harks, E. G., J. J. Torres, et al. (2003). "Ionic basis for excitability of normal rat kidney (NRK) fibroblasts." J Cell Physiol **196**(3): 493-503.

Kim, N., J. Han, et al. (2003). "Effects of prostaglandin F2alpha on membrane currents in rabbit middle cerebral arterial smooth muscle cells." Am J Physiol Heart Circ Physiol **284**(3): H1018-1027.

Kulkarni, S., J. S. Rader, et al. (2001). "Cyclooxygenase-2 is overexpressed in human cervical cancer." Clin Cancer Res **7**(2): 429-434.

Kusano, K. and H. Gainer (1991). "Bombesin-like peptides induce Ca2(+)-activated K+ conductance increases in mouse fibroblasts." Am J Physiol **260**(4 Pt 1): C701-707.

Lahaye, D. H., M. G. Camps, et al. (1998). "Epidermal growth factor (EGF) receptor density controls mitogenic activation of normal rat kidney (NRK) cells by EGF." J Cell Physiol **174**(1): 9-17.

Lahaye, D. H., F. Walboomers, et al. (1999). "Phenotypic transformation of normal rat kidney fibroblasts by endothelin-1. Different mode of action from lysophosphatidic acid, bradykinin, and prostaglandin f2alpha." Biochim Biophys Acta **1449**(2): 107-118.

Narko, K., A. Ristimaki, et al. (1997). "Tumorigenic transformation of immortalized ECV endothelial cells by cyclooxygenase-1 overexpression." J Biol Chem **272**(34): 21455-21460.

Narumiya, S., Y. Sugimoto, et al. (1999). "Prostanoid receptors: structures, properties, and functions." Physiol Rev **79**(4): 1193-1226.

Pierce, K. L., T. J. Bailey, et al. (1997). "Cloning of a carboxyl-terminal isoform of the prostanoid FP receptor." J Biol Chem **272**(2): 883-887.

Schenning, M., C. M. van Tiel, et al. (2007). "The anti-apoptotic MAP kinase pathway is inhibited in NIH3T3 fibroblasts with increased expression of phosphatidylinositol transfer protein beta." Biochim Biophys Acta.

Trifan, O. C. and T. Hla (2003). "Cyclooxygenase-2 modulates cellular growth and promotes tumorigenesis." Journal of cellular and molecular medicine **7**(3): 207-222.

van Zoelen, E. J. (1991). "Phenotypic transformation of normal rat kidney cells: a model for studying cellular alterations in oncogenesis." Crit Rev Oncog **2**(4): 311-333.

van Zoelen, E. J., D. R. Twardzik, et al. (1984). "Neuroblastoma cells produce transforming growth factors during exponential growth in a defined hormone-free medium." Proc Natl Acad Sci U S A **81**(13): 4085-4089.

van Zoelen, E. J., T. M. van Oostwaard, et al. (1986). "PDGF-like growth factor induces EGF-potentiated phenotypic transformation of normal rat kidney cells in the absence of TGF beta." Biochem Biophys Res Commun **141**(3): 1229-1235.

van Zoelen, E. J., T. M. van Oostwaard, et al. (1988). "The role of polypeptide growth factors in phenotypic transformation of normal rat kidney cells." J Biol Chem **263**(1): 64-68.

Vichai, V., C. Suyarnsesthakorn, et al. (2005). "Positive feedback regulation of COX-2 expression by prostaglandin metabolites." Inflamm Res **54**(4): 163-172.

Vielhauer, G. A., H. Fujino, et al. (2004). "Cloning and localization of hFP(S): a six-transmembrane mRNA splice variant of the human FP prostanoid receptor." Arch Biochem Biophys **421**(2): 175-185.

Wigler, M., S. Silverstein, et al. (1977). "Transfer of purified herpes virus thymidine kinase gene to cultured mouse cells." Cell **11**(1): 223-232.

Woodward, D. F. and R. A. Lawrence (1994). "Identification of a single (FP) receptor associated with prostanoid-induced Ca2+ signals in Swiss 3T3 cells." Biochem Pharmacol **47**(9): 1567-1574.

CHAPTER 3

Different Roles of Inositol 1,4,5-triphosphate Receptor Subtypes in PGF2α-Induced Calcium Oscillations and Pacemaker Activity in NRK Fibroblasts

Almirza WH, Peters PH, van Meerwijk WP, van Zoelen EJ, Theuvenet AP

Cell Calcium. 2010 Jun; 47(6):544-553

Abstract

We investigated the role of inositol 1, 4, 5-trisphosphate (IP_3) - receptor isoforms in the prostaglandin $F_{2\alpha}$ ($PGF_{2\alpha}$)-induced calcium oscillations and pacemaking activity of normal rat kidney (NRK) fibroblasts. Reverse transcription polymerase chain reaction (RT-PCR) studies revealed that NRK fibroblasts express only the IP_3-receptor subtypes IP_3R1 and IP_3R3. Quantitative RT-PCR analysis demonstrated that their expression levels varied as a function of the growth status of NRK cells; NRK cells made quiescent (Q) by serum deprivation expressed significantly higher levels of subtype 1 and 3 than cells grown to density-arrest (DA). Using Ca^{2+}- imaging techniques, we show that the frequency of $PGF_{2\alpha}$-induced calcium oscillations in DA-cells is lower than in Q-cells. To study whether these differences in the frequency of calcium oscillations relate to the relative amounts of IP_3-receptor subtypes expressed by the cells, we knocked down the genes for either IP_3-receptor subtype by using an shRNA approach. Knockdown of the IP_3R1 gene significantly decreased the frequency of the $PGF_{2\alpha}$-induced calcium oscillations in both Q- and DA-cells. It also reduced the frequency of the repetitive firing of calcium action potentials by DA-cells. In contrast, knockdown of the IP_3R3 gene caused an increase in the frequency of both processes, suggesting a role for this receptor subtype as an anti-Ca^{2+}-oscillatory unit in NRK fibroblasts. Our findings indicate that the reduction in the frequency of $PGF_{2\alpha}$-induced calcium oscillations in DA-cells compared with Q-cells results from the reduced expression ratio of IP_3R1 versus IP_3R3 receptors in DA-cells. Moreover, these data provide direct evidence that the frequency of IP_3-dependent calcium oscillations determines the periodicity of action potential firing by density-arrested NRK fibroblasts.

Keywords: IP_3-receptor subtypes, Calcium oscillations, Pacemaking activity, NRK fibroblasts, $PGF_{2\alpha}$.

Introduction

Changes in intracellular free Ca^{2+} concentration ($[Ca^{2+}]_i$) represent one of the most widespread and important signaling events, controlling a diverse range of cellular processes, including gene transcription, cell proliferation and cell-cell communication (Nathanson, Burgstahler et al. 1995; Dolmetsch, Lewis et al. 1997; Dolmetsch, Pajvani et al. 2001; Berridge, Bootman et al. 2003). Various studies have indicated that the frequency of stimulus-induced Ca^{2+} oscillations is very important for the decoding of the Ca^{2+}-signal by Ca^{2+}-dependent downstream events. A ubiquitous mechanism of modulating $[Ca^{2+}]_i$ involves activation of phospholipase C (PLC)-β and PLC-γ by trimeric G protein- or tyrosine kinase-coupled receptors, respectively. The resulting degradation of inositol-containing lipids leads to the generation of soluble inositol 1,4,5-trisphosphate (IP_3), which binds IP_3-receptors (IP3R) on the endoplasmic reticulum (ER) membrane and thereby causes a rapid but transient liberation of Ca^{2+} into the cytoplasm. Due to positive and negative feedback control of the IP_3Rs by cytosolic and luminal Ca^{2+}, IP_3 may induce sustained Ca^{2+} oscillations in the cell (Berridge 1993; Clapham 1995). It has been shown that multiple IP_3R subtypes exist, designated IP_3R1, IP_3R2 and IP_3R3, which differ in their Ca^{2+} sensitivity, and therefore dictate another frequency of Ca^{2+} oscillations upon IP_3 activation (Foskett, White et al. 2007).

In a number of studies we have shown that normal rat kidney (NRK) fibroblasts adapt their Ca^{2+} homeostasis to the growth status of the cells. In cells grown to confluence in a monolayer culture and made quiescent by serum deprivation, prostaglandin $F_{2\alpha}$ ($PGF_{2\alpha}$) is able to induce sustained calcium oscillations, which are asynchronous between cells in spite of the gap junction-mediated metabolic and electrical coupling of the cells (Harks, Scheenen et al. 2003). On the other hand, if these fibroblasts are grown to density-arrest in the presence of epidermal growth factor (EGF) as the sole polypeptide growth factor, they exhibit spontaneous, almost synchronous periodic changes in $[Ca^{2+}]_i$ associated with the firing of repetitive Ca^{2+} action potentials (de Roos, Willems et al. 1997). If these density-arrested cells are subsequently treated with $PGF_{2\alpha}$, they lose the ability to generate action potentials and respond again with asynchronous Ca^{2+} oscillations. In the present study we show that the frequency of $PGF_{2\alpha}$-induced Ca^{2+} oscillations is significantly higher in quiescent than in density-arrested NRK cells. We also show that NRK cells express the genes for IP_3R1 and IP_3R3, but not for IP_3R2, and that selective knockdown of either gene

alters the frequency of $PGF_{2\alpha}$-induced Ca^{2+} oscillations. In combination with quantitative RT-PCR data, our results indicate that IP_3R1 enhances and IP_3R3 reduces the frequency of IP_3-mediated Ca^{2+} oscillations in NRK cells. In agreement with that notion, it appears that the significantly higher frequency of $PGF_{2\alpha}$-induced Ca^{2+} oscillations in quiescent than in density-arrested NRK cells correlates with the higher expression level of IP_3R1 in the quiescent than in the density-arrested cells.

Materials & Methods

Cell culturing

Normal rat kidney fibroblasts (NRK clone 49F) were seeded at a density of $1.25x10^4$ cells/cm^2 in bicarbonate-buffered Dulbecco's modified Eagle's medium (DMEM; Invitrogen, Carlsbad, CA) supplemented with 10% newborn calf serum (HyClone Laboratories, Logan, UT). *Confluency was reached after four days. Cells were then incubated for three days in* serum-free DF medium (1:1 mixture of DMEM and Ham's F-12 medium (Invitrogen) supplemented with 30 nM Na_2SeO_3 and 10 μg/ml human transferrin, to obtain quiescent cells. Density-arrested monolayers were obtained *by incubation of quiescent cells for 48 hours with 5 ng/ml EGF (*Collaborative Research Incorporated, Bedford, MA*) in combination with 5 μg/ml insulin (Sigma-Aldrich, St. Louis, MO)*.

RNA extraction and reverse transcription polymerase chain reaction (RT-PCR) analysis

Total RNA was purified by applying Trizol reagent (Invitrogen) to NRK monolayer cells according to the manufacturer's instructions. Total RNA was quantified at 260 nm and the quality was analyzed by electrophoresis on 1% agarose/formaldehyde denaturing gels. For complementary DNA (cDNA) synthesis, 2 μg of total RNA were reverse transcribed from random hexamer primers using the SUPER SCRIPT II ribonuclease H^- reverse transcriptase kit (Invitrogen). For studying the expression of IP3R subtype genes in NRK cells, PCR amplification was performed on a PERKIN ELMER Gene Amp PCR System 2400 (Norwalk, CT), using 2 μl of first stranded cDNA reaction, 150 pmol of each degenerate primer, 50 μM dNTPs, 2 U Bio Therm Taq polymerase and 2.5 mM $MgCl_2$ in total volume of 50 μl. Following a hot start (3 min at 94 ^{0}C), the sample was subjected to 30 cycles of 30 sec at 94 ^{0}C, 30 sec at 60 ^{0}C and 30 sec at 72 ^{0}C. This procedure was followed by a final extension for 7 min at 72 ^{0}C. Reaction products were separated by standard agarose gel electrophoresis and subsequently cloned into the pCR-2.1 TOPO (Invitrogen) vector according to the manufacturer's protocol. The identity of the inserts was confirmed by DNA sequencing. Table 1 shows the primers used for expression analysis of rat *Itpr1* (encoding IP_3R1), *Itpr2* (encoding IP_3R2) and *Itpr3* (encoding IP_3R3) with the corresponding size of the amplified product.

Real-time quantitative PCR analysis

Quantitative RT-PCR analysis was carried out on a Detection System 5700 ABI Prism (Applied Biosystems, Foster City, CA). An amount of 0.2 μg of total cDNA was amplified using SYBR Green PCR Mastermix (Applied Biosystems) under the following conditions: initial denaturation for 10 min at 95 ^{0}C, followed by 40 cycles consisting of 15 sec at 94 ^{0}C and 1 min at 60 ^{0}C. For rat *Itpr1* the following primers were used: forward primer 5'- gagatgagcctggctgaggttcaa -3' and reverse primer 5'- tgttgcctccttccagaagtgcga-3'. For rat *Itpr3* the following primers were used: forward

primer 5'-cggctaccacatccaaggaa-3' and reverse primer 5'- gtcaggaactggcagatggcaggt–3'. Expression data were indicated relative to rat 18S rRNA, for which the following primers were used: forward primer 5'-cggctaccacatccaaggaa-3' and reverse primer 5'-gctggaattaccgcggct-3'. All samples gave rise to amplicons of 110–144 base pairs with a melting temperature of 60 ^{0}C. Expression values were calculated from threshold cycles at which an increase in reporter fluorescence above the baseline signal was first detected.

shRNA constructs

In order to knock down expression of rat *Itpr1* and *Itpr3*, two different sets of shRNAs sequences were chosen by entering the nucleotide sequence of both genes (Accession No. NM_001007235 and Accession No. NM_013138, respectively) into the web-based design tool from Dharmacon (http://design.dharmacon.com). The chosen siRNA target and scrambled sequences for both genes were then verified for their specificity by BLAST database search and did not show significant homology to any other known gene sequence in the human, mouse and rat genome. Specific shRNA oligonucleotides were designed by entering the siRNA target sequences into the siRNA Wizard web-based design tool (http://www.sirnawizard.com/construct.php). The derived complementary oligonucleotides, as well as their scrambled variants with similar nucleotide composition, were synthesized by Sigma-Aldrich, annealed, and ligated into the linearized pSUPER.retro puro vector (Oligo Engine, Seattle, WA) according to the pSUPER RNAi system protocol.

Virus production and cell infections

The resulting specific shRNAs and scrambled constructs, as well as the pSUPER-empty vector (not expressing shRNA as control) were transfected into Phoenix packaging cell line (Nolan Lab, Stanford, CA) in order to produce ecotropic retroviral supernatants. Phoenix cells were seeded in tissue culture dishes in DMEM supplemented with 10% NCS and pre-treated with chloroquine at a final concentration of 25 μM. One day before transfection, Phoenix cells were seeded in culture dishes at a density of $4.0x10^4$ cells/cm^2 in order to reach 60% confluence at the time of transfection. Cells were then transfected with 20 μg of viral vector DNA using the calcium–phosphate precipitation method (Wigler, Silverstein et al. 1977; Chen and Okayama 1987). After 48 hours, the culture medium was filtered through a 0.45 μm filter and the viral supernatant was used for infection of NRK cells pre-treated with 4 μg/ml of polybrene (Sigma-Aldrich). After infection, NRK cells were incubated for 24 hours at 37 ^{0}C. Subsequently, the medium was replaced by fresh, virus-free medium and the cells allowed to recover for 48 hours at 37 ^{0}C. Infected cells were selected by culturing them for 5 days in the presence of puromycin (6 μg/ml). *Itpr1* and *Itpr3*

expression in NRK cells was analyzed by quantitative RT-PCR, both before and after infection with specific or scrambled shRNA containing virus, as well as with the empty vector.

Western blot analysis

NRK cells were plated on dishes at a density of $1.4x10^4$ cells/cm^2 under the conditions described above. Cells were then treated with lysis buffer (50 mM Tris-HCl pH 7.5, 2 mM EDTA, 100 mM NaCl, 1% Triton X-100 and protease inhibitors mixture), supplemented with 50 mM NaF, 1 mM Na_3VO_4, and 10 mM β-glycerol phosphate. Cell lysates were incubated for 1 hour on ice and centrifuged at 12,000xg to collect supernatants. Protein concentration in the supernatants was evaluated by the Bradford method (Bradford 1976). After addition of sample buffer and boiling, 50 μg of the denatured proteins were separated on 8% SDS–PAGE gels and subsequently transferred to nitrocellulose paper. After a 1 hour blocking period, nitrocellulose papers were incubated with specific antibodies. The following primary antibodies used were: polyclonal anti-IP_3R1 antibodies were purchased from Abcam plc (Cambridge, UK), anti-IP_3R3 antibodies from Millipore (Amsterdam, The Netherlands) and anti-actin antibodies from Sigma-Aldrich. HRP-conjugated secondary antibodies were purchased from Santa Cruz Biotechnology (Santa Cruz, CA). Immunolabelling was visualized using the ECL procedure (Amersham Biosciences, Uppsala, Sweden). Bands were quantified by densitometric image analysis software (Image Master VDS, Pharmacia Biotech, Uppsala, Sweden). Signal quantification was performed with Photoshop software (Adobe systems). Briefly, mean pixel value was calculated for a predefined rectangle-encompassing signal of interest after subtracting the background signal. Similar data calculation was carried out for loading control samples (e.g α-actin) as indicated in the legend to the figures. The data plotted in the graphs represent mean pixel value (MPV) of the signal of interest divided by the MPV of the loading control.

Intracellular Ca^{2+} measurements

NRK cell lines were plated on glass cover slips coated with 0.1% gelatin at a density of $1.4x10^4$ cells/cm^2, as described above, and subsequently placed in a Leiden cell chamber where they were loaded for 30 min at room temperature with 4 μM Fura-2 AM (Invitrogen) in serum-free DF medium. Prior to measuring intracellular calcium concentrations, the loading medium was replaced by Ca^{2+} containing HEPES-buffered saline (Ca-HBS; 141.5 mM NaCl, 5.0 mM KCl, 1.0 mM $CaCl_2$, 10 mM glucose, 1.0 mM $MgCl_2$, 10 mM HEPES, pH 7.4). Dynamic calcium video imaging was performed as described elsewhere (Harks, Scheenen et al. 2003). Excitation wavelengths of 340 and 380 nm (bandwidth 8-15 nm) were provided by a 150-W xenon lamp (UXL S150 MO; Ushio, Tokyo, Japan), while fluorescence emission was monitored above 440 nm, using a 440 nm

DCLP dichroic mirror and a 510 nm emission filter (40 nm bandwidth) in front of the camera. Image acquisition, using camera pixel binning of 4, and computation of ratio images (F340/F380) was performed every 4 sec using MetaFluor software v.6.2 (Universal Imaging Corporation, Downingtown, PA). Camera acquisition time was 100 msec per excitation wavelength.

Patch-clamp measurements

NRK cell lines were seeded at a density of $1.4x10^4$ cells/cm^2 in culture dishes, as described above, to obtain monolayer of density-arrested cells. Whole cell current-clamp experiments were performed in order to study the propagation of spontaneous calcium action potentials. During the experiment cells were perfused with Sr^{2+}-containing HEPES-buffered saline (Sr-HBS; 135.5 mM NaCl, 5.0 mM KCl, 5.0 mM $SrCl_2$, 10 mM glucose, 1.0 mM $MgCl_2$, 10 mM HEPES, pH 7.4). Borosilicate patch pipettes (GC 150-15; Clark, Reading, UK) with resistances of 4-6 MΩ were used, filled with an intracellular pipette solution containing 25 mM NaCl, 120 mM KCl, 1.0 mM $CaCl_2$, 1.0 mM $MgCl_2$, 3.5 mM EGTA, and 10 mM HEPES-KOH (pH 7.4). Data were acquired with an EPC-10 patch-clamp amplifier in conjugation with Pulse/Pulsefit v8.74 software (HEKA Elektronik, Lambrecht, Germany) at a sampling frequency of 0.1 kHz. Data analysis was performed offline using Microcal Origin software version 6.0 (Microcal Software, Northampton, MA).

Statistics

Numerical data are represented as mean ± S.E.M throughout this article, with n representing the number of replicates in each experiment. The frequency of calcium oscillations was determined by counting the number of transients within a set time interval using the 'pick peak' algorithm of Microcal Origin 6.0, whereby a minimal peak height of 10% of the total signal was used as selection criterion. The Mann-Whitney U ranking test was applied for comparing the frequency of calcium oscillations/ transients in different cell groups. Statistical significance was defined at $p< 0.05$ and depicted by an asterisk in the figures.

Table 1. Primers for RT-PCR analysis

Gene	Accession No.	Size (bp)	Primers	Location
Rat Itpr1	NM_001007235	355	For: 5'-AACTGTGGGACCTTCACCAG-3' Rev: 5'-GCCCACAATTGAGAACAGGT-3'	7449-7703
Rat Itpr2	NM_031046	335	For: 5'-CGCCTTGATTCTGAGTGACA-3' Rev: 5'-ATCATCTCCTCCCTCCTCGT-3'	6303-6537
Rat Itpr3	NM_013138	324	For: 5'-AAGACCGAGGTGGAAACCTT-3' Rev: 5'-TCGATGCTGAGGTACTCGTG-3'	1968-2191

Table 2. shRNA oligonucleotide sequences for Itpr1 and Itpr3

Gene	Accession No.	Hairpin oligonucleotide sequences (5'-3') target sequence printed in bold	Location
Rat Itpr1	NM_001007235	For:5' GATCCCC**CCAAGCTTTGCTACATAAATT**CA AGAGATTTATGTAGCAAAGCTTGGTTTTTA-3' Rev:5'AGCTTAAAAACCAAGCTTTGCTACATAAATCTCT TGAATTTATGTAGCAAAGCTTGGGGG-3'	4082
Scr-IP_3R1		For:5'GATCCCCGAATAACTGGAGAGGCTATGACAA GAGATCATAGCCTCTCCAGTTATTCTTTTTA 3' Rev:5'AGCTTAAAAAGAATAACTGGAGAGGCTATG ATCTCTTGTCATAGCCTCTCCAGTTATTCGGG 3'	
Rat Itpr3	NM_013138	For:5'-GATCCCC**GAACATCATTGAGAAGTTATT**CA AGAGATAACTTCTCAATGATGTTCTTTTTA-3' Rev:5'AGCTTAAAAAGAACATCATTGAGAAGTTATCTCT TGAATAACTTCTCAATGATGTTCGGG-3'	4901
Scr-IP_3R3		For:5'GATCCCCGCTGGAAGATCAACTTATTCACAA GAGATGAATAAGTTGATCTTCCAGCTTTTTA 3' Rev:5'AGCTTAAAAAGCTGGAAGATCAACTTATTCA TCTCTTGTGAATAAGTTGATCTTCCAGCGGG 3'	

Results

Expression of IP_3-receptor genes in NRK fibroblasts

We have previously shown that $PGF_{2\alpha}$ is able to induce sustained Ca^{2+} oscillations in quiescent NRK cells (Harks, Scheenen et al. 2003). In order to understand which role the various IP_3R subtypes play in this process, we first studied the expression of their genes by RT-PCR analysis. Figure 1A shows that NRK cells express the genes encoding IP_3R1 (*Itpr1*) and IP_3R3 (*Itpr3*), but not the gene encoding IP_3R2 (*Itpr2*). In contrast, control rat brain tissue contained mRNA for all three IP_3R genes. The expected PCR product sizes of 355bp for *Itpr1* and 324bp for *Itpr3* were confirmed by gel electrophoresis. Furthermore, the nature of the PCR products was identified by DNA sequencing and found in agreement with the original GenBank sequences. For our further studies on NRK fibroblasts we therefore focused specifically on the roles of IP_3R1 and IP_3R3.

In order to test if the expression of IP_3R1 and IP_3R3 depends on the growth stage of the NRK cells, we used quantitative RT-PCR analysis and Western blot analysis. At the mRNA level expression of the IP_3R1 gene was reduced by 43% (Figure 1B) and that of the IP_3R3 gene by 13% (Figure 1C), when quiescent NRK cells were grown for an additional cell cycle to induce density-arrest. Figures 1D and 1E show that also at the protein level expression of the two IP_3R subtypes was reduced (by 33% in the case of IP_3R1 and 10% for IP_3R3), when quiescent cells were grown to density-arrest. These data show that expression of the IP_3R1 and IP_3R3 genes is differently regulated with increasing density in NRK cells.

Calcium oscillations in NRK cells are growth stage dependent

$PGF_{2\alpha}$-induced Ca^{2+} oscillations in NRK cells are generally characterized by an initial large Ca^{2+} transient, which is often followed by secondary repetitive oscillations that appear as large sharp transients. Between different cells within the same monolayer culture, however, Ca^{2+} oscillations may greatly differ with respect to their amplitude and frequency (see examples in Figure 2A). Analysis of 225 cells in five independent monolayer cultures revealed that the $PGF_{2\alpha}$-induced cellular Ca^{2+} responses can be divided best into four categories, characterized by the number of oscillations after the initial transient, as follows: (i) no secondary transients; (ii) one to four; (iii) five to eight; (iv) nine or more secondary Ca^{2+} transients per 15 min (see Figure 2B).

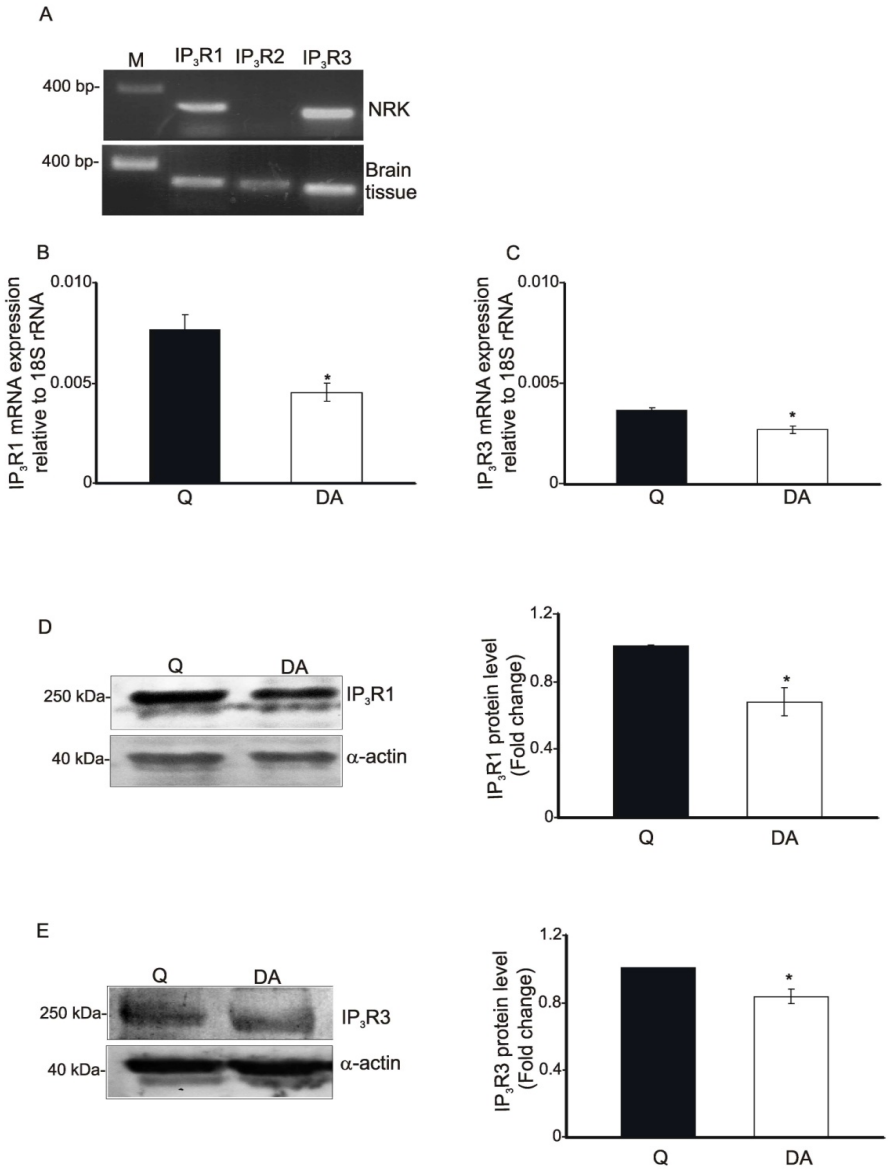

Fig. 1. Expression of IP_3R subtypes in NRK fibroblasts. (A) Reverse transcription polymerase chain reaction (RT-PCR) analysis for the rat IP_3R1 (*Itpr1*), IP_3R2 (*Itpr2*) and IP_3R3 (*Itpr3*) genes in NRK cells and whole brain extract as a positive control using subtype-specific primers (table 1). Single band products were identified in brain tissue for the IP_3R1, IP_3R2 and IP_3R3 genes of the expected size, whereas in NRK cells only expression of the IP_3R1 and IP_3R3, but not of the IP_3R2 gene was observed. M denotes the marker for the base-pair length. Real-time quantitative PCR analysis of growth stage-dependent expression of the IP_3R1 (B) and the IP_3R3 (C) gene in NRK fibroblasts, relative to 18S rRNA. mRNA expression levels of IP_3R1 and IP_3R3 in quiescent (Q) (black bar) and density-arrested (DA) (white bar) NRK fibroblasts. Data are represented as mean ± S.E.M (significance: *, $p<0.05$, n=3). (D) and (E) Western blots of IP_3R1 and IP_3R3 protein levels in NRK cells at the quiescent (Q) and density-arrested (DA) stage of growth. Whole cell lysates were blotted and stained with specific antibodies against rat IP_3R1 (D left) and IP_3R3 (E left), whereby staining with antibodies against rat α-actin (α-actin) was used as a loading control. Densitometric

analysis of IP_3R1 protein and IP_3R3 protein signal in quiescent (Q) and density-arrested (DA) cells is shown in (D right) and (E left), respectively. Data were plotted as a fold change relative to the mean intensity of quiescent stage according to procedures described in Materials and Methods. Data are representative of 3 independent experiments.

The presented data show that the majority of quiescent cells (62%) show 5-8 secondary transients after stimulation with 100 nM $PGF_{2\alpha}$, while most density-arrested cells (48%) fall in the category 1-4 secondary transients. Figure 2C shows in a box-plot that for quiescent cells the number of Ca^{2+} oscillations per 15 min corresponds to a median of 6 (90% range 2-11; n=228), which is significantly higher than for density-arrested cells with a median of 3 (90% range 0-7; n=180). These data show that quiescent and density-arrested NRK cells differ in the frequency of $PGF_{2\alpha}$-induced Ca^{2+} oscillations.

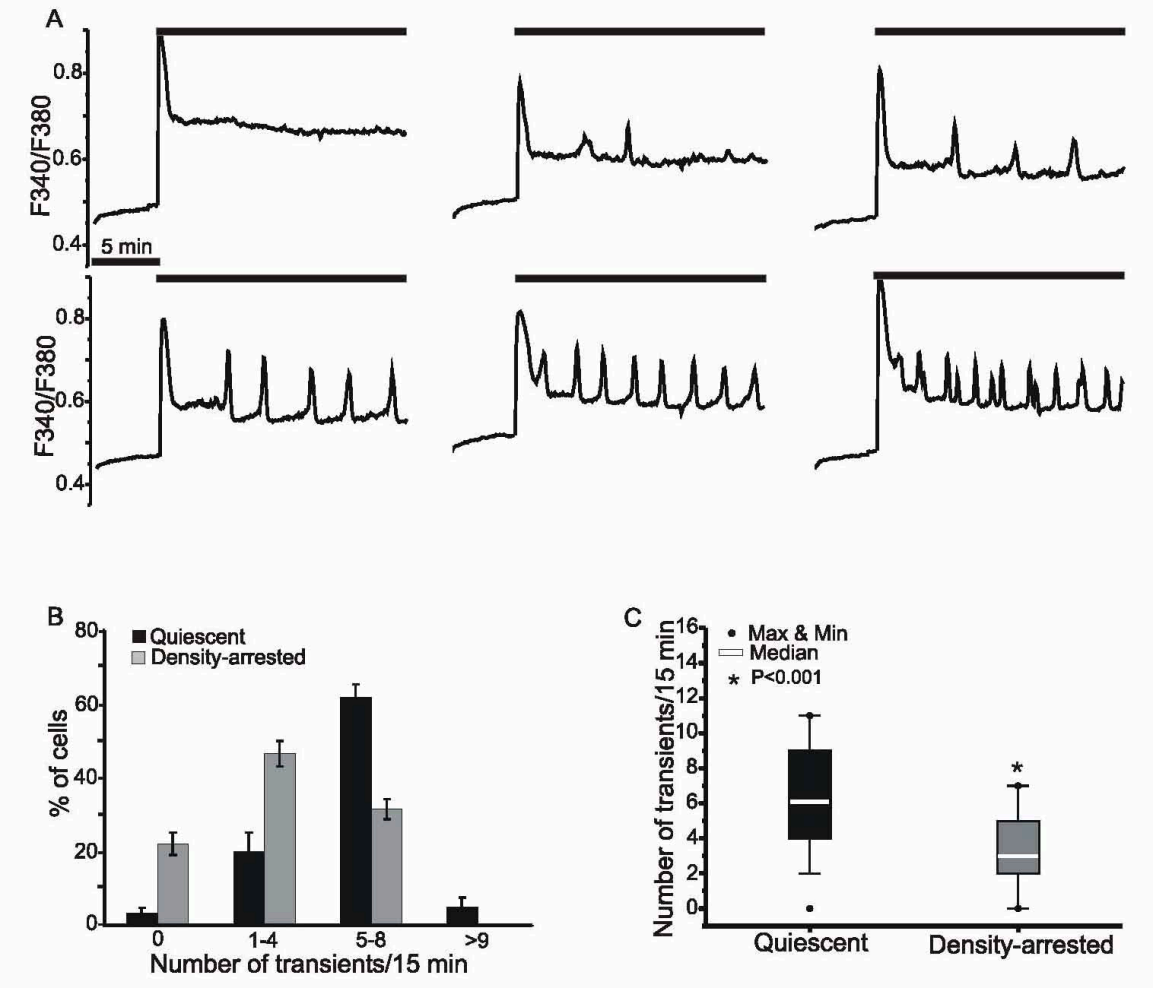

Fig. 2. Quiescent and density-arrested NRK cells exhibit different frequencies of $PGF_{2\alpha}$-induced Ca^{2+} oscillations. (A) Typical cellular responses of six individual cells with different frequency of Ca^{2+} oscillations within the same monolayer of quiescent (Q) NRK cells, as measured by dynamic Ca^{2+} video

imaging upon stimulation with 100 nM $PGF_{2\alpha}$. The presence of $PGF_{2\alpha}$ is indicated by the upper black bar and time (5 min) by the lower black bar. (B) Classification of the number of Ca^{2+} oscillations within 15 min after the initial peak response of a cell. Percentage of cells showing no secondary response after the initial peak response, one to four, five to eight and nine or more Ca^{2+} oscillations in quiescent (Q) (black bar) and density- arrested (DA) (grey bar) NRK cells. (C) Box plots depicting the median and distribution of $PGF_{2\alpha}$–induced Ca^{2+} oscillations per 15 min in quiescent (Q) (black box) and density-arrested (DA) (grey box) NRK cells. Boxes represent the 25th and 75th percentiles, while the whiskers determine the 5th and 95th percentiles.

Knockdown of individual IP_3-receptor subtype genes in NRK fibroblasts

The above data show that upon growth of NRK cells from a quiescent state to density-arrested state, the expression of particularly IP_3R1 is reduced and that concomitantly the frequency of $PGF_{2\alpha}$-induced Ca^{2+} oscillations is reduced. In order to test if a causal relation exists between these two phenomena, we knocked down the expression of the IP_3R1 and IP_3R3 receptor genes and studied the effect on the frequency of $PGF_{2\alpha}$- induced Ca^{2+} oscillations in both quiescent and density-arrested NRK cells. Quantitative RT-PCR analysis shows that knockdown of *Itpr1* in NRK cells resulted in a 65% reduction of its mRNA level (Figure 3A light gray bar), while knockdown of *Itpr3* resulted in a 60% reduction in mRNA level (Figure 3B light gray bar). No reduction in IP_3R1 and IP_3R3 receptor gene expression was observed if NRK cells were infected with empty vector and scrambled shRNAs (Figure 3A and 3B; black and dark gray bar respectively). Moreover, no effect of the *Itpr1*-directed shRNA was observed on IP_3R3 receptor gene expression, and vice versa compared to empty vector and scrambled shRNA (Figure 3A and 3B; white bar). Western blot analysis revealed a similar degree of suppression of individual IP_3R proteins (Figures 3C and 3D). These data show that expression of IP_3R1 and IP_3R3 can be efficiently and selectively reduced in NRK cells.

Effect of knockdown of IP_3-receptor subtype genes on the $PGF_{2\alpha}$-induced Ca^{2+} oscillations in NRK cells

Figure 4A shows examples of $PGF_{2\alpha}$-induced Ca^{2+} oscillations in quiescent NRK cells in which either *Itpr1* or *Itpr3* has been knocked down. Reduction of IP_3R1 gene expression resulted in a lower frequency of $PGF_{2\alpha}$- induced Ca^{2+} oscillations, while knockdown of the IP_3R3 gene tended to increase the frequency of these oscillations. Figure 4B shows that

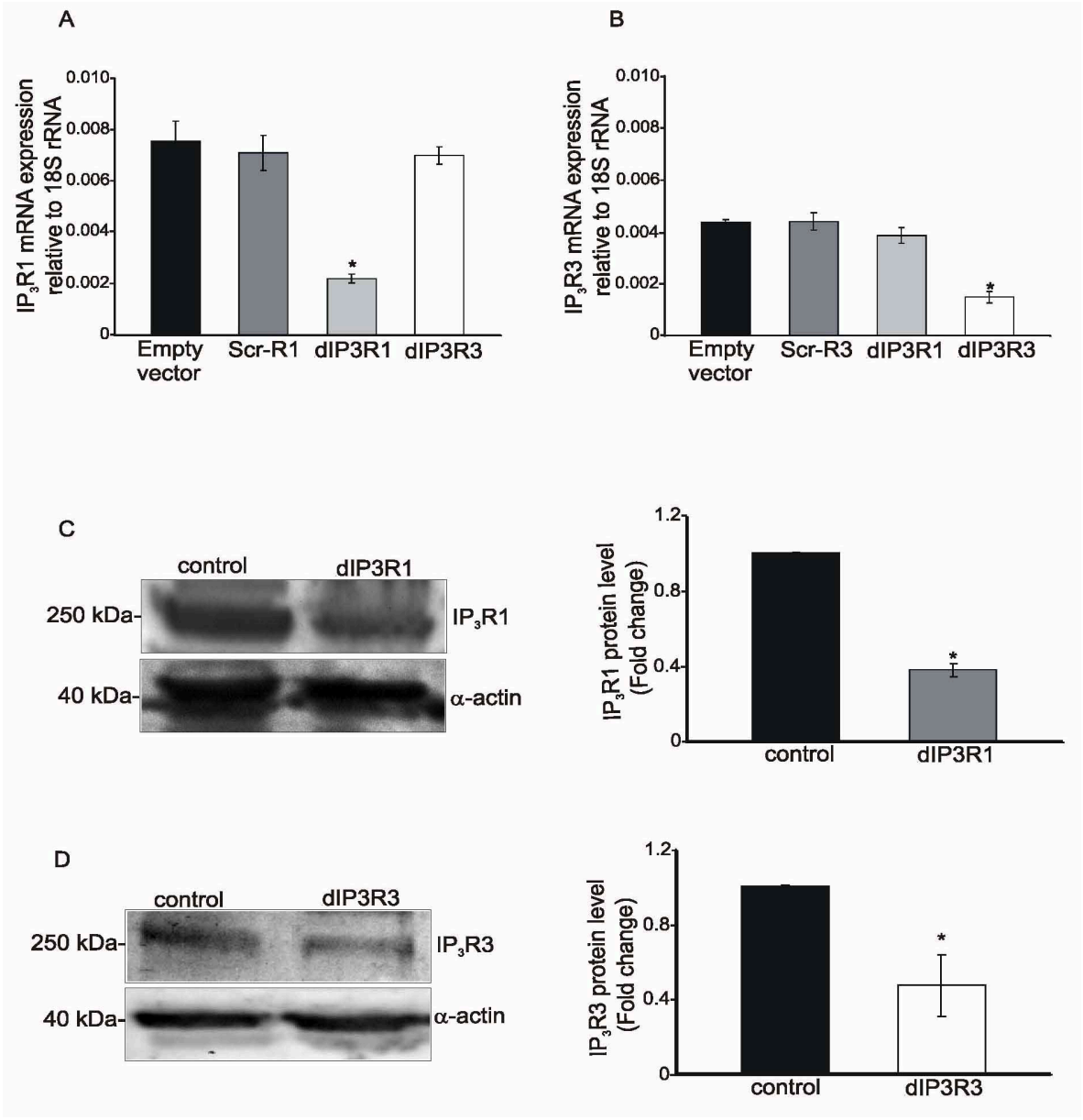

Fig. 3. Assessment of *Itpr1* and *Itpr3* knockdown by shRNA. (A and B) Quantitative PCR analysis of shRNA-mediated reduction on the *Itpr1* and *Itpr3* mRNA levels in NRK cells stably transfected with *Itpr1* specific shRNA vector (dIP3R1 cells), *Itpr3* specific shRNA vector (dIP3R3 cells) scrambled IP3R1-shRNA (Scr-R1), scrambled IP3R3-shRNA (Scr-R3) and empty vector (control cells), respectively. Expression values are represented as mean ± SEM (significance: *, $p<0.05$, n=4). (C and D; right) Western blots of the expression of IP_3R1 and IP_3R3 in control cells, dIP3R1 and dIP3R3 cells, respectively. Staining with antibodies against rat α-actin (α-actin) was used as a loading control. (C and D; right) Densitometric analysis of the corresponding Western blots, plotted as a fold change relative to the mean intensity of the control, as described under Materials and Methods. Data are representative of 3 independent experiments.

control cells mostly gave rise to 5-8 oscillations/15 min, while *Itpr1* knockdown cells (dIP3R1) mainly fell in the category of 1-4, and the *Itpr3* knockdown cells (dIP3R3) in the category 9-14 oscillations/15 min. Figure 4C shows box-plots for the significant differences in the distribution of the number of Ca^{2+} oscillations per 15 min, resulting for control cells in a median of 6 (90% range 2-11; n=228), for dIP3R1 cells in a median of 4 (90% range 0-9; n=200), and for dIP3R3 cells in a median of 8 (90% range 3-13; n=225). Interestingly, the distribution of Ca^{2+} oscillations in dIP3R1 cells is very similar and statistically not different (p=0.5) from that of the density-arrested wild-type cells. This suggests that the reduced frequency of Ca^{2+} oscillations in density-arrested cells indeed results from a reduced expression of IP_3R1.

Similar studies in density-arrested NRK cells (see Figure 5) also showed that knockdown of the IP_3R1 gene resulted in a significant reduction, and knockdown of the IP_3R3 gene in a significant increase in the frequency of $PGF_{2\alpha}$-induced Ca^{2+} oscillations (n=180 for all three analyses). For a proper comparison of the $PGF_{2\alpha}$-induced Ca^{2+} oscillations in the two growth stages, these oscillations were measured in the presence of 1 μM nifedipine in order to prevent the disturbance of the Ca^{2+} oscillations in density-arrested cells by the action potential-associated repetitive influx of Ca^{2+} via voltage-dependent L-type Ca^{2+} channels. Figure 5C shows box-plots summarizing the variation of Ca^{2+} oscillations per 15 min, resulting for control cells in a median of 4 (90% range 0-7; n=180), for dIP3R1 cells in a median of 3 (90% range 0-6; n=180), and for dIP3R3 cells in a median of 7 (90% range 2-11; n=180). In conclusion, our data show that IP_3R1 enhances and IP_3R3 decreases the frequency of Ca^{2+} oscillations in NRK cells.

Role of IP_3R1 and IP_3R3 in the generation of action potentials in density-arrested NRK cells

We have previously shown that density-arrested NRK cells exhibit spontaneous periodic Ca^{2+} action potentials (De Roos, Van Zoelen et al. 1997), which result from the concerted activity of an L-type calcium channel, a calcium-activated chloride channel and an inward rectifying potassium channel. Instantaneous depolarization occurs upon opening of the L-type Ca^{2+} channel, a process that is enforced in the presence of strontium ions (De Roos, Van Zoelen et al. 1997; Harks, Torres et al. 2003). These action potentials propagate through the monolayer at a speed of 0.6 cm/sec, resulting in near synchronous Ca2+ tran-

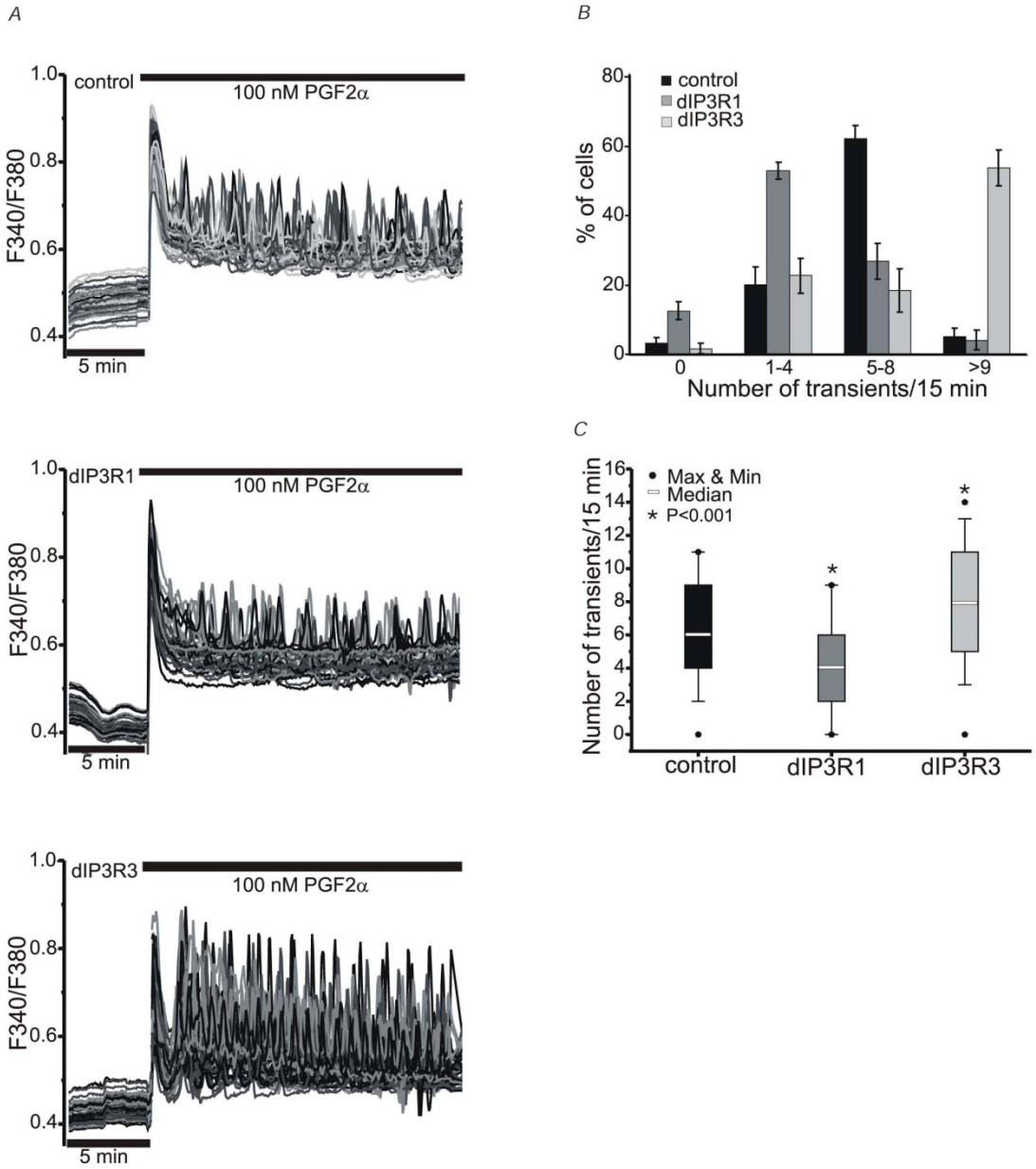

Fig. 4. Effect of *Itpr1* and *Itpr3* knockdown on PGF2α-induced Ca^{2+} oscillations in quiescent NRK cells. (A) Typical calcium responses of control (top), dIP3R1 (middle) and dIP3R3 (down) quiescent NRK cells upon stimulation with 100 nM $PGF_{2\alpha}$. In each panel the responses of 45 individual cells are shown. The presence of $PGF_{2\alpha}$ is indicated by the upper black bar and time (5 min) by the lower black bar. (B) Classification of Ca^{2+} oscillations within 15 min after the initial peak. Percentage of cells showing no calcium response, one to four, five to eight and nine or more oscillations for control (black bar), dIP3R1 (grey bar) and dIP3R3 cells (light grey bar), respectively. (C) Box plots depicting the median and distribution of $PGF_{2\alpha}$-induced Ca^{2+} oscillations per 15 min in control cells (black box), dIP3R1 cells (grey box) and dIP3R3 cells (light grey box). Boxes represent the 25^{th} and 75^{th} percentiles, while the whiskers determine the 5^{th} and 95^{th} percentiles.

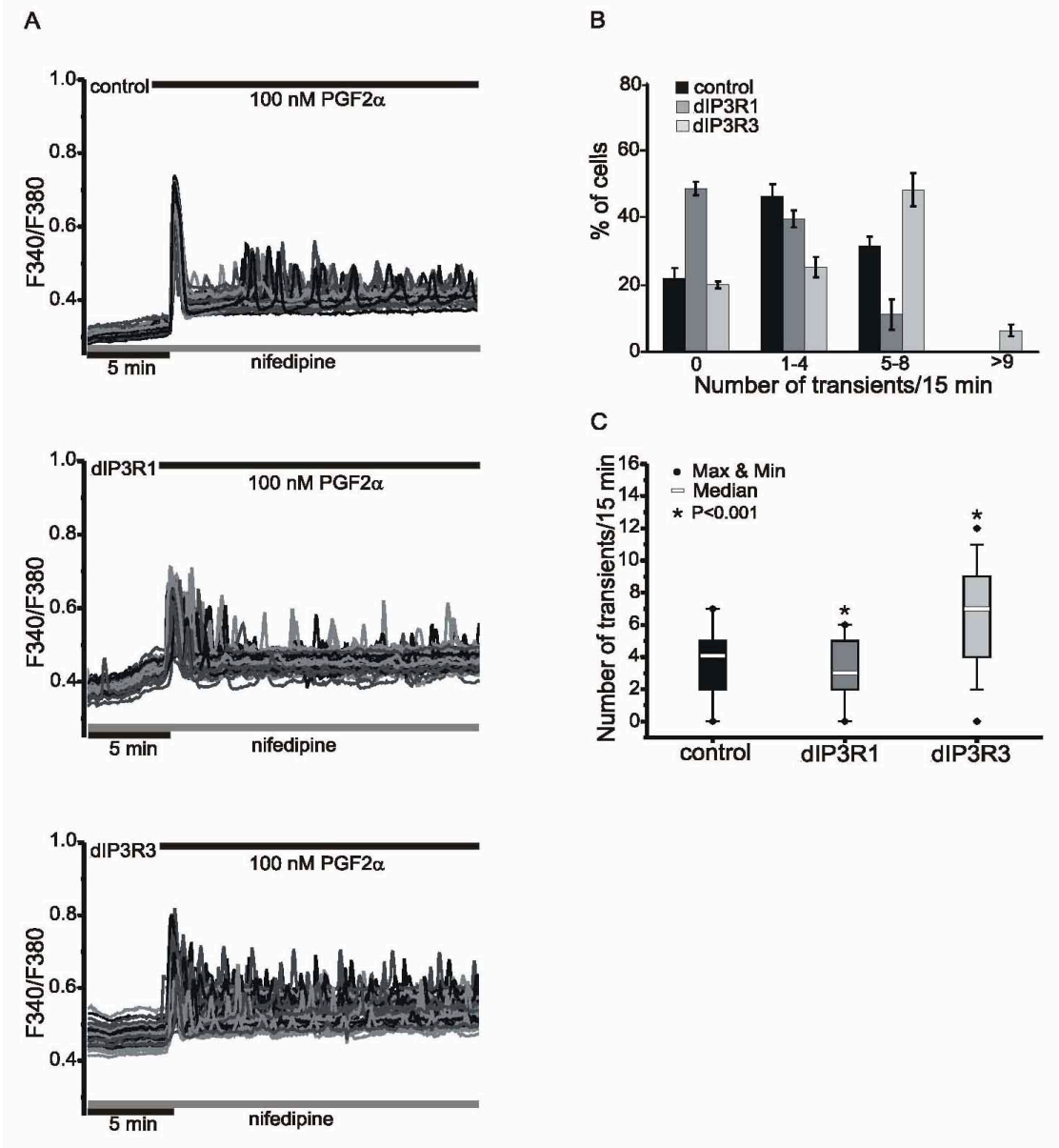

Fig. 5. **Effect of *Itpr1* and *Itpr3* knockdown on PGF2α-induced Ca^{2+} oscillations in density-arrested NRK cells.** (A) Typical calcium responses of control (top), dIP3R1 (middle) and dIP3R3 (down) density-arrested NRK cells upon stimulation with 100 nM $PGF_{2\alpha}$ in the presence of 1 μM nifedipine. In each panel the responses of 45 individual cells are shown. The presence of $PGF_{2\alpha}$ is indicated by the upper black bar, the presence of nifedipine by the lower grey bar and the time (5 min) by the lower black bar. (B) Classification of Ca^{2+} oscillations within 15 min after the initial peak. Percentage of cells showing no calcium response, one to four, five to eight and nine or more oscillations for control cells (black bar), dIP3R1 cells (grey bar) and dIP3R3 cells (light grey bar), respectively. (C) Box-plots depicting the median and distribution of $PGF_{2\alpha}$–induced Ca^{2+} oscillations per 15 min in control cells (black box), dIP3R1 cells (grey box) and dIP3R3 cells (light grey box). Boxes represent the 25^{th} and 75^{th} percentiles, while the whiskers determine the 5^{th} and 95^{th} percentiles.

-sients in all cells of the monolayer. Based on our observation that growing NRK cells produce and secrete $PGF_{2\alpha}$, particularly upon phenotypic transformation (Harks, Peters et al. 2005), we have postulated that locally enhanced production of $PGF_{2\alpha}$ in density-arrested NRK fibroblasts induces Ca^{2+} oscillations, which generate a pacemaker activity that is required for the induction of propagating action potentials in the remainder of cells in the monolayer (Harks 2003). According to this hypothesis, the periodicity of action potential firing will depend on the frequency of the $PGF_{2\alpha}$-induced Ca^{2+} oscillations in the pacemaker cells. Since this latter process is controlled by the various IP_3-receptor subtypes, we have tested the above hypothesis by studying the effect of knockdown of *Itpr1* and *Itpr3* on the frequency of spontaneous action potential firing in cultures of density-arrested NRK cells.

Figure 6A shows synchronous Ca^{2+} transients in density-arrested control cells, dIP3R1 cells and dIP3R3 cells, which result from periodic spontaneous Ca^{2+} action potentials in these cells. In dIP3R1 cells, in which *Itpr1* has been knocked down, the number of Ca^{2+} transients per 15 min (median 5; range 4-6; n=5) was lower ($p<0.03$) than in control cells (median 7; range 5-8; n=5), while in dIP3R3 cells, in which *Itpr3* has been knocked down, the frequency (media 9; range 7-11; n=5) was higher ($p<0.05$) than in control cells. These data indicate that the frequency of Ca^{2+} action potentials in density-arrested NRK cells is reduced upon knockdown of the IP_3R1 gene, and enhanced upon knockdown of the IP_3R3 gene.

Comparable results were observed if the propagation of action potentials was measured in a single follower cell by patch-clamp technology. Figure 6B shows that a reduced frequency was observed in dIP3R1 cells, and an enhanced frequency in dIP3R3 cells. Since the propagation of Ca^{2+} action potentials in NRK cells occurs independently of IP_3-signaling, the observed effects must result from the effects of IP_3-receptor subtypes on the processes that underlie the generation of such action potentials in the pacemaker cells.

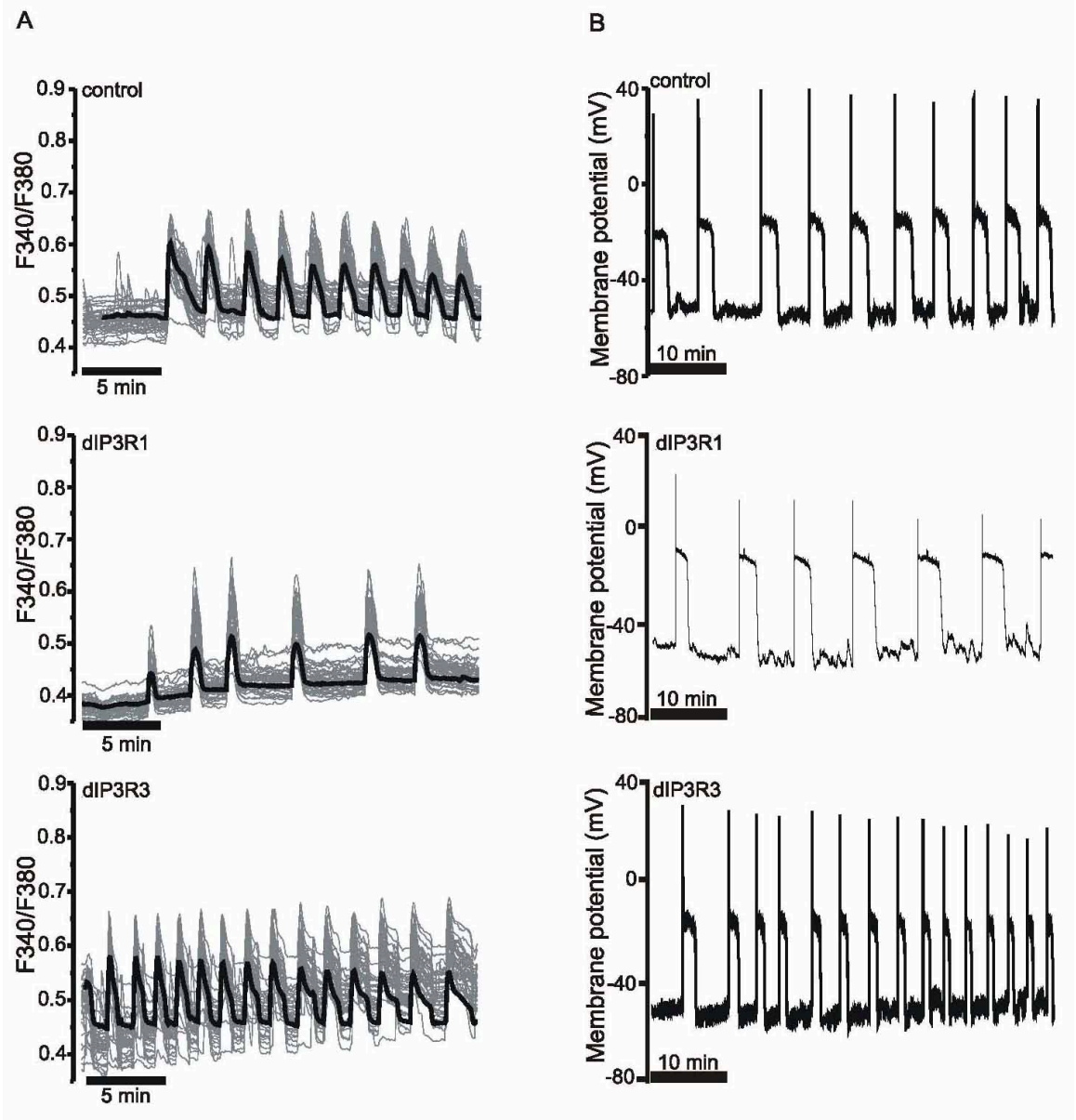

Fig. 6. Effect of *Itpr1* and *Itpr3* knockdown on the spontaneous synchronized Ca^{2+}/Sr^{2+} transients and action potentials in density-arrested NRK cells. (A) Typical examples of spontaneous synchronous repetitive Ca^{2+} transients in density-arrested control cells (top), dIP_3R1 (middle) and dIP_3R3 (down) NRK cells, respectively. Cells were loaded with Fura-2 in order to measure changes in intracellular Ca^{2+} concentration. A typical response of 45 cells is displayed (n=5 experiments). Individual traces are shown in grey, while the mean response is shown in black. Time (5 min) is indicated by lower black bar. (B) Typical patch-clamp measurements of spontaneous action potential firing by density-arrested control cells (top), dIP_3R1 (middle) and dIP_3R3 (down) NRK cells. Time (5 min) is indicated by lower black bar. Membrane potential was recorded in the current clamp mode of the whole cell patch-clamp technique during continuous perfusion with Sr^{2+}- HBS medium.

Discussion

In the present study we have shown that NRK cells express the IP_3-receptor (IP_3R) subtypes IP_3R1 and IP_3R3. The expression of these receptors varied as a function of the growth status of NRK cells, such that particularly the expression of IP_3R1 was reduced when quiescent cells were grown to density-arrest. The observation that the frequency of $PGF_{2\alpha}$-induced Ca^{2+} oscillations in these cells was also reduced upon growing these cells from the quiescent to the density-arrested stage, prompted us to investigate the role of the various IP_3R subtypes in this process. Knockdown of the IP_3R1 gene resulted in reduced, while knockdown of the IP_3R3 gene resulted in an enhanced frequency of $PGF_{2\alpha}$-induced Ca^{2+} oscillations in cells at both growth stages. These data indicate that the reduction in the frequency of $PGF_{2\alpha}$-induced Ca^{2+} oscillations, which is observed when quiescent NRK cells are grown to density-arrest, most likely results from the reduction in expression of the IP_3R1 receptor, relative to IP_3R3. Moreover, our observation that knockdown of either the IP_3R1 or IP_3R3 gene affected the frequency of spontaneous Ca^{2+} action potentials in density-arrested NRK cells provides the first direct evidence that IP_3-mediated Ca^{2+} oscillations actually do control the activity of the pacemaking cells that generate these action potentials.

In NRK monolayer individual cells respond to the stimulation with $PGF_{2\alpha}$ by displaying a variable Ca^{2+} oscillation frequency and this variation in Ca^{2+} oscillation frequency still persists after the knockdown of respective IP_3R subtypes. This suggests that there are more factors besides the expression level of IP_3Rs that modulate calcium signaling in these cells. In an earlier study we found that a high concentration of ryanodine (50 μM), an inhibitor of ryanodine-sensitive (i.e. cyclic ADP-ribose (cADPR)-sensitive) calcium stores, was without effect on the frequency of Ca^{2+} oscillations induced by $PGF_{2\alpha}$ in quiescent NRK cells (Harks 2003)**.** That observation would suggest that then $PGF_{2\alpha}$–induced Ca^{2+} oscillations in NRK cells are also not much affected by eventual variations in ryanodine receptor expression. On the other hand, recently we discovered that changes in calcium dynamics upon growing quiescent NRK cells to density-arrest particularly coincide with a regulation of the expression and activity of Trpc5, Trpc6 and Orai1 calcium channels, as well as of the calcium sensor Stim1 (Dernison, Almirza et al.). These findings suggest that in addition to a modulation of the expression of IP_3R subtypes, also that of calcium sensor Stim1 and the calcium entry channels Trpc5, Trpc6 and Orai1

contribute to the growth stage-dependent differences in the $PGF_{2\alpha}$-induced Ca^{2+}oscillations. We are currently testing this hypothesis by using a shRNA approach to selectively knockdown the genes for these proteins.

Our data show that normal rat kidney fibroblasts express IP_3R1 and IP_3R3, but not IP_3R2. Monkawa et al. (Monkawa, Hayashi et al. 1998) have shown that in the rat kidney IP_3R1 is expressed in the glomerular mesangial cells and vascular smooth muscle cells, while IP_3R2 is exclusively expressed in intercalated cells of the collecting ducts from the cortex to the inner medulla, and IP_3R3 is expressed in the vascular smooth muscle cells, glomerular mesangial cells, and some cells of cortical collecting ducts, probably principal cells. These data show that expression of IP_3-receptor subtypes is cell type specific. Others studies have provided evidence for the importance of Ca^{2+}-release channels, particularly IP_3Rs, in the spontaneous electrical activity of interstitial cells of Cajal (ICCs) and myocytes (Mackenzie, Bootman et al. 2002; Liu, Ohya et al. 2005; McHale, Hollywood et al. 2006; Kapur and Banach 2007; Domeier, Zima et al. 2008), but a specific role for the various IP_3R subtypes has not been studied in these systems.

The present results show that the IP_3-receptor subtypes expressed in NRK cells have a different role in shaping the Ca^{2+} signal induced by $PGF_{2\alpha}$. We show that a low expression level of IP_3R1 results in reduction or even disappearance of Ca^{2+} oscillations, whereas lowering of IP_3R3 expression is associated with an increase in the Ca^{2+} oscillations with high amplitude. This means that Ca^{2+} oscillations induced by $PGF_{2\alpha}$ seem to be dependent on a sufficient expression level of IP_3R1. Our results are in line with those of Hattori et al. (Hattori, Suzuki et al. 2004), who showed that knockdown of the IP_3R1 gene in HeLa cells decreased the total Ca^{2+} signalling, whereas knockdown of the IP_3R3 gene increased the frequency of Ca^{2+} oscillations. It has been established that IP_3R1 is more sensitive to $[IP_3]$ than IP_3R3 (Missiaen, Parys et al. 1998; Miyakawa, Maeda et al. 1999; Hagar and Ehrlich 2000), which implies that IP_3R1 can be activated by a lower $[IP_3]$ than IP_3R3. Second, the open probability of IP_3R1 is decreased by a high Ca^{2+} concentration, whereas IP_3R3 is less sensitive to increased Ca^{2+} concentrations, and may in fact not be inactivated at all by elevated Ca^{2+} (Bezprozvanny, Watras et al. 1991; Finch, Turner et al. 1991). As a result IP_3R1 will inactivate more rapidly upon an increase of the intracellular Ca^{2+} concentration than IP_3R3. Probably, the recovery from inactivation by elevated Ca^{2+} also occurs more rapidly in IP_3R1 than in IP_3R3.

Dupont and Combettes (Dupont and Combettes 2006) have modelled the effect of different combinations of IP_3- receptor subtypes on Ca^{2+} oscillations. Based on the steady state activity curve of each subtype, they concluded that receptors with a classical "bell-shaped curve" (IP_3R1) generate the most robust oscillations, whereas receptors with a sigmoidal dependence of activity on the Ca^{2+} concentration (IP_3R3) cannot sustain oscillations. Also the range of IP_3-receptor subtype expression levels and the IP_3-concentrations that allow Ca^{2+} oscillations are more restricted for sigmoidal than for the bell-shaped receptors. Moreover, systems that combine sigmoidal and bell-shaped receptors tend to have less robust oscillations, because they are prone to reach an elevated intracellular Ca^{2+} concentration that prevents the reactivation of Ca^{2+}-induced Ca^{2+} release. This conclusion agrees mostly with our results and that of Hattori et al. (Hattori, Suzuki et al. 2004), such that we see a reduction in Ca^{2+} oscillations without a significant elevation of $[Ca^{2+}]_i$ concentration. Our observation that the oscillation frequency is higher in the dIP3R3 than in the control cells agrees with observations by Hattori et al. (Hattori, Suzuki et al. 2004) on Hela and COS-7 cells. It therefore appears that IP_3R1 exerts a pro-oscillatory and IP_3R3 an anti-oscillatory effect on cytosolic Ca^{2+}. However, our results do not agree with those of Foskett et al. (Foskett, White et al. 2007), who showed that Xenopus IP_3R1 and IP_3R3 have other probability curves with much higher maximum open probabilities. Their experiments show that Xenopus IP_3R1 is a sigmoidal and rat IP_3R3 a bell-shaped receptor, exactly the opposite from our conclusions on NRK cells.

We have previously postulated that propagation of action potentials in density-arrested NRK fibroblast monolayers is generated by a pacemaker area, which shows elevated levels of intracellular IP_3 due to locally enhanced secretion of $PGF_{2\alpha}$ in these cultures (Harks, Peters et al. 2005). Recently, we have shown that localized administration of $PGF_{2\alpha}$ (inside a small ring placed on a monolayer of quiescent NRK cells) generates an artificial pacemaker that exhibits Ca^{2+} oscillations in the cells under the ring, which periodically induces propagating Ca^{2+} action potentials in the follower cells outside the ring (Dernison, Kusters et al. 2008). In the present study, we show that the knockdown of individual IP_3-receptor subtype genes has the same effect on spontaneous propagating action potentials in density-arrested monolayer of NRK fibroblasts as it has on $PGF_{2\alpha}$-induced Ca^{2+} oscillations. In our view, the 'pacemaker' cells in the monolayer experience a locally elevated concentration of $PGF_{2\alpha}$ that induce a Ca^{2+} oscillation [31], which in its turn activates the Ca^{2+}-dependent Cl-channels to depolarize these cells. This depolarization is

then electrically propagated to 'follower' cells that react by the firing of action potentials using their L-type Ca^{2+} channels. These data are the first experimental support for the hypothesis that IP_3-receptor mediated Ca^{2+}-oscillations provides NRK cells a timing mechanism for periodic action potential firing in the density-arrested stage of growth.

Acknowledgements

We gratefully thank Dr. Jeroen van Leeuwen (Department of Cell Biology, Radboud University Nijmegen) for his interest and valuable advices during the course of this study. This research project was funded in part by the Physical Biology Research Program (No. 805.47.066) of the Stichting voor Fundamenteel Onderzoek der Materie (FOM) and the Gebiedsbestuur Aard en Levenswetenschappen (ALW), which are financially supported by the Netherlands Organization for Scientific Research (NWO).

References

Berridge, M. J. (1993). "Inositol trisphosphate and calcium signalling." Nature **361**(6410): 315-325.

Berridge, M. J., M. D. Bootman, et al. (2003). "Calcium signalling: dynamics, homeostasis and remodelling." Nat Rev Mol Cell Biol **4**(7): 517-529.

Bezprozvanny, I., J. Watras, et al. (1991). "Bell-shaped calcium-response curves of Ins(1,4,5)P3- and calcium-gated channels from endoplasmic reticulum of cerebellum." Nature **351**(6329): 751-754.

Bradford, M. M. (1976). "A rapid and sensitive method for the quantitation of microgram quantities of protein utilizing the principle of protein-dye binding." Anal Biochem **72**: 248-254.

Chen, C. and H. Okayama (1987). "High-efficiency transformation of mammalian cells by plasmid DNA." Mol Cell Biol **7**(8): 2745-2752.

Clapham, D. E. (1995). "Calcium signaling." Cell **80**(2): 259-268.

De Roos, A. D., E. J. Van Zoelen, et al. (1997). "Membrane depolarization in NRK fibroblasts by bradykinin is mediated by a calcium-dependent chloride conductance." J Cell Physiol **170**(2): 166-173.

de Roos, A. D., P. H. Willems, et al. (1997). "Synchronized calcium spiking resulting from spontaneous calcium action potentials in monolayers of NRK fibroblasts." Cell Calcium **22**(3): 195-207.

Dernison, M. M., W. H. Almirza, et al. "Growth-dependent modulation of capacitative calcium entry in normal rat kidney fibroblasts." Cell Signal.

Dernison, M. M., J. M. Kusters, et al. (2008). "Local induction of pacemaking activity in a monolayer of electrically coupled quiescent NRK fibroblasts." Cell Calcium.

Dolmetsch, R. E., R. S. Lewis, et al. (1997). "Differential activation of transcription factors induced by Ca2+ response amplitude and duration." Nature **386**(6627): 855-858.

Dolmetsch, R. E., U. Pajvani, et al. (2001). "Signaling to the nucleus by an L-type calcium channel-calmodulin complex through the MAP kinase pathway." Science **294**(5541): 333-339.

Domeier, T. L., A. V. Zima, et al. (2008). "IP3 receptor-dependent Ca2+ release modulates excitation-contraction coupling in rabbit ventricular myocytes." Am J Physiol Heart Circ Physiol **294**(2): H596-604.

Dupont, G. and L. Combettes (2006). "Modelling the effect of specific inositol 1,4,5-trisphosphate receptor isoforms on cellular Ca2+ signals." Biol Cell **98**(3): 171-182.

Finch, E. A., T. J. Turner, et al. (1991). "Calcium as a coagonist of inositol 1,4,5-trisphosphate-induced calcium release." Science **252**(5004): 443-446.

Foskett, J. K., C. White, et al. (2007). "Inositol trisphosphate receptor Ca2+ release channels." Physiol Rev **87**(2): 593-658.

Hagar, R. E. and B. E. Ehrlich (2000). "Regulation of the type III InsP(3) receptor by InsP(3) and ATP." Biophys J **79**(1): 271-278.

Harks, E. G. (2003). Excitable Fibroblasts. Ph.D., Radboud University Nijmegen.

Harks, E. G., P. H. Peters, et al. (2005). "Autocrine production of prostaglandin F2alpha enhances phenotypic transformation of normal rat kidney fibroblasts." Am J Physiol Cell Physiol **289**(1): C130-137.

Harks, E. G., W. J. Scheenen, et al. (2003). "Prostaglandin F2 alpha induces unsynchronized intracellular calcium oscillations in monolayers of gap junctionally coupled NRK fibroblasts." Pflugers Arch **447**(1): 78-86.

Harks, E. G., J. J. Torres, et al. (2003). "Ionic basis for excitability of normal rat kidney (NRK) fibroblasts." J Cell Physiol **196**(3): 493-503.

Hattori, M., A. Z. Suzuki, et al. (2004). "Distinct roles of inositol 1,4,5-trisphosphate receptor types 1 and 3 in Ca2+ signaling." J Biol Chem **279**(12): 11967-11975.

Kapur, N. and K. Banach (2007). "Inositol-1,4,5-trisphosphate-mediated spontaneous activity in mouse embryonic stem cell-derived cardiomyocytes." J Physiol **581**(Pt 3): 1113-1127.

Liu, H. N., S. Ohya, et al. (2005). "Co-contribution of IP3R and Ca2+ influx pathways to pacemaker Ca2+ activity in stomach ICC." J Biol Rhythms **20**(1): 15-26.

Mackenzie, L., M. D. Bootman, et al. (2002). "The role of inositol 1,4,5-trisphosphate receptors in Ca(2+) signalling and the generation of arrhythmias in rat atrial myocytes." J Physiol **541**(Pt 2): 395-409.

McHale, N., M. Hollywood, et al. (2006). "Origin of spontaneous rhythmicity in smooth muscle." J Physiol **570**(Pt 1): 23-28.

Missiaen, L., J. B. Parys, et al. (1998). "Functional properties of the type-3 InsP3 receptor in 16HBE14o- bronchial mucosal cells." J Biol Chem **273**(15): 8983-8986.

Miyakawa, T., A. Maeda, et al. (1999). "Encoding of Ca2+ signals by differential expression of IP3 receptor subtypes." Embo J **18**(5): 1303-1308.

Monkawa, T., M. Hayashi, et al. (1998). "Localization of inositol 1,4,5-trisphosphate receptors in the rat kidney." Kidney Int **53**(2): 296-301.

Nathanson, M. H., A. D. Burgstahler, et al. (1995). "Ca2+ waves are organized among hepatocytes in the intact organ." Am J Physiol **269**(1 Pt 1): G167-171.

Wigler, M., S. Silverstein, et al. (1977). "Transfer of purified herpes virus thymidine kinase gene to cultured mouse cells." Cell **11**(1): 223-232.

CHAPTER 4

Growth-Dependent Modulation of Capacitative Calcium Entry in NRK Fibroblasts

Dernison MM, Almirza WH, Kusters JM, van Meerwijk WP, Gielen CC, van Zoelen EJ, Theuvenet AP

Cell Signal. 2010 Jul; 22(7): 1044-53

Abstract

Normal rat kidney (NRK) fibroblasts have electrophysiological properties and intracellular calcium dynamics that are dependent upon their growth stage. In the present study we show that this differential behavior coincides with a differential calcium entry that can be either capacitative or non-capacitative. Confluent cells made quiescent by serum deprivation, which have a stable membrane potential near –70 mV and do not show spontaneous intracellular calcium oscillations, primarily exhibit the capacitative mechanism for calcium entry, also called store-operated calcium entry (SOCE). When the quiescent cells are grown to density-arrest in the presence of EGF as the sole polypeptide growth factor, these cells characteristically fire spontaneously repetitive calcium action potentials, which propagate throughout the whole monolayer and are accompanied by intracellular calcium transients. These density-arrested cells appear to exhibit in addition to SOCE also receptor-operated calcium entry (ROCE) as a mechanism for calcium entry. Furthermore we show that, in contrast to earlier studies, the employed SOCs and ROCs are permeable for both calcium and strontium ions. We examined the expression of the canonical transient receptor potential channels (Trpcs) that may be involved in SOCE and ROCE. We show that NRK fibroblasts express the genes encoding Trpc1, Trpc5 and Trpc6, and that the levels of their expression are dependent upon the growth stage of the cells. In addition we examined the growth-stage dependent expression of the genes encoding Orai1 and Stim1, two proteins that have recently been shown to be involved in SOCE. Our results suggest that the differential expression of *Trpc5, Trpc6, Orai1 and Stim1* in quiescent and density-arrested NRK fibroblasts is responsible for the difference in regulation of calcium entry between these cells. Finally, we show that inhibition or potentiation of SOCE and ROCE by pharmacological agents has profound effects on calcium dynamics in NRK fibroblasts.

Introduction

There is currently a great interest in the cellular and molecular mechanisms that underlie store-operated calcium entry (SOCE). Upon release of intracellular calcium ions from stores in the endoplasmic reticulum (ER), calcium channels in the plasma membrane are opened, which results in an influx of calcium ions and a refilling of the intracellular stores. A breakthrough in the understanding of this process has come from the identification of the proteins Stim1 and Stim2 as sensors of Ca^{2+} within the ER. Stim proteins sense the depletion of Ca^{2+} from the ER, oligomerize, translocate to junctions adjacent to the plasma membrane, organize plasma membrane calcium channels into clusters and open these channels to bring about SOCE (Cahalan 2009; Putney 2009). Recent studies have identified particular members of the Orai and Trpc family as the plasma membrane calcium channels that are activated by this calcium-store depletion mechanism (Salido, Sage et al. 2009).

Although the components that play a role in store-operated calcium entry may have been identified, relatively few studies have functionally characterized this process under physiological conditions. Calcium entry into cells can take place through voltage-dependent calcium channels, including L-type and N-type channels, or through voltage-independent calcium channels. The latter group can be subdivided into store-operated calcium channels (SOCs) and receptor-operated calcium channels (ROCs). SOCs are activated by depletion of calcium stores after calcium-release, whereas ROCs are activated through PLC-coupled receptors involving second messengers such as diacylglycerol (DAG), inositol 1,4,5-trisphosphate (IP_3) and arachidonic acid (AA). Orai channels work according to a SOC mechanism, whereas certain members of the Trpc channel family operate as SOC, and others as ROC.

In a number of studies we have made a detailed characterization of the calcium homeostasis in normal rat kidney (NRK) fibroblasts as a function of their growth status (Harks, Scheenen et al. 2003; Harks, Peters et al. 2005). When cultured at high density in serum-free medium these cells become quiescent, which is characterized by a stable membrane potential near – 70 mV. Addition of prostaglandin $F_{2\alpha}$ ($PGF_{2\alpha}$) to such quiescent cells, which activates the G-protein-coupled $PGF_{2\alpha}$- receptor (Ptgfr), results in degradation of inositol lipids and the production of IP_3, which releases calcium ions from the ER by activation of the IP_3-receptor. This process results in calcium oscillations, which are uncorrelated between different cells, and is accompanied by depolarization of the cells to a

stable membrane potential of -20 mV. Upon addition of epidermal growth factor (EGF) and insulin to quiescent NRK cells, they can undergo one additional round of duplication, after which they stop proliferating as a result of density-dependent growth arrest. These density-arrested cells maintain a membrane potential near – 70 mV, but show in addition periodically propagating calcium action potentials during which cells temporarily depolarize to positive values as a result of the opening of L-type calcium channels.

In an integrated model of calcium fluxes in NRK cells, we have previously shown that constitutive activation of plasma membrane calcium channels is essential for long-term calcium oscillations in $PGF_{2\alpha}$-treated quiescent cells, as well as for periodic calcium action potentials in density-arrested cells (Kusters, Dernison et al. 2005). In the present study we have characterized experimentally the contribution of store-operated and receptor-operated calcium channels in the calcium homeostasis of quiescent and density-arrested NRK cells. Our results show that changes in calcium dynamics upon growing quiescent NRK cells to density-arrest coincide particularly with regulation of expression and activity of Trpc5, Trpc6 and Orai1 calcium channels, as well as of the calcium sensor Stim1.

Materials & Methods

Cell culturing

Normal rat kidney fibroblasts (NRK clone 49F) were seeded at a density of $1.25x10^4$ cells/cm^2 in bicarbonate-buffered Dulbecco's modified Eagle's medium (DMEM; Invitrogen, Carlsbad, CA) supplemented with 10% newborn calf serum (HyClone Laboratories, Logan, UT). Confluency was reached after four days. Cells were then incubated for three days in serum-free DF medium (1:1 mixture of DMEM and Ham's F-12 medium (Invitrogen) supplemented with 30 nM Na_2SeO_3 and 10 µg/ml human transferrin, to obtain quiescent cells. Density-arrested monolayers were obtained by incubation of quiescent cells for 48 hours with 5 ng/ml EGF (Collaborative Research Incorporated, Bedford, MA) in combination with 5 µg/ml insulin (Sigma-Aldrich, St. Louis, MO). For calcium imaging experiments $1.2x10^5$ NRK cells were seeded on 0.1% gelatin-coated glass coverslips with a diameter of 25 mm in 9.6 cm^2 wells.

Intracellular calcium measurements

Glass coverslips grown with quiescent monolayers of NRK fibroblasts were placed in a cell chamber and loaded for 30 min with 4 µM Fura-2/AM (Molecular Probes, Eugene, OR) in serum-free DF medium at room temperature. Medium was replaced by Ca^{2+}-free HEPES-buffered saline (Ca^{2+}-free HBS, containing 143 mM NaCl, 5 mM KCl, 1 mM $MgCl_2$, 10 mM glucose, 10 mM HEPES-KOH, pH 7.4). Ca^{2+} or Sr^{2+}-containing HBS (128 mM NaCl, 10 mM $CaCl_2$ or $SrCl_2$, 5 mM KCl, 1 mM $MgCl_2$, 10 mM glucose, 10 mM HEPES-KOH, pH 7.4) was mixed with an equal amount of Ca^{2+}-free medium to obtain a 5 mM Ca^{2+} or Sr^{2+}-containing medium in the chamber. Dynamic calcium video imaging was performed as described elsewhere (Cornelisse, Deumens et al. 2002). Excitation wavelengths of 340 nm and 380 nm (bandwidth 8-15 nm) were provided by a 150 W Xenon lamp (Ushio UXL S150 MO, Ushio, Tokio, Japan), while fluorescence emission was monitored above 440 nm, using a 440 nm DCLP dichroic mirror and a 510 nm emission filter (40 nm bandwidth) in front of the camera. Image acquisition, using a camera pixel binning of 4 and computation of ratio images (F340/F380), was every 4 sec and operated through Metafluor v.6.2 (Universal Imaging Corporation, Downingtown, PA). Camera acquisition time was 100 msec per excitation wavelength. The agents U73122, SKF96365, Gö6976 and OAG were purchased from *Sigma-Aldrich (St. Louis, MO), BHQ was purchased from Calbiochem (Darmstadt, Germany) and 2-APB from Tocris (Avonmouth, UK).*

Data analysis

At each measurement variations in intracellular calcium concentration as a function of time were measured simultaneously in 50 to 70 cells. The Mann-Whitney U ranking test was applied for comparing the frequency of calcium oscillations/ transients in different cell groups. The increase of

the F340/F380 ratio due to calcium influx through membrane channels or by calcium release from intracellular stores was determined by subtracting the mean ratio before (basal level) and after (peak) the calcium influx or release. Numerical data are represented as mean ± S.E.M throughout this article, with n representing the number of replicates in each experiment. Significance levels (denoted p) have been determined by double-sided student's T-test unless otherwise stated.

PCR Primers and Total RNA isolation

PCR primers for rat *Trpc1-7, Orai1* and *Stim1* were designed based on published sequences in GenBank (see supplementary table S1) using Oligo Perfect designed tool (Invitrogen),. Total RNA was isolated from NRK cells using Trizol (Invitrogen) according to manufacturer's protocol.

RT-PCR

First strand cDNA was prepared from 1 µg of total RNA using SuperScript^{TM} II RNase H^{-} reverse transcriptase (Invitrogen) and 0.25 µg of hexamer primer. Thereto RNA samples were denaturated at 65 ^{0}C for 55 min and reverse transcription was performed for 50 min at 42 ^{0}C and stopped by heating the samples for 15 min at 70 ^{0}C. The cDNA was amplified by PCR using the specific primers for individual *Trpc* genes (see list in supplementary table S1) and Taq polymerase^{TM} (Invitrogen) PCR amplification was performed using a PERKIN ELMER Gene Amp PCR System 2400 (Norwalk, CT) using 1 µl of first stranded cDNA reaction, 150 pmol of each degenerate primer, 50 µM of dNTPs, 2 units of Taq polymerase and 2.5 mM $MgCl_2$ in total volume of 50 µl. PCR conditions were as follows: 3 min at 94 ^{0}C, 40 cycles consisting of 30 sec at 94 ^{0}C, followed by 1 min at 72 ^{0}C. After completion of the 30 cycles, samples were incubated at for 10 min 72 ^{0}C. The PCR products were visualized on an ethidium bromide-stained agarose gel.

Quantitative Real-time RT-PCR

The mRNA levels for genes of interest were analyzed by using quantitative RT-PCR (Detection System 5700 ABI Prism, Applied Biosystems, Foster City, CA). A total of 1 µg of cDNA, synthesized as described above using the primers shown in supplementary table S2, was amplified using SYBR Green PCR Mastermix (Applied Biosystems) under the following conditions: initial denaturation for 10 min at 95 ^{0}C, followed by 40 cycles consisting of 15 sec at 94 ^{0}C and 1 min at 60 ^{0}C. Expression values were calculated from threshold cycles at which an increase in reporter fluorescence above baseline signal could first be detected

Results

ResultsCharacterization of store-operated calcium entry in quiescent and density-arrested NRK fibroblasts

Store-operated calcium entry (SOCE) was studied in quiescent (Q) and density-arrested (DA) NRK fibroblasts by measuring calcium influx after release of calcium from intracellular stores. Emptying of these stores was induced by placing the cells in a nominal calcium-free medium in the additional presence of the sarco-endoplasmatic reticulum Ca^{2+}-ATPase (SERCA) inhibitor BHQ. SOCE was subsequently measured by increasing the extracellular calcium concentration to 5 mM.

Figure 1 shows on the basis of the F340/F380 ratio of Fura-2 fluorescence that release of calcium from the stores results in an increase in cytoplasmic calcium ions, which are rapidly pumped out of the cells by the plasma membrane Ca^{2+}-ATPase. Subsequent addition of calcium to the extracellular medium results in a strong, transient increase in cytoplasmic calcium concentration due to the activity of store-operated calcium channels. Figure 1A shows that the release of calcium from intracellular stores in Q-cells resulted in an increase in F340/F380 ratio of 0.080 ± 0.008 (mean ± SEM, n=19), as measured from the basal level to the peak value after addition of BHQ. Addition of extracellular calcium ions resulted in a rise of the F340/F380 ratio of 0.14 ± 0.01 (mean ± SEM, n=19), as measured from the basal level to the peak value after addition of Ca^{2+}. Comparable experiments for DA-cells (see Figure 1B) resulted in an increase in F340/F380 ratio of 0.10 ± 0.02 (mean ± SEM, n=6) for BHQ treatment and of 0.19 ± 0.02 (mean ± SEM, n=6) upon subsequent calcium addition. Figure 1C shows that addition of extracellular calcium to Q-cells without prior depletion of calcium stores by BHQ treatment resulted in a small increase in the F340/F380 ratio of only 0.030 ± 0.021 (mean ± SEM, n=4). These data show that SOCE in density-arrested NRK cells is higher than in quiescent cells, although the difference was below the 95% confidence interval for statistical significance ($p = 0.08$).

Since DA-cells can undergo spontaneous calcium action potentials, accompanied by calcium influx due to transient opening of the L-type calcium channel, the above experiments were carried out in the presence of the L-type channel inhibitor nifedipine. Control experiments showed that nifedipine had no effect on the intracellular calcium level of both Q- and DA-cells (data not shown).

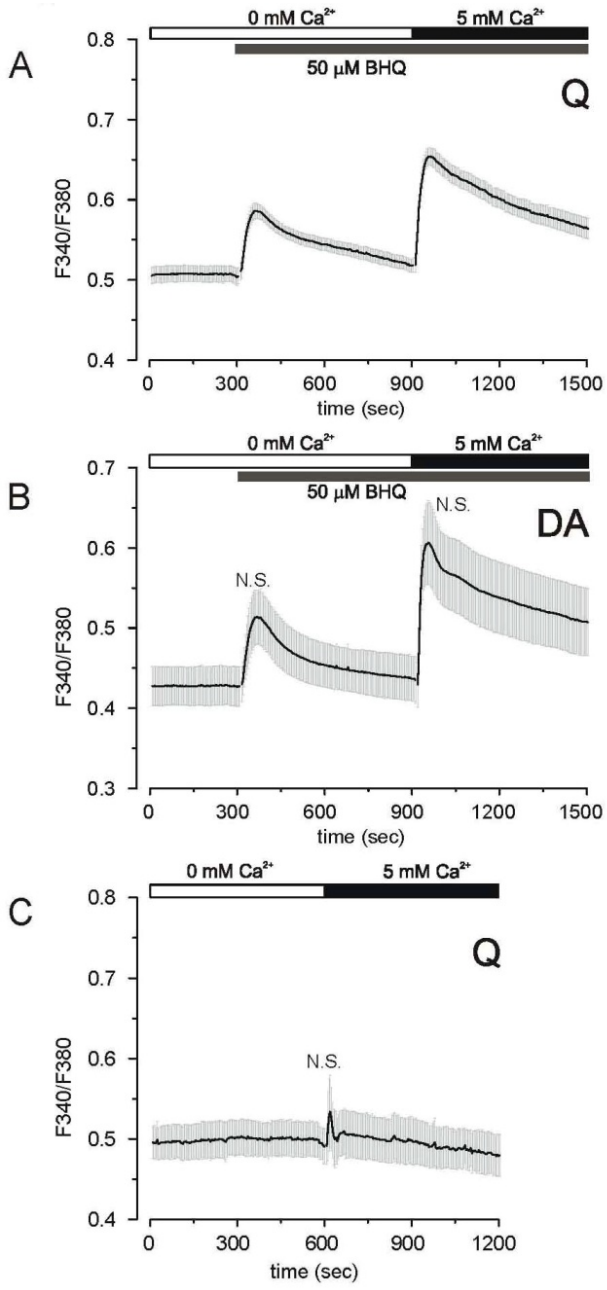

Fig 1. Demonstration of store-operated calcium entry in NRK fibroblasts.

Store-operated calcium entry is present in both quiescent (A) and density-arrested (B) NRK fibroblasts. BHQ (50 µM) was added to deplete intracellular calcium stores (first phase of calcium increase) and subsequently 5 mM extracellular calcium was added to induce store-operated calcium entry (second phase). Recordings in density-arrested cells were performed in the presence of nifedipine to prevent activation of L-type channels. Difference in the calcium entry between quiescent and density-arrested fibroblasts was not significant (N.S.). Addition of extracellular calcium to quiescent cells without previous stimulation did not induce a significant increase (N.S.) in the intracellular calcium level (C). The gray band around the traces represents the SEM-error bars for every data point.

Characterization of receptor-operated calcium entry in quiescent and density-arrested NRK fibroblasts

Receptor-operated calcium entry (ROCE) was studied in quiescent (Q) and density-arrested (DA) NRK fibroblasts by pre-incubating the cells in nominal calcium-free medium with the DAG-analogue OAG and measuring the increase in intracellular calcium concentration upon addition of 5 mM extracellular Ca^{2+}. Nifedipine was added in the experiments to prevent calcium influx through voltage-dependent L-type calcium channels.

Figure 2A shows that addition of extracellular calcium to Q-cells in the presence of OAG resulted in a F340/F380 increase of 0.045 ± 0.013 (mean ± SEM, n=10) above the basal fluorescence level. Figure 2B shows that addition of calcium ions to OAG-treated DA-cells resulted in an increase in F340/F380 of 0.11 ± 0.01 (mean ± SEM, n=10), which is 2.4 times higher ($p<0.01$) than the value observed in Q-cells. When these experiments were carried out in DA-cells without prior incubation with OAG (Figure 2C), a value of 0.11 ± 0.01 (mean ± SEM, n=10) was found, which is not significantly different from the increase found in the presence of OAG. This suggests that density-arrested NRK cells may already contain sufficient DAG to activate receptor-operated calcium channels. Figure 2D shows that pretreatment of DA-cells with PLC-inhibitor U73122 in order to prevent PIP_2 degradation and concomitant DAG production, reduced the increase in F340/F380 to 0.061±0.007 (mean ± SEM, n=7), which is indeed 45% lower than the value observed for these cells in the absence of this inhibitor, either with or without additional OAG. These results show that density-arrested NRK cells display significantly higher levels of ROCE than quiescent cells. Furthermore they suggest that at least in density-arrested cells activation of receptor-operated calcium entry takes place in a PLC-dependent manner.

Mechanism of strontium uptake in NRK cells

We have previously shown that $PGF_{2\alpha}$-mediated calcium oscillations in quiescent, as well as spontaneous calcium action potentials in density-arrested NRK cells, also occur in the presence of externally added strontium ions (de Roos, Willems et al. 1997). These studies provided evidence that during an action potential L-type calcium channels can mediate the uptake of strontium ions into NRK cells. However, the ion channels involved in strontium uptake in the absence of an action potential have not been characterized yet. Figures 3A and B compare the uptake of calcium and strontium ions, respectively, by store-operated ion channels in DA-cells. In BHQ-treated cells 5 mM Ca^{2+} induced a F340/F380 increase -

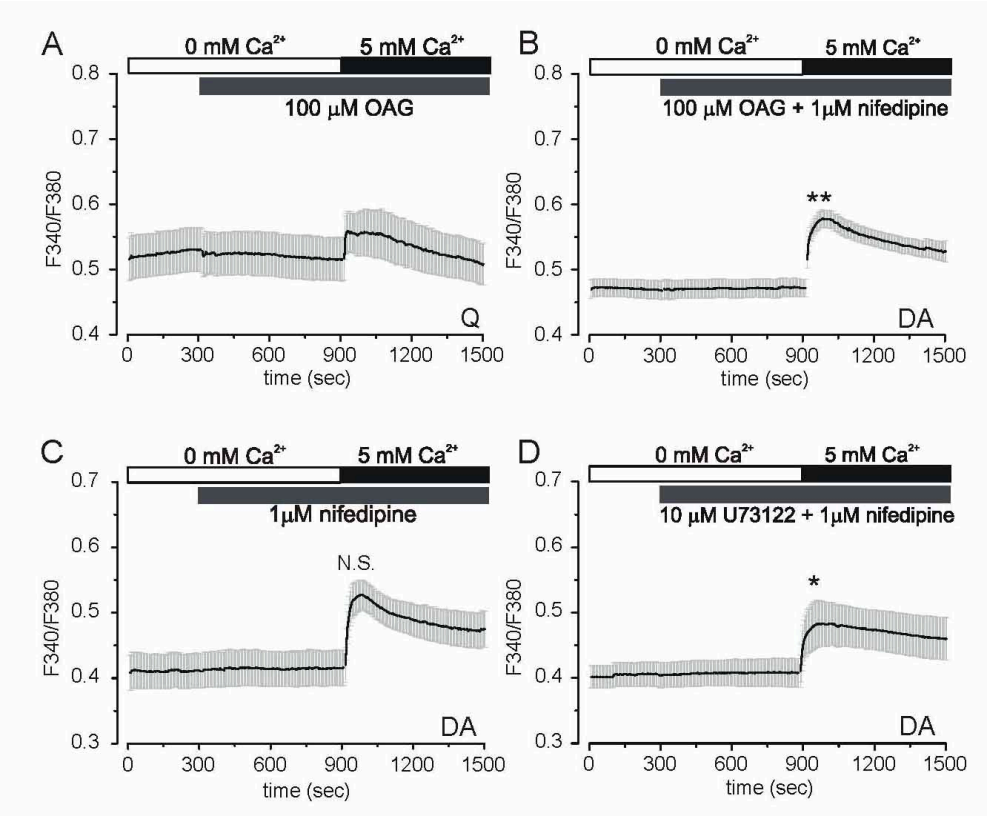

Fig 2. Non-store operated calcium entry is larger in density-arrested than in quiescent cells.

Increase in intracellular calcium upon re-addition of calcium in the presence of 100 µM OAG to quiescent cells (A) and density-arrested cells (B) (significance: **, $p<0.001$, compared to A, n=10). Increase in intracellular calcium upon re-addition of calcium to density-arrested cells in the absence of OAG (N.S., compared to B, n=10) (C). Calcium entry upon re-addition of calcium to density-arrested cells in presence of the PLC-inhibitor U73122 (D) (significance: *, $p<0.05$, compared to C, n=7). All recordings in density-arrested cells were performed in presence of nifedipine to prevent entry of calcium through L-type calcium channels. The gray band around the traces represents the SEM-error bars for every data point.

- of 0.14 ± 0.01 (mean ± SEM, n=19), while 5 mM Sr^{2+} induced a fluorescence increase of 0.034 ± 0.008 (mean ± SEM, n=11). Figures 3C and D show the rise in fluorescence ratio by the uptake of calcium or strontium ions, respectively, through receptor-operated channels in OAG-treated DA-cells. Addition of calcium ions resulted in a F340/F380 increase of 0.11 ± 0.01 (mean ± SEM, n=12), while strontium ions induce an increase in fluorescence ratio of 0.075 ± 0.019 (mean ± SEM, n=6). These data indicate that strontium ions can be taken up by NRK cells through both store-operated and receptor-operated ion channels. All the measured increases of the fluorescence ratio in these experiments were significant compared to the baseline values.

When interpreting these data it should be taken into account that calcium and strontium ions both change the fluorescence properties of Fura-2, but do so with a different affinity (Ca^{2+}: K_d = 224 nM; Sr^{2+}: K_d = 9.2 μM (Hatae, Fujishiro et al. 1996)). The relatively small change in fluorescence upon addition of strontium ions therefore corresponds to a relatively high permeability of the plasma membrane for Sr^{2+}, when compared to calcium ions. Calibration of the Fura- 2 ratio signal by the method of Grynkewic (Robinson, Jenkins et al. 2004) was not conclusive due to the small increase in the fluorescence ratio when strontium was added. Based on the above K_d-values and the known Hill coefficient of Fura-2, the observed increase in fluorescence ratio from 0.52 to 0.65 after addition of extracellular calcium (Figure 3A) corresponds to an increase in intracellular calcium concentration of 0.44 μM. In comparison, the relatively small increase from 0.49 to 0.52 upon addition of extracellular strontium (Figure 3B) corresponds to an intracellular strontium concentration up to 10 μM. This indicates that strontium ions can permeate through store-operated ion channels at least as good as calcium ions. Moreover, the relatively high fluorescence increases for strontium versus calcium ions during receptor-operated ion uptake indicates that strontium ions are well taken up by NRK cells by both SOCE and ROCE mechanisms.

Endogenous expression of Trpc family members, Orai1 and Stim1 in NRK fibroblasts

In order to test which calcium channels may be involved in the observed SOCE and ROCE, we tested NRK cells for expression of channel encoding genes by RT-PCR analysis. Figure 4A shows that of the various Trpc channels, NRK cells expressed particularly the genes encoding Trpc1, Trpc5 and Trpc6. As a comparison, rat brain tissue expressed at least the genes encoding Trpc1, Trpc3, Trpc4, Trpc5, and Trpc6, but possibly also those encoding Trpc2 and Trpc7. Trpc1 is generally considered as a channel involved in SOCE (Liu, Singh et al. 2003), while Trpc6 is known to be DAG dependent (Lemonnier, Trebak et al. 2008). Trpc5 is less well characterized in this respect. The observation that NRK cells express these three genes, confirms our functional studies that NRK cells contain both SOCs and ROCs. As shown in Figure 4B, quantitative RT-PCR analysis indicated that particularly *Trpc5* (10-fold) and *Trpc6* (6-fold) are strongly up-regulated when quiescent NRK cells are grown to density-arrest. In contrast, the high expression level of *Trpc1* is not enhanced upon density-arrest of the cells.

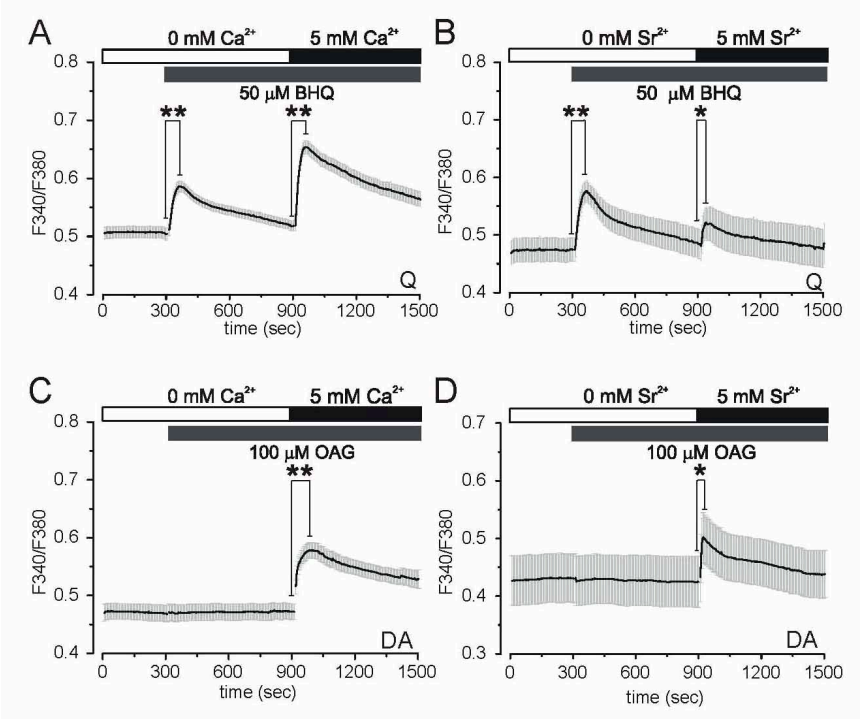

Fig. 3. ROCE and SOCE are permeable for calcium as well as strontium ions.

Calcium (A) and strontium (B) entry after depletion of calcium stores induced by BHQ (50 µM) in quiescent cells. Receptor-operated calcium (C) and strontium (D) entry in density-arrested cells in presence of OAG (100 nM) and nifedipine (1 µM). All changes in the F340/F380 fluorescence ratio where significant (peak values compared to the baseline) (significance: *, $p < 0.002$; **, $p < 10^{-6}$). The gray band around the traces represents the SEM-error bars for every data point.

Under similar experimental conditions, transcripts of both Stim1 and Orai1 were detected in NRK fibroblasts by RT-PCR. Figure 5A and 5C show the PCR products obtained for Stim1 and Orai1, respectively. Gel electrophoresis confirmed that the PCR product sizes corresponded to rat Stim1 (293bp) and rat Orai1 (375bp). Sequencing of the PCR products showed agreement with the original GenBank sequences. Upon density-arrest, the expression of *Stim1* and *Orai1* was up-regulated 1.6 and 5.5 fold, respectively (Figure 5B and D).

Although these data do not necessarily reflect changes in channel densities, the results indicate that the genes for most calcium channels tested and for the calcium sensor Stim1 are strongly up-regulated, when NRK cells are grown from quiescence to density-arrest. These data agree with our functional studies showing that both SOCE and ROCE are clearly enhanced upon growing NRK cells to density-arrest (see section 3.1 and 3.2).

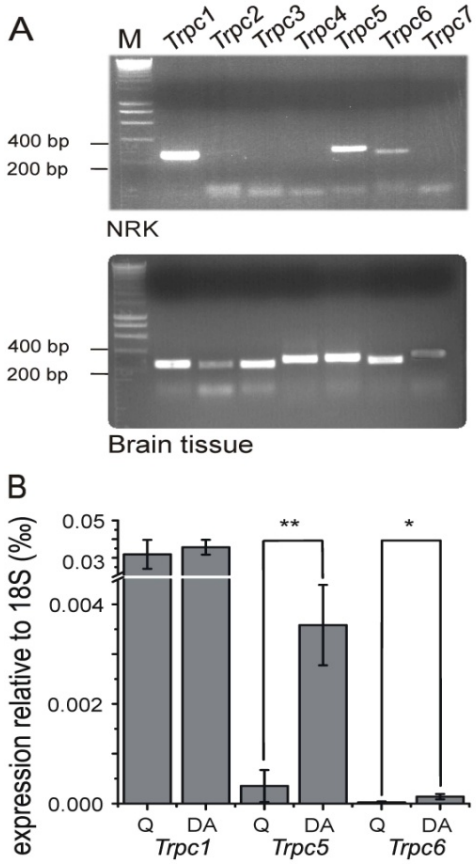

Fig. 4. Differential expression of *Trpc1, Trpc5* and *Trpc6* genes in quiescent and density-arrested NRK fibroblasts. A) RT-PCR analysis of the expression of *Trpc* genes in NRK fibroblasts. Equal amounts of cDNA, prepared from quiescent NRK cells and rat brain tissue as a positive control, were added in combination with specific primers for individual *Trpc* genes (see supplementary table S1). Data are representative of three independent experiments. M denotes marker for base-pair length. B) mRNA levels for Trpc1, Trpc5 and Trpc6 in quiescent (Q) and density-arrested (DA) NRK fibroblasts determined by quantitative RT-PCR using *Trpc* specific primers (see Table 2), and expressed relative to 18S rRNA levels. (significance: *, $p<0.05$; **, $p<0.005$, n=4).

Calcium influx limits calcium oscillations

We have previously shown that calcium influx is required for the persistent calcium oscillations that are induced by $PGF_{2\alpha}$ in quiescent NRK cells (Harks, Scheenen et al. 2003). Several pharmaceutical agents are known to inhibit or enhance SOCE and ROCE. We have determined the inhibitory or enhancing effect of three of these compounds. In figure 6 we show that 2-APB and SKF96365 had profound inhibitory effects on SOCE in quiescent (Figure 6A and 6C, respectively) and ROCE in density-arrested cells (Figure 6B and 6D, respectively) (see also supplementary table S3). In the remainder of figure 6 we

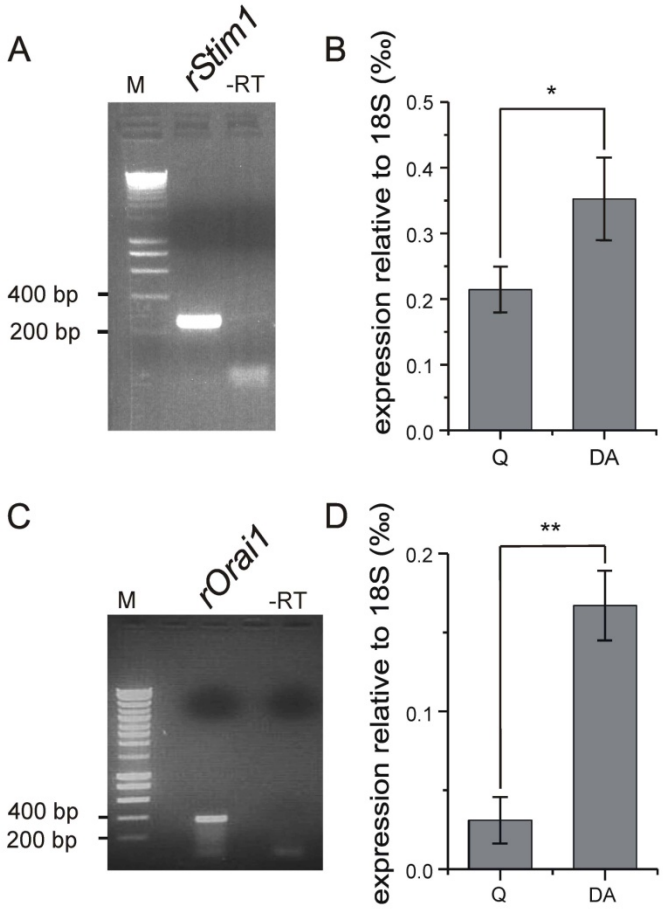

Fig. 5. Differential expression of Stim1 and Orai1 genes in quiescent and density-arrested NRK fibroblasts. RT-PCR analysis of Stim1 (A) and Orai1 (C) expression in NRK fibroblasts. Equal amounts of cDNA, prepared from quiescent NRK cells and rat brain tissue as a positive control, were added in combination with gene specific primers (see supplementary table S1). Data are representative of three independent experiments. mRNA levels of Stim1 (B) and Orai1 (D) in quiescent (Q) and density-arrested (DA) NRK fibroblasts determined by quantitative RT-PCR using gene specific primers (see Table 2), and expressed relative to 18S rRNA levels (significance: *, $p<0.05$; **, $p<0.005$, n=3).

show that pre-incubation with the protein kinase C inhibitor Gö6976 potentiated SOCE in quiescent cells (Figure 6E) and also ROCE in density-arrested cells (Figure 6F) (see also supplementary table S3). The present observations show that calcium entry into NRK cells can be either inhibited or enhanced by pharmacological treatments. Because of the inhibitory effects of 2-APB on IP_3 receptors (Siefjediers, Hardt et al. 2007), we choose SKF96365 and Gö6976 to test their inhibitory and potentiating effects, respectively, on $PGF_{2\alpha}$-induced calcium oscillations and spontaneous action potential induced calcium transients.

In figure 7 we show typical responses of individual quiescent cells upon inhibition and potentiation of SOCE. Figure 7B shows that pre-incubation of Q-cells with Gö6976 resulted in an inhibition of $PGF_{2\alpha}$-induced calcium oscillations after approximately 10 min. In contrast, addition of SKF96365 resulted in an immediate decrease in the frequency of calcium oscillations (Figure 7C). Density-arrested NRK cells display spontaneous action potentials with concomitant calcium transients. In figure 8 we show the typical responses of whole monolayers of density-arrested cells upon inhibition and potentiation of ROCE. Figure 8B shows that pre-incubation with Gö6976 had no significant effect on the frequency of the action potential-induced calcium transients in DA-cells. The addition of SKF96365 resulted in an immediate extinction of the spontaneous calcium spikes (Figure 8C). Table 1 summarizes the results of the Mann-Whitney analysis of the effects of SKF96365 and Gö6976 on the $PGF_{2\alpha}$-induced calcium oscillations and the spontaneous calcium spikes, as exemplified in the Figures 7 and 8, respectively. The analysis revealed that in Q-cells potentiation by Gö6976 as well as inhibition by SKF96365 of calcium entry both significantly reduced the frequency of the $PGF_{2\alpha}$-induced calcium oscillations, while in DA-cells only inhibition of calcium entry caused a significant reduction in the frequency of the action potential-induced calcium transients.

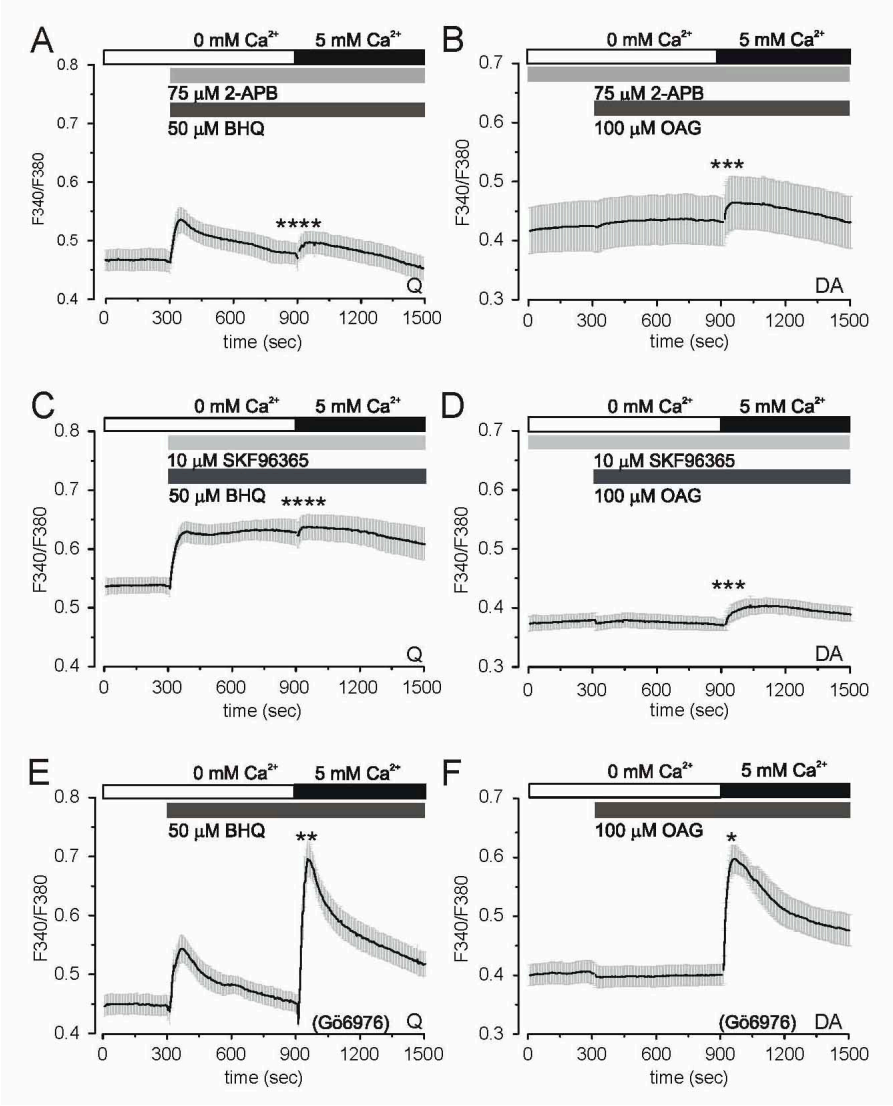

Fig. 6. Effects of pharmacological agents on calcium entry in NRK fibroblasts.

Figure 6A and 6B show the effect of 75 µM 2-APB on BHQ-induced store-operated calcium entry in quiescent cells (A) and receptor-operated calcium entry in density-arrested cells in presence of OAG (B). Figure 6C and 6D show the effect of SKF9365 (10 µM) on SOCE and ROCE in quiescent (C) and density-arrested cells (D), respectively. The inhibition calcium entry by 2-APB and SKF96365 in quiescent cells is compared with control experiments (Figure 1A) (significance: ****, $p < 10^{-8}$). The inhibition of 2-APB and SKF96365 in density-arrested cells is compared with control experiments (Figure 2B) (significance: ***, $p < 10^{-6}$). Figure 6E and 6F show the effect of pre-incubation (30 min) with 100 nM Gö6976 (assigned by (Gö6976) in the figure) on SOCE in quiescent (E) and ROCE in density-arrested cells (F). Potentiation of calcium entry in quiescent and density-arrested cells is compared with control experiments (Figure 1A and 2B, respectively) (significance: **, $p < 10^{-4}$; *, $p < 0.01$). All recordings in density-arrested cells were performed in the presence of the L-type calcium channel blocker nifedipine to prevent entry of calcium through this type of calcium channels.

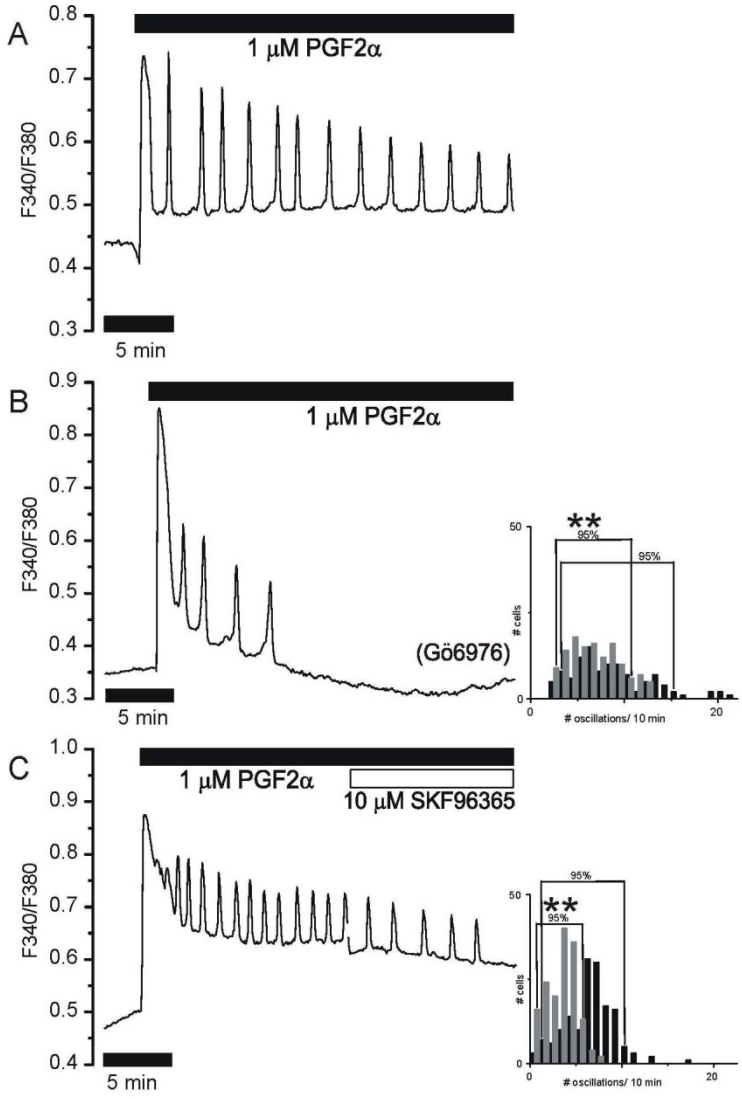

Fig. 7. SOCE modulators have a profound effect on $PGF_{2\alpha}$-induced intracellular calcium oscillations in quiescent NRK fibroblasts. A) Intracellular calcium oscillations induced by $PGF_{2\alpha}$ in quiescent NRK fibroblasts. B) $PGF_{2\alpha}$-induced intracellular calcium oscillations in NRK fibroblasts after 30 min pre-incubation with 100 nM Gö6976, assigned by (Gö6976) in the figure. C) Effect of inhibition of calcium entry by 10 μM of SKF96365 on $PGF_{2\alpha}$-induced intracellular calcium oscillations in quiescent NRK fibroblasts. Each trace shown in this figure represents a typical calcium response induced by $PGF_{2\alpha}$ in an individual cell selected from a panel of 100-150 cells of data obtained in 3 independent experiments. (See Table 1 for a quantitative Mann-Whitney analysis of the significance level of the changes represented in the traces)

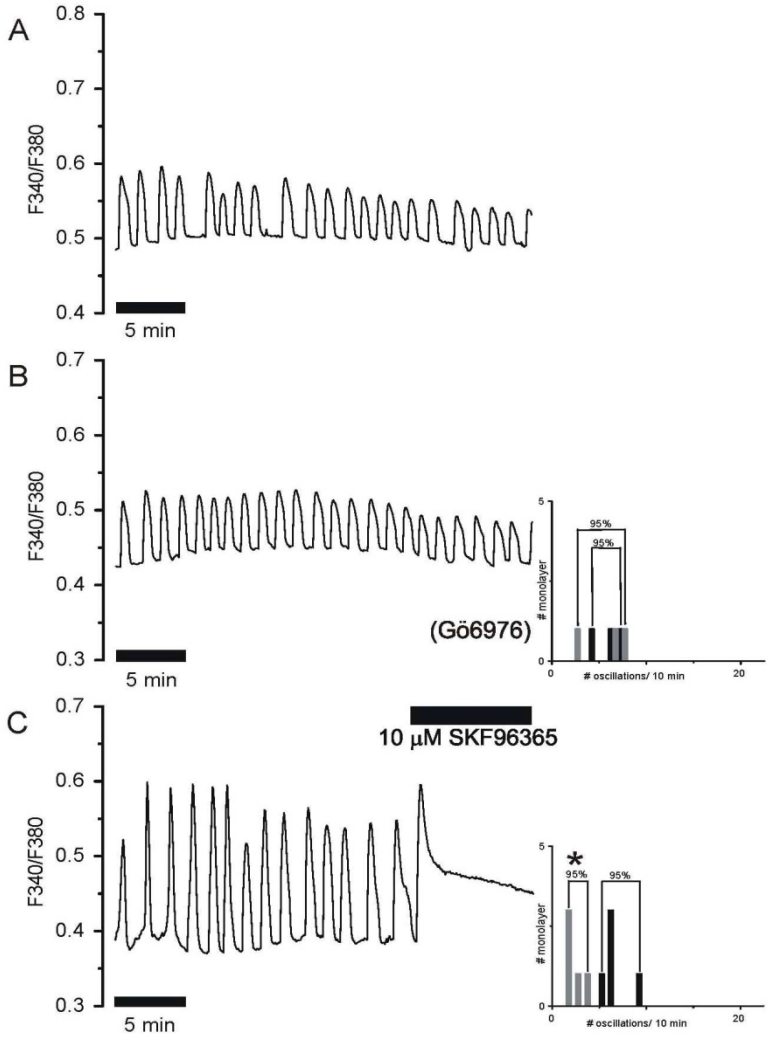

Fig. 8. Effect of either potentiating or inhibiting calcium entry on action potential-induced calcium transients in density-arrested NRK fibroblasts. A) Calcium transients induced by propagating action potentials in density-arrested NRK fibroblasts. B) Calcium transients induced by propagating action potentials in density-arrested NRK fibroblasts after 30 min pre-incubation with 100 nM of Gö6976, assigned by (Gö6976) in the figure. C) Calcium transients induced by propagating action potentials in density-arrested NRK fibroblasts disappear in the presence of 10 µM SKF96365. Each trace shown in this figure represents a typical example out of 3 (pre-incubation with Gö6976) and out of 5 (addition of SKF96365) independent experiments of spontaneous synchronized calcium responses of a whole monolayer of density-arrested NRK fibroblasts, respectively. (See Table 1 for a quantitative Mann-Whitney analysis of the significance level of the changes represented in the traces).

Number of calcium oscillations/ transients per 10 min

	Q-cells				DA-cells			
	median	95% range	n	p	median	range	n	p
control	7	3-16	107		7	4-8	3	
Gö6976	6	2-11	128	<0.001	6	2-7	3	>0.05
control	6	1-10	155		6	5-9	5	
SKF96365	3	0-5	155	<0.001	1	1-3	5	<0.01

Table 1. Effect of Gö6976 and SKF96365 on the frequency of $PGF_{2\alpha}$-induced intracellular calcium oscillations in Q-cells and action potential-induced calcium transients in DA-cells. The effect of pre-incubation with Gö6976 is compared to separate control experiments. The effects of SKF96365 are compared to the $PGF_{2\alpha}$-induced calcium oscillations and the action potential-induced calcium transients, respectively, before addition of the agent. Number of calcium oscillations in a period of 10 min was counted in n individual quiescent cells from data obtained in three independent experiments. In density-arrested cells the number of synchronized calcium transients due to action potentials in the whole cellular monolayer was determined in a number (n) of independent experiments. The significance level (p) following Mann-Whitney analysis is indicated.

Discussion

In this study we show a differential role for SOCs and ROCs in the calcium dynamics of quiescent and density-arrested NRK fibroblasts. For the first time the occurrence of both types of calcium entry has been demonstrated experimentally in quiescent and density-arrested NRK cells. In an earlier study we already predicted the necessity of a calcium entry pathway, dependent on the filling state of the intracellular calcium stores, which could have a stabilizing role in intracellular IP_3-mediated calcium dynamics and cell membrane excitability [6]. Here we show experimentally that this calcium store-dependent calcium entry is differentially regulated via SOCs and ROCs in quiescent and density-arrested fibroblasts.

In contrast to previous studies (Tesfai, Brereton et al. 2001; Gamberucci, Giurisato et al. 2002; Venkatachalam, Zheng et al. 2003) we have shown that both SOCs and ROCs have a significant permeability for Sr^{2+}-ions. Due to the low affinity of Fura-2 for Sr^{2+}, influx of Sr^{2+} into the cells resulted in only a rather small increase in the fluorescence ratio.

This modest increase represents, however, a quite large Sr^{2+} influx. Previously we have shown that density-arrested cells can repetitively fire action potentials in calcium-free medium supplemented with strontium for prolonged periods of time (de Roos, Willems et al. 1997). Our results suggest that strontium entry is facilitated by the same activation pathways as calcium entry and that those pathways are different from L-type voltage-gated channels.

In quiescent cells, addition of extracellular calcium after calcium deprivation without SERCA inhibition resulted in a small calcium influx (Figure 1C). In density-arrested cells, however, calcium addition after calcium deprivation resulted in a significantly higher calcium influx (Figure 2C). These results indicate that density-arrested cells have another ensemble of calcium influx pathways than quiescent cells. Besides store-operated calcium entry, the density-arrested cells also exhibit a receptor-operated calcium entry mechanism. The addition of OAG, a DAG-derivative, did not result in an additional increase of the calcium influx. However, incubation of the density-arrested cells with PLC-inhibitor U73122 inhibited the calcium entry in these cells (Figure 2D). This indicates that in density-arrested NRK cells a PLC-dependent hydrolysis of PIP_2 into IP_3 and DAG plays a role in the stimulation of ROCs. This is supported by earlier findings by Harks et al(Harks, Peters et al. 2005), which have shown that density-arrested cells produce and secrete low amounts of $PGF_{2\alpha}$. This low concentration of $PGF_{2\alpha}$ activates the G-protein coupled FP receptor and activates PLC. These results suggest that the low concentrations of $PGF_{2\alpha}$ present in the culture medium of the density-arrested cells can result in an increased intracellular DAG level activating ROCE. Earlier studies(Flourakis, Van Coppenolle et al. 2006) have proposed an $iPLA_2$-dependent pathway as an activation mechanism for SOCE. However, inhibition of $iPLA_2$ did not affect SOCE, showing that this pathway is not relevant in NRK fibroblasts (data not shown).

Our findings are further supported by the differential expression pattern of *Trpc* genes in quiescent and density-arrested cells. Trpc channels have been described earlier as candidate channels for mediating SOCE and ROCE (Parekh and Putney 2005). While the expression level of *Trpc1* was found to be independent of cell density, expression levels of *Trpc5* and *Trpc6* were clearly increased in density-arrested cells. Trpc1 is generally considered as the channel involved in SOC formation (Liu, Singh et al. 2003), while Trpc6 is known to be DAG dependent (Lemonnier, Trebak et al. 2008). Although the exact activation pathway is not conclusive, Trpc5 seems to be activated by receptors coupled to

PLC, suggesting a role together with Trpc6 in ROCE (Blair, Kaczmarek et al. 2009). On the other hand, Zhu et al. (Zhu, Chae et al. 2005) have shown that Trpc5 is desensitized by phosphorylated PKC. The binding of DAG to the C1 domain results in activation and translocation of PKC (Newton 2001), whereby the production of DAG would inhibit the activity of Trpc5. The potentiating effect of PKC inhibitor Gö6976 suggests that a PKC-dependent calcium entry channel is present. However, we have shown that the PLC inhibitor U73122, expected to decrease DAG levels, just attenuated instead of potentiated ROCE in the density-arrested NRK cells.

The six-fold increase of *Trpc6* mRNA expression coinciding with ROCE in density-arrested NRK fibroblasts suggests a prominent role of Trpc6 in ROCE. Large et al. (Large, Saleh et al. 2009) have suggested a model in which PIP_2 binds to the same binding site as DAG in the resting state of Trpc6. Cleavage of PIP_2 into IP_3 and DAG makes the DAG/PIP_2-binding site available for DAG and subsequently activates Trpc6. The requirement of both cleavage of PIP_2 and elevated DAG levels might explain the limited effect of additional OAG in combination with a significant effect of inhibiting PLC activity. Our results show a differential expression of *Trpcs*, *Orai1* and *Stim1* mRNA in quiescent and density-arrested cells coinciding with a differential regulation of ROCE and SOCE. Recently it has been reported that Stim1 converts Trpc1 from a ROC into a SOC (Alicia, Angelica et al. 2008; Jardin, Lopez et al. 2008; Cahalan 2009) and that Trpc3, Trpc6 and Trpc7 facilitate DAG-sensitive calcium entry (Lemonnier, Trebak et al. 2008). These studies show that an intricate interplay between Trpcs, Stim1 and Orai1 subunits may constitute the channels responsible for calcium entry, whether receptor-operated or store-operated. Our results therefore suggest that quiescent and density-arrested NRK fibroblasts differ in their calcium entry mechanisms.

The effect of SOCE inhibition and potentiation on $PGF_{2\alpha}$ -induced calcium oscillations in both quiescent and spontaneously action potential firing density-arrested cells is puzzling. It was expected that an increased calcium entry in both quiescent and density-arrested cells would result in a higher frequency or amplitude of calcium oscillations and action potential-induced calcium transients, since increased calcium would fasten the recovery of the IP_3-receptor. However, in quiescent cells the calcium oscillations extinguished while density-arrested cells seemed to be unaffected by calcium entry potentiation. On the other hand, nearly complete SOCE inhibition only reduced the calcium oscillation frequency in quiescent cells by 50% (Table 1). Although inhibition of

ROCE by SKF96365 in density-arrested cells was less effective than in quiescent cells (Table S3), the reduced calcium entry completely attenuated the action potential-induced calcium transients in the DA-cells (Table 1).

In NRK cells we found SOCE in quiescent cells and both SOCE and ROCE in density-arrested cells. In a previous study Kusters et al. have explored the dynamical properties of a single cell model, reproducing experimental observations on calcium oscillations and action potential generation in NRK fibroblasts (Kusters, Cortes et al. 2007). An analysis of increasing SOC conductance and the effect on intracellular calcium oscillations is visualized in the bifurcation diagrams shown in supplementary Figure S1 (modified from (Kusters, Dernison et al. 2005)). This diagram shows how the range of IP_3 concentrations whereby the cells exhibit calcium oscillations, depends on store- and/or receptor-operated calcium entry. Quiescent cells start calcium oscillations after addition of $PGF_{2\alpha}$, assuming an $[IP_3]_{cyt}$ of 1 μM and a low calcium entry conductance of 0.02 nS (see Supplementary Figure S1A). Sufficient potentiation might bring these cells to an equivalent SOC level of 0.10 nS (Figure S1C), where they become silent and depolarized. Density-arrested cells, however, behave in a more complex manner. In a previous study (Dernison, Kusters et al. 2008) we have suggested a pacemaker-follower system to explain the spontaneous calcium action potentials in density-arrested cells. Under conditions of density-arrest an inhomogeneity in the local production of $PGF_{2\alpha}$ might give rise to localized islands of depolarized cells with increased intracellular IP_3. In these 'pacemaker'-islands IP_3-induced intracellular calcium oscillations synchronize resulting in depolarization at the border between polarized and depolarized cells, giving rise to propagating action potentials, which depolarize the surrounding 'follower'-cells. According to Harks et al. (Harks, Peters et al. 2005) density-arrested cells have a $PGF_{2\alpha}$ concentration of only 1.5 nM in the extracellular medium. Therefore the cytosolic level of IP_3 in density-arrested cells is presumably much lower than in quiescent cells stimulated with 1 μM $PGF_{2\alpha}$. Density-arrested cells, however, seem to have a larger calcium entry facilitated by SOCs and ROCs, so in pacemaking cells the concentration of IP_3 might be in a regime near 0.2 μM in combination with a membrane calcium conductance of 0.04 nS (Figure S1B). An increase/ potentiation of calcium entry conductance (to 0.10 nS, Figure S1C), while maintaining a constant level of $[IP_3]_{cyt}$, would not stop the calcium oscillations. This shows that the higher calcium influx in density-arrested cells results in a broader range of IP_3 concentrations that can induce calcium oscillations. Apparently,

density-arrested cells are more sensitive to IP_3 with respect to the ability to induce calcium oscillations.

The effect of increasing calcium entry on the calcium oscillations in NRK cells suggests that proliferation of these cells from the quiescent to the density-arrested stage may not only result in an increased production of $PGF_{2\alpha}$, but also in an enhanced expression of both SOCs and ROCs. This differential mechanism of calcium entry provides NRK fibroblasts with an elegant pathway to meet their calcium requirements under the different growth conditions. Our previous study (Kusters, Dernison et al. 2005) has shown that a regulated calcium entry is required to couple membrane excitability with calcium dynamics, in order to maintain calcium homeostasis in NRK fibroblasts. Our results thereby suggest that Trpc channels, most likely in combination with Stim1 and Orai1, are able to provide this calcium entry pathway. We are currently testing this hypothesis by using a shRNA approach to selectively knockdown the genes for these proteins.

Conclusions

In this study we have shown that Trpc1, Trpc5 and Trpc6, Stim1 and Orai1 are expressed in NRK fibroblasts. Moreover, Trpc5, Trpc6 and Orai1 are differentially expressed in quiescent and density-arrested cells. The increased expression of these genes in density-arrested cells coincides with an increase of SOCE and ROCE at this growth stage. The involvement of Trpc6 in ROCE is supported by our observation that ROCE is a PLC-dependent process. Earlier observations of sustained oscillations in Sr^{2+}- containing media are supported by our findings that in NRK fibroblasts SOCs as well as ROCs are not only permeable Ca^{2+} but also for Sr^{2+}. The earlier notion from the mathematical model of NRK fibroblasts that calcium entry limits the range, in which IP_3-dependent calcium oscillations and action potentials can occur, is supported by the present experimental findings.

Acknowledgement

We gratefully thank professor D.L.Ypey (Department of Cell Biology, Radboud University Nijmegen) for his interest and valuable advices during the course of this study. This research project was funded by the Physical Biology Research Program (No. 805.47.066) of the Stichting voor Fundamenteel Onderzoek der Materie (FOM) and the Gebiedsbestuur

Aard en Levenswetenschappen (ALW), which are financially supported by the Netherlands Organization for Scientific Research (NWO).

Supplementary data

Theoretical background of Figure S1

Modeling the dependence of calcium oscillations on the extent of calcium influx

In an earlier study a mathematical single cell model of the NRK fibroblast has been developed to describe the dynamics of the calcium oscillations in these cells (Cornelisse, Deumens et al. 2002; Kusters, Dernison et al. 2005). In a subsequent model we have studied the role of store-operated calcium entry in the stabilization of the calcium dynamics by changing the SOC conductance [22, 23]. In that model the presence of calcium oscillations depends on the concentration of both IP_3 and Ca^{2+}. For low IP_3 concentrations, there is a balance between removal of calcium from the cytosol and leak into the cytosol from the ER and the extracelullar medium. In this condition, the cytosolic calcium concentration is low. For higher IP_3 concentrations, calcium oscillations occur. During IP_3-mediated calcium oscillations, the increased Ca^{2+}-concentration causes inactivation of the IP_3 receptor. The inactivation time constant is governed by both the calcium and IP_3-concentration. At high calcium concentrations the inactivation time constant is small. Therefore, the inactivation rate is fast at the peak of the calcium spike. When the calcium concentration decreases due to removal from the cytosol, the inactivation time constant increases, causing a slow de-inactivation of the IP_3 receptor. Calcium oscillations occur as long as the inactivation time constant is long relative to the duration of the calcium spike. As the concentration of IP_3 increases, the inactivation time constant decreases and calcium oscillations stop when the duration of the inactivation time constant has become sufficiently short to follow the changes in calcium concentration. In that condition, the calcium concentration settles to a constant elevated level in a range between 2 and 5 μM depending on the concentration of IP_3.

Figure S1

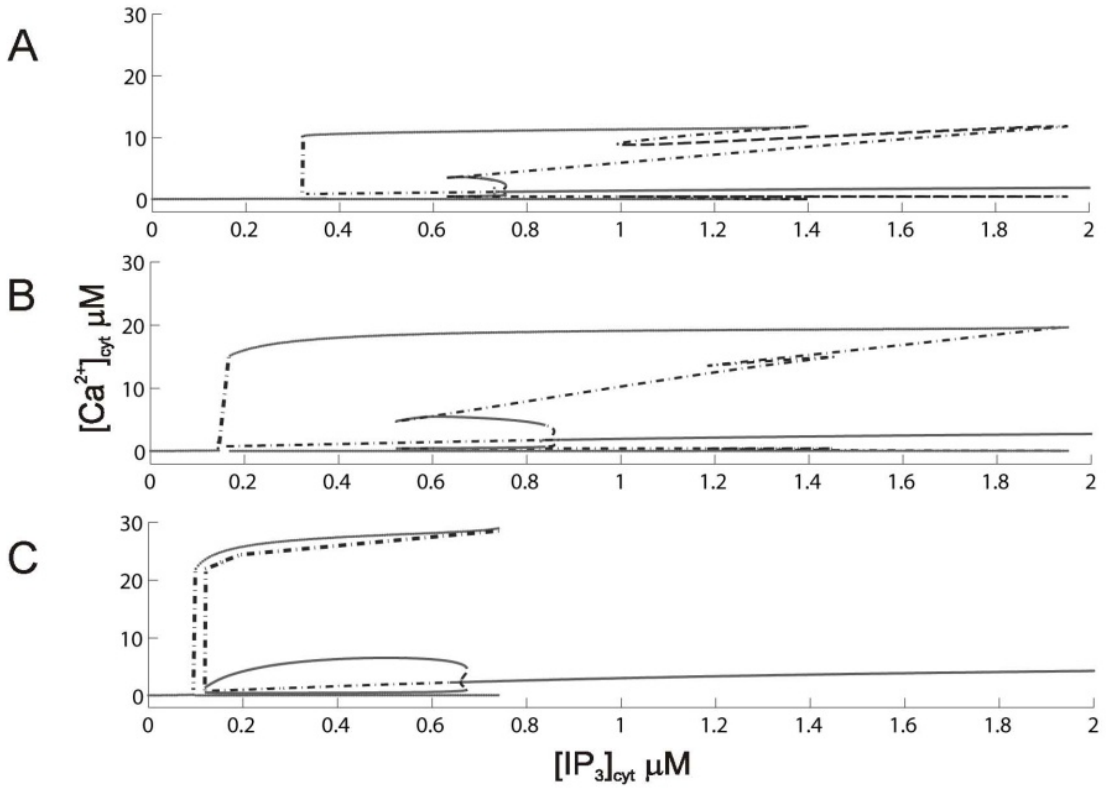

Figure S1 (modified from Fig.3 in (Kusters, Cortes et al. 2007)) shows bifurcation diagrams for intracellular calcium concentration as a function of $[IP_3]$ at three different levels of SOC conductance: 0.02 nS (A), 0.04 nS (B) and 0.10 nS (C), respectively. The increase in SOC conductance causes an increase in the intracellular calcium entry from the extracellular medium. The increased entry of calcium gives rise to a larger removal by pumps in the plasma membrane and in the ER. The slight increase in cytosolic calcium concentration with increased SOC conductance makes the IP_3 receptor more sensitive for calcium oscillations at lower IP_3 concentrations. At a low IP_3 concentration of 0.2 µM and a low SOC conductance of 0.02 nS (panel A), the cytosolic calcium concentration is too low to activate the IP_3-receptor. Increasing this conductance to 0.04 nS (panel B) will activate the IP_3-receptor and results in calcium oscillations. For 0.10 nS (panel C) the calcium level is still low enough to produce calcium oscillations, but the range of $[IP_3]$ in which oscillations can occur is much smaller. These simulations show that store-operated calcium entry does have a great impact on calcium dynamics in NRK cells.

Table S1. Oligonucleotide sequences of primers used for RT-PCR

Gene	Accession No.	Size (bp)	Primers	Location
rTrpc1	AF061266	248	For: 5'-T C A C G A T T G G A C T G A C A C A G C-3' Rev: 5'-A A G C A C G A T C A C A A C C A C G A-3'	1571-1819
rTrpc2	AF136401	261	For: 5'-G G G T C A C A G G C T T T C T G T G G-3' rev:5'-A G C A T G C T C G T G A C A G C A A A-3'	1326-1587
rTrpc3	NM_021771	250	For: 5'-T C G G C T A C T G G A T T G C A C C T-3' Rev: 5'-A T C C C G A G A A C C C A G A C C A T-3'	836-1086
rTrpc4	NM_053434	283	For: 5'-A T G T T G G C G A T G C G C T A C T T-3' Rev:5'-T G A G G C T G T C C A C G T C T G A G-3'	400-683
rTrpc5	NM_080898	301	For: 5'-T C G C T C A G C C A A A C T G T C A A-3' Rev: 5'-A G T T G G G G G A G G T C C T T G A A-3'	1235-1536
rTrpc6	NM_053559	275	For: 5'-T G C A G C A A G A T G G G G A A G A T-3' Rev: 5'-G G G G C C T T G A G T C C A G A T T T-3'	1281-1556
rTrpc7	XM_001067646	391	For: 5'-A T C T G G T C C G A A T G C A A G G A-3' Rev:5'-C G T A C A G C C C T T C C G A G A T G-3'	1621-2012
rOrai1	NM_001013982	375	For: 5'-A C G T C C A C A A C C T C A A C T C C-3' Rev: 5'-A C T G T C G G T C C G T C T T A T G G-3'	546-921
rStim1	XM_341896.2	293	For: 5'-A A G C T T A T C A G C G T G G A G G A-3' Rev: 5'-T G A T T G T G G C G A G T C A A G A G-3'	905-1197

Table S2. Oligonucleotide sequences of primers used for Quantitative RT-PCR

Gene	Accession No.	Size(bp)	Primers	Location
rTrpc1	AF061266	105	For: 5'- G G C A G A A C A G C T T G A A G G A G -3' Rev: 5'- G T C G C A T G G A G G T C A G G T A T -3'	2057-2161
rTrpc5	NM_080898	116	For: 5'- T G A G G A G C T C T C C C A A C A G T -3' Rev: 5'- C A A G T T C T T C G C T G T G G T C A -3'	1054-1169
rTrpc6	NM_053559	114	For: 5'- G C A T C A T C G A T G C A A A T G A C -3' Rev: 5'- T G A T C T G A G G A T C G G T A G G G -3'	1664-1777
rOrai1	NM_001013982	117	For: 5'-T C A C T T C T A C C G C T C A C T G G-3' Rev:5'-A G A G A A T G G T C C C C T C T G T G-3'	859-975
rStim1	XM_341896	100	For: 5'-A G C T C C T G G T A T G C T C C T G A-3' Rev:5'-G C C T C T C T G C A T T T T G C T T C-3'	1583-1682

Table S3 Effects of pharmacological agents on calcium entry in NRK fibroblasts.

	SOCE/ ROCE	Growth state	mean	SEM	%	p	n
BHQ (control)	SOCE	Q	0.14	0.01	0		19
BHQ + 2-APB	SOCE	Q	0.028	0.007	-80	<0.001	10
BHQ + SKF96365	SOCE	Q	0.0088	0.0053	-94	<0.001	10
BHQ + Gö6976	SOCE	Q	0.25	0.02	86	<0.001	10
OAG (control)	ROCE	DA	0.11	0.01	0		10
OAG + 2-APB	ROCE	DA	0.044	0.007	-59	<0.001	10
OAG + SKF96365	ROCE	DA	0.033	0.006	-70	<0.001	7
OAG + Gö6976	ROCE	DA	0.20	0.03	82	<0.01	10

Several agents have a profound effect on calcium entry in quiescent and density- arrested NRK fibroblasts. In this table the effect of the agents (2-APB, SKF96365 and Gö6976) on BHQ-induced store-operated calcium entry (SOCE) in quiescent cells (Q) and OAG-induced receptor-operated calcium entry (ROCE) in density-arrested cells (DA), respectively, are shown. The table shows the mean rise of fluorescence ratio (mean) with standard error of means (SEM). In column '%' the percent increase and decrease compared to the control is shown. Significance level of this increase/decrease is shown in column 'p' compared to the control, n denotes the number of experiments. All experiments were performed at room temperature.

References

Alicia, S., Z. Angelica, et al. (2008). "STIM1 converts TRPC1 from a receptor-operated to a store-operated channel: moving TRPC1 in and out of lipid rafts." Cell Calcium **44**(5): 479-491.

Blair, N. T., J. S. Kaczmarek, et al. (2009). "Intracellular calcium strongly potentiates agonist-activated TRPC5 channels." J Gen Physiol **133**(5): 525-546.

Cahalan, M. D. (2009). "STIMulating store-operated Ca(2+) entry." Nat Cell Biol **11**(6): 669-677.

Cornelisse, L. N., R. Deumens, et al. (2002). "Sauvagine regulates Ca2+ oscillations and electrical membrane activity of melanotrope cells of Xenopus laevis." J Neuroendocrinol **14**(10): 778-787.

de Roos, A. D., P. H. Willems, et al. (1997). "Synchronized calcium spiking resulting from spontaneous calcium action potentials in monolayers of NRK fibroblasts." Cell Calcium **22**(3): 195-207.

Dernison, M. M., J. M. Kusters, et al. (2008). "Local induction of pacemaking activity in a monolayer of electrically coupled quiescent NRK fibroblasts." Cell Calcium **44**(5): 429-440.

Flourakis, M., F. Van Coppenolle, et al. (2006). "Passive calcium leak via translocon is a first step for iPLA2-pathway regulated store operated channels activation." FASEB J, **20**(8): 1215-1217.

Gamberucci, A., E. Giurisato, et al. (2002). "Diacylglycerol activates the influx of extracellular cations in T-lymphocytes independently of intracellular calcium-store depletion and possibly involving endogenous TRP6 gene products." Biochem J **364**(Pt 1): 245-254.

Harks, E. G., P. H. Peters, et al. (2005). "Autocrine production of prostaglandin F2alpha enhances phenotypic transformation of normal rat kidney fibroblasts." Am J Physiol Cell Physiol **289**(1): C130-137.

Harks, E. G., W. J. Scheenen, et al. (2003). "Prostaglandin F2 alpha induces unsynchronized intracellular calcium oscillations in monolayers of gap junctionally coupled NRK fibroblasts." Pflugers Arch **447**(1): 78-86.

Hatae, J., N. Fujishiro, et al. (1996). "Spectroscopic properties of fluorescence dye fura-2 with various divalent cations." Jpn J Physiol **46**(5): 423-429.

Jardin, I., J. J. Lopez, et al. (2008). "Orai1 mediates the interaction between STIM1 and hTRPC1 and regulates the mode of activation of hTRPC1-forming Ca2+ channels." J Biol Chem **283**(37): 25296-25304.

Kusters, J. M., J. M. Cortes, et al. (2007). "Hysteresis and bistability in a realistic cell model for calcium oscillations and action potential firing." Phys Rev Lett **98**(9): 098107.

Kusters, J. M., M. M. Dernison, et al. (2005). "Stabilizing role of calcium store-dependent plasma membrane calcium channels in action-potential firing and intracellular calcium oscillations." Biophys J **89**(6): 3741-3756.

Large, W. A., S. N. Saleh, et al. (2009). "Role of phosphoinositol 4,5-bisphosphate and diacylglycerol in regulating native TRPC channel proteins in vascular smooth muscle." Cell Calcium.

Lemonnier, L., M. Trebak, et al. (2008). "Complex regulation of the TRPC3, 6 and 7 channel subfamily by diacylglycerol and phosphatidylinositol-4,5-bisphosphate." Cell Calcium **43**(5): 506-514.

Liu, X., B. B. Singh, et al. (2003). "TRPC1 is required for functional store-operated Ca2+ channels. Role of acidic amino acid residues in the S5-S6 region." J Biol Chem **278**(13): 11337-11343.

Newton, A. C. (2001). "Protein kinase C: structural and spatial regulation by phosphorylation, cofactors, and macromolecular interactions." Chem Rev **101**(8): 2353-2364.

Parekh, A. B. and J. W. Putney, Jr. (2005). "Store-operated calcium channels." Physiol Rev **85**(2): 757-810.

Putney, J. W. (2009). "Capacitative calcium entry: from concept to molecules." Immunol Rev **231**(1): 10-22.

Robinson, J. A., N. S. Jenkins, et al. (2004). "Ratiometric and nonratiometric Ca2+ indicators for the assessment of intracellular free Ca2+ in a breast cancer cell line using a fluorescence microplate reader." J Biochem Biophys Methods **58**(3): 227-237.

Salido, G. M., S. O. Sage, et al. (2009). "TRPC channels and store-operated Ca(2+) entry." Biochim Biophys Acta **1793**(2): 223-230.

Siefjediers, A., M. Hardt, et al. (2007). "Characterization of inositol 1,4,5-trisphosphate (IP3) receptor subtypes at rat colonic epithelium." Cell Calcium **41**(4): 303-315.

Tesfai, Y., H. M. Brereton, et al. (2001). "A diacylglycerol-activated Ca2+ channel in PC12 cells (an adrenal chromaffin cell lin) correlates with expression of the TRP-6 (transient receptor potential) protein." Biochemical Journal **358**(pt 3): 717-726.

Venkatachalam, K., F. Zheng, et al. (2003). "Regulation of canonical transient receptor potential (TRPC) channel function by diacylglycerol and protein kinase C." J Biol Chem **278**(31): 29031-29040.

Zhu, M. H., M. Chae, et al. (2005). "Desensitization of canonical transient receptor potential channel 5 by protein kinase C." Am J Physiol Cell Physiol **289**(3): C591-600.

CHAPTER 5

Role of TRPC Channels, STIM1 and ORAI1 in PGF2α-Induced Calcium Signaling in NRK Fibroblasts

Almirza WH, Peters PH, van Zoelen EJ, Theuvenet AP

Submitted to Cell Calcium

Abstract

Normal rat kidney (NRK) fibroblasts exhibit growth-dependent changes in electrophysiological properties and intracellular calcium dynamics. The transition from a quiescent state to a density-arrested state results in altered calcium entry characteristics. This coincides with modulation of the expression of the genes encoding the calcium channels Trpc1, Trpc6 and Orai1, and of the intracellular calcium sensor Stim1. In the present study we have used gene selective short hairpin (sh) RNAs against these various genes to investigate their role in a) capacitative store-operated calcium entry (SOCE); b) non-capacitative OAG-induced receptor-operated calcium entry (ROCE); and c) prostaglandin $F_{2\alpha}$ ($PGF_{2\alpha}$)-induced Ca^{2+}-oscillations in NRK fibroblasts. Intracellular calcium measurements revealed that knockdown of the genes encoding Trpc1, Orai1 and Stim1 each caused a significant reduction of SOCE in NRK cells, whereas knockdown of the gene encoding Trpc6 reduced only the OAG-induced ROCE. Furthermore, our data show that knockdown of the genes encoding Trpc1, Orai1 and Stim1, but not Trpc6, substantially reduced the frequency (up to 60%) of $PGF_{2\alpha}$-induced Ca^{2+} oscillations in NRK cells. These results indicate that in NRK cells distinct calcium channels control the processes of SOCE, ROCE and $PGF_{2\alpha}$-induced Ca^{2+} oscillations.

Key words: NRK; $PGF_{2\alpha}$; Trpc; SOCE; ROCE; Stim1; Orai1Ca2+ oscillation.

Introduction

In many cell types activation of phospholipase C (PLC)-coupled receptors does not only result in an IP_3-mediated increase in intracellular calcium concentration, but also in enhanced calcium entry across the plasma membrane. In general, two distinct mechanisms for calcium uptake can be discriminated; one is referred to as receptor-operated calcium entry (ROCE), which involves non-selective calcium channels that are activated by phosphatidylinositol 4,5-bisphosphate (PIP_2) metabolites. The other mechanism is referred to as store-operated calcium entry (SOCE) and involves calcium channels that are activated by IP_3-induced depletion of intracellular calcium stores (Putney 1986; Takemura, Hughes et al. 1989; Thastrup, Dawson et al. 1989; Putney 1990; Hoth and Penner 1992; Fasolato, Hoth et al. 1993; Franzius, Hoth et al. 1994). Despite intensive studies the calcium channels specifically involved in ROCE and SOCE have not been identified yet in a conclusive manner.

During the last decade, the mammalian homologues of *Drosophila* canonical Transient Receptor Potential Channels (TRPCs) have been proposed to be involved in both SOCE and ROCE (Fasolato, Hoth et al. 1993; Hardie and Minke 1993; Selinger, Doza et al. 1993). There are seven related members of the TRPC family, designated in humans as TRPC1-7. Based on biochemical and functional similarities, the TRPC family of ion channels can be divided into a number of subfamilies, one consisting of TRPC1, TRPC4 and TRPC5, and another one consisting of TRPC3, TRPC6 and TRPC7 (Parekh and Putney 2005). Based on overexpression and knockdown studies, as well as on pharmacological approaches, it has been proposed that TRPC1 is particularly involved in SOCE and becomes activated upon depletion of intracellular calcium stores (Salido, Sage et al. 2009). Moreover, there is general agreement that members of the TPRC3/TRPC6/TRPC7 subfamily are involved in ROCE, since they can be activated by the diacylglycerol analogue 1-oleoyl-2-acetyl-sn-glycerol (OAG) (Inoue, Okada et al. 2001; Trebak, St et al. 2003; Venkatachalam, Zheng et al. 2003).

The recent identification of two new protein families has helped greatly to better understand the nature and regulation of ion channels involved in SOCE. It has been shown that STIM1 (Stromal Interaction Molecule 1) acts as a Ca^{2+} sensor inside the cell, which links the filling state of the intracellular Ca^{2+} stores to the regulation of plasma membrane Ca^{2+} channels (Williams, Senior et al. 2002; Liou, Kim et al. 2005; Roos, DiGregorio et al. 2005; Zhang, Yu et al. 2005). Knockdown of STIM1 gene expression by siRNA reduced

SOCE in HEK293, SH-SY5Y, Jurkat T, and HeLa cells significantly, indicating that STIM1 plays an essential role in the regulation of this process. In contrast, over-expression of the STIM1 gene only modestly enhanced SOCE in HEK293 cells, indicating that physiological levels of STIM1 are already optimal for SOCE control (Spassova, Soboloff et al. 2006).

Secondly, a new calcium release-activated calcium channel (CRACM1 or ORAI1) has been identified, which acts as a STIM-1 activated calcium channel in lymphocytes (Feske, Gwack et al. 2006; Prakriya, Feske et al. 2006; Vig, Beck et al. 2006; Vig, Peinelt et al. 2006; Yeromin, Zhang et al. 2006; Zhang, Yeromin et al. 2006). Experimental evidence indicates that knockdown of the ORAI1 gene decreases SOCE. A mutation in the ORAI1 gene, resulting in an R91W substitution, has been shown to be responsible for a familial form of Severe Combined Immunodeficiency (SCID) in humans. Interestingly, human cells transfected with the R91W-ORAI1 mutant gene did not only show a reduction in SOCE, but also in ROCE (Liao, Erxleben et al. 2008). Furthermore, there is increasing evidence that STIM1 and ORAI1 can form dynamic complexes with both TRPC1 and TRPC6 (Ong, Cheng et al. 2007; Brechard, Melchior et al. 2008). Several recent studies have revealed that STIM1 regulates the opening of ORAI and TRPC channels. Whereas STIM1 is obligatory for the functioning of ORAI channels (Lalioti, Zhang et al. 2006; Mercer, Dehaven et al. 2006; Peinelt, Vig et al. 2006), TRPC channels appear to be able to function both as STIM1-dependent and STIM1-independent channels. Structural studies have indicated that binding of the so-called SOAR domain of STIM1 is sufficient to mediate activation of ORAI1, but that in the case of TRPC channels this requires the additional binding of the STIM1 polylysine domain (Lee, Yuan et al. 2010). However, the exact mechanism by which STIM1 and ORAI1 regulate SOCE and ROCE, both in the presence and absence of TRPC proteins, is still largely unknown.

Normal rat kidney fibroblasts (NRK) represent an excellent in vitro model system for studying the control mechanisms of cellular growth and phenotypic alterations upon cellular transformation (van Zoelen 1991). Normal rat kidney (NRK) fibroblasts have intracellular calcium dynamics that strongly depend on their growth stage. NRK cells can be grown to confluence in monolayer culture and made quiescent by serum deprivation. The exposure of these quiescent cells to prostaglandin $F_{2\alpha}$ ($PGF_{2\alpha}$) causes individual cells in the monolayer to exhibit calcium oscillations at variable frequency, in spite of their metabolic and electrical, gap junction-mediated coupling (Harks, Scheenen et al. 2003).

When grown to density-arrest following incubation with EGF and insulin, these fibroblasts start to exhibit spontaneous firing of repetitive calcium action potentials, which are associated with near-synchronous Ca^{2+} transients. We have previously shown that $PGF_{2\alpha}$ plays an important role in both processes, since knockdown of the FP receptor gene *(Ptgfr)*, which is specifically activated by $PGF_{2\alpha}$, completely abolishes both the Ca^{2+} transients and the action potentials (Almirza, Dernison et al. 2008).

Previous studies have shown that in NRK cells SOCE is essential for maintaining intracellular calcium homeostasis, including membrane excitability and the refilling of calcium stores (Kusters, Dernison et al. 2005; Parekh and Putney 2005). We have recently presented pharmacological evidence that in NRK fibroblasts SOCE and ROCE are differentially regulated in quiescent and density-arrested cultures (Dernison, Almirza et al. 2010). The aim of the present study was to investigate the role of TRPCs, STIM1 and ORAI1 in these calcium entry mechanisms and in $PGF_{2\alpha}$-induced calcium oscillation in NRK cells, by using a knockdown approach against their individual genes.

Abbreviations

SOCE, store-operated calcium entry; ROCE, receptor-operated calcium entry; TRPC, Transient Receptor Potential Channels; STIM1, Stromal Interaction Molecule 1; CRACM1, calcium release-activated calcium channel; NRK, normal rat kidney; $PGF_{2\alpha}$, Prostaglandin $F_{2\alpha;}$ OAG, 1-Oleoyl-2-*acetyl*-sn-*glycerol*; BHQ, 2,5-Di-*t*-butyl-1,4-benzohydroquinone; ER,endoplasmatic reticulum; IP_3, inositol 1,4,5-trisphosphate; Q-cells, quiescent NRK cells; DA-cells, density-arrested NRK cells.

Materials & Methods

Cell culturing

NRK fibroblasts, NRK-49F (a cell line established from a mixed population of rat kidney and fibroblasts cells), were cultured in bicarbonate-buffered Dulbecco's modified Eagle's medium (DMEM; Invitrogen, Paisley, UK) supplemented with 10% newborn calf serum (NCS; HyClone Laboratories, Logan, UT). Confluent cultures were made quiescent by subsequent incubation for 2-3 days in serum-free DF medium (1:1 mixture of DMEM-Ham's F-12 medium; Invitrogen, UK) supplemented with 30 nM Na_2SeO_3 and 10 μg/ml human transferrin. Density-arrested monolayers were obtained by a subsequent 2-days incubation in the presence of 5 ng/ml EGF (Collaborative Biomedical Products, Bedford, MA) in combination with 5 μg/ml insulin (Sigma, St. Louis, MO).

Total RNA extraction and reverse transcription Polymerase Chain Reaction analysis

Total RNA was isolated and purified by applying Trizol reagent (Invitrogen, Paisley, UK) to NRK monolayer cells according to the manufacturer's instructions. For complementary DNA (cDNA) synthesis, 2 μg of total RNA were reverse transcribed from random hexamer primers using the SUPER SCRIPT II Ribonuclease H^- reverse transcriptase kit (Invitrogen, Paisley, UK). Reverse transcriptase PCR was performed in order to determine mRNA levels of *Stim1* and *Orai1* in NRK cells. Specific primers were designed using Oligo Perfect designed tool (Invitrogen, Paisley, UK). PCR amplification was performed using a PERKIN ELMER Gene Amp PCR System 2400 (Norwalk, CT, USA) using 2 μl of first-stranded cDNA reaction, 150 pmol of each degenerate primer, 50 μM dNTPs, 2 U Bio Therm Taq polymerase and 2.5 mM $MgCl_2$ in total volume of 50 μl. Following a hot start (3 min at 94 ^{0}C), the sample was subjected to 30 cycles of 30 sec at 94 ^{0}C, followed by 30 sec at 60 ^{0}C, 30 sec at 72 ^{0}C, and a final extension for 7 min at 72 ^{0}C. Reaction products were separated by standard agarose gel electrophoresis and cloned into the pCR-2.1 TOPO vector (Invitrogen) using the protocol supplied by the manufacturer. The identity of the inserts was subsequently confirmed by ABI PRISM sequencing. Table 1 shows the designed primers used for *Stim1* and *Orai1* (rat sequences) with their amplified product size, whereby the identity of the products was confirmed by direct sequencing.

Real-Time quantitative PCR analysis

For real-time quantitative RT-PCR analysis, the ABI Prism Sequence Detection System 5700 and Primer Expressk software (PE Biosystems, USA) were used. For each gene, a set of primers was designed using sequences obtained from Genbank (Table 2). Prior to complementary DNA (cDNA) synthesis, 2 μg of total RNA were treated with DNase for 15 min at 37 ^{0}C, after which RNA was reverse transcribed from random hexamer primers using the SUPERSCRIPTk II reverse

transcriptase kit (Invitrogen, Paisley, UK). Subsequently, 0.2 μg of total cDNA was amplified using SYBR Green PCR Mastermix (Applied Biosystems, USA) under the following conditions: initial denaturation for 10 min at 95 ^{0}C, followed by 40 cycles consisting of 15 sec at 94 ^{0}C and 1 min at 60 ^{0}C. Expression values were calculated from threshold cycles at which an increase in reporter fluorescence above baseline signal was first detected (CT).

shRNA constructs, virus production and cell infections

In order to knockdown the expression of rat *Trpc1, Trpc6, Stim1 and Orai1*, at least two different sets of siRNAs sequences were chosen by entering the nucleotide sequence of each gene into the web-based design tool from Dharmacon (http://design.dharmacon.com). Verification of these siRNA sequences for their specificity by BLAST database search did not show significant homology to any other known gene sequence in the human, mouse and rat genome. Specific and control short hairpin (shRNA) template oligonucleoties were designed by entering the siRNA target sequences into the siRNA Wizard web-based design tool (http://www.sirnawizard.com/construct.php) (Table 3).

The obtained complementary oligonucleotides were synthesized by Sigma-Aldrich (UK), annealed, and ligated into the linearized pSUPER.retro puro vector (Oligo Engine, Seattle WA, USA) according to pSUPER RNAi system protocol.

The resulting constructs, shRNA-Trpc1, shRNA-Trpc6, shRNA-Stim1, shRNA-Orai1 and control shRNA, were transfected into the Phoenix packaging cell line (Nolan Lab, Stanford, USA) in order to produce ecotropic retroviral supernatants. A negative control vector, expressing a hairpin shRNA with limited homology to any known sequences in rat genome, was used as a control. Phoenix cells were seeded in tissue culture dishes in DMEM supplemented with 10% NCS and pre-treated with chloroquine at a final concentration of 25 μM. One day before transfection, Phoenix cells were seeded in culture dishes at a density of $4.0x10^4$ cells/cm^2 in order to reach 60% confluence at the time of transfection. Cells were then transfected with 20 μg of viral vector DNA using the calcium–phosphate precipitation method (Wigler, Silverstein et al. 1977; Chen and Okayama 1987). After 48 hours of transfection, the culture medium was filtered through a 0.45 μm filter and the viral supernatant was used for infection of NRK cells pre-treated with 4 μg/ml of polybrene (Sigma, USA). After infection, NRK cells were incubated for 24 hours at 37 ^{0}C. Subsequently, the medium was replaced by fresh virus-free medium and NRK cells were allowed to recover for 48 hours at 37 ^{0}C. Infected cells were selected by culturing them in the presence of puromycin (6 μg/ml) for 5 days. Target gene expression in NRK wild-type cells, empty vector cells and shRNA producing cells was analyzed by real-time quantitative RT-PCR and Western blot analysis, as described in detail below.

Western blot analysis

NRK cells were plated in dishes at a density of $1.9x10^4$ cells/cm^2 under the conditions described above. Cells were then lysed in lysis buffer (50 mM Tris-HCl, pH 7.5, 2 mM EDTA, 100 mM NaCl, 1% Triton X-100 and protease inhibitor mixture), supplemented with 50 mM NaF, 1 mM Na_3VO_4, and 10 mM β-glycerol phosphate. Cell lysates were incubated for 1 hour on ice and centrifuged at 12,000xg to collect supernatants. Protein concentration in the supernatants was measured by the Bradford method (Bradford 1976). After addition of sample buffer and boiling of this suspension, 75 μg of the denatured proteins were separated on 10% SDS–PAGE gels and subsequently transferred to nitrocellulose papers. After a 1-hour blocking period, nitrocellulose papers were incubated with specific antibodies. The primary antibodies used were: monoclonal anti-Stim1 and polyclonal anti-Trpc1, both form Santa Cruz Biotechnology (Santa Cruz, USA); polyclonal anti-Orai1 antibodies from Bio Cat GmbH (Germany) and polyclonal anti-Trpc6 and anti-Actin antibodies from Sigma Aldrich (UK). HRP-conjugated secondary antibodies were purchased from Santa Cruz Biotechnology. Immunolabelling was visualized using the ECL procedure (Amersham Biosciences, USA). Bands were quantified by densitometric image analysis software (Image Master VDS, Pharmacia Biotech, Uppsala, Sweden).

Intracellular Ca^{2+} measurements

Glass coverslips grown with quiescent monolayers of NRK fibroblasts were placed in a Leiden cell chamber and loaded for 30 min at room temperature with 4 μM Fura-2/AM (Invitrogen, Paisley, UK) in serum-free DF medium. Medium was replaced by Ca^{2+}-free HEPES-buffered saline (Ca^{2+}-free HBS, containing 143 mM NaCl, 5 mM KCl, 1 mM $MgCl_2$, 10 mM glucose, 10 mM HEPES-KOH, pH 7.4). Ca^{2+}-containing HEPES-buffered saline (Ca^{2+}-containing HBS, containing 128 mM NaCl, 10 mM $CaCl_2$) was added to an equal amount of Ca^{2+}-free medium to obtain a 5 mM Ca^{2+}-containing medium in the Leiden chamber. Dynamic calcium video imaging was performed as described (Cornelisse, Deumens et al. 2002). Excitation wavelengths of 340 nm and 380 nm (bandwidth 8-15 nm) were provided by a 150 W Xenon lamp (Ushio UXL S150 MO, Ushio, Tokio, Japan), while fluorescence emission was monitored above 440 nm, using a 440 nm DCLP dichroic mirror and a 510 nm emission filter (40 nm bandwidth) in front of the camera. Image acquisition, using a camera pixel binning of 4 and computation of ratio images (F340/F380), was every 4 sec and operated through Metafluor software v.6.2 (Universal Imaging Corporation, Downingtown, PA, US). Camera acquisition time was 100 msec per excitation wavelength.

Data analysis

Each experiment was performed at least 5 times; per experiment 50 to 60 cells were recorded. The traces of these cells were averaged per experiment and further analyzed. Mean values of cytosolic calcium increase via release and influx was determined by dividing the mean value of 5 data points

before increase (R0 and R2 for respectively Ca^{2+}-release and –influx) by the mean value at maximum ratio levels after release and influx (R1 and R3 respectively). Student's *t*-test was used for statistical comparisons. Numeric data are represented as mean ± SEM throughout this article, whereby *n* represents the number of replicates of each experiment. Frequency of calcium oscillations was determined by counting the peaks using 'pick peak' algorithm of Origin 6.0 (Microcal, Northampton, MA, US), using a minimal peak height of 10% of the total signal as selection criteria.

Table 1. Oligonucleotide sequences of primers used for Quantitative RT-PCR

Gene	Accession No.	Size bp	Primers	Location
rTrpc1	AF061266	105	For: 5-GGCAGAACAGCTTGAAGGAG-3 Rev:5-GTCGCATGGAGGTCAGGTAT-3	2057-2161
rTrpc6	NM_053559	114	For: 5-GCATCATCGATGCAAATGAC-3 Rev:5-TGATCTGAGGATCGGTAGGG-3	1664-1777
rOrai1	NM_001013982	117	For: 5-TCACTTCTACCGCTCACTGG-3 Rev:5-AGAGAATGGTCCCCTCTGTG-3	859-975
rStim1	XM_341896	100	For: 5-AGCTCCTGGTATGCTCCTGA-3 Rev:5-GCCTCTCTGCATTTTGCTTC-3	1583-1682
Rat 18s rRNA	XM_341896	109	For: 5-CGGCTACCACATCCAAGGAA-3 Rev:5-GCTGGAATTACCGCGGCT-3	462-571

Table 2. Target sequences for constructing shRNA specific for TRPC homologs

Gene	Accession No.	Hairpin oligonucleotide sequences (5'-3') target sequence printed in bold	Location
rTrpc1	AF061266	For:GATCCCC**GGGTGACTATTATATGGTT**TTCAAGAGAAACCATATAATAGTCACCCTTTTTA Rev:AGCTTAAAAAGGGTGACTATTATATGGTTTCTCTTGAAAACCATATAATAGTCACCCGGG	246-264
rTrpc6	NM_053559	For:GATCCCC**TCGAGGACCAGCATACATGTT**CAAGAGACATGTATGCTGGTCCTCGATTTTTA Rev:AGCTTAAAAATCGAGGACCAGCATACATGTCTCTTGAACATGTATGCTGGTCCTCGAGGG	670-678
rOrai1	NM_001013982	For:GATCCCC**GCAACGTCCACAACCTCAACT**TTCAAGAGAAGTTGAGGTTGTGGACGTTGCTTTTTA Rev:AGCTTAAAAAGCAACGTCCACAACCTCAACTTCTCTTGAAAGTTGAGGTTGTGGACGTTGCGGG 3	543-563
rStim1	XM_341896	For:GATCCCC**GCATGGAAGGCATCAGAAGTGTAT A**TTCAAGAGATATACACTTCTGATGCCTTCCATGCTTTTTA Rev:AGCTTAAAAAGCATGGAAGGCATCAGAAGTGTATATCTCTTGAATATACACTTCTGATGCCTTCCATGCGGG	635-655
control		For:GTACCCC**AATTCTCCGAACGTGTCAG**TTCAAGAGACTGACACGTTCGGAGAATTTTTTTA Rev:AGCTTAAAAAAATTCTCCGAACGTGTCAGTCTCTTGAACTGACACGTTCGGAGAATTGGG	

Results

Effect of knockdown of Trpc1 and Trpc6 on SOCE in NRK cells

We recently reported on the differential role for SOCE and ROCE in the calcium dynamics of quiescent and density-arrested NRK fibroblasts. Furthermore, we have shown that NRK fibroblasts express Trpc1 and Trpc6, and that expression of these proteins depends on the growth stage of the NRK fibroblasts (Dernison, Almirza et al. 2010). In the present study we have investigated the role of these various calcium channel proteins in mediating Ca^{2+} entry during the different NRK growth stages. For this we employed an shRNA approach to generate stable NRK cell lines in which the expression of specific *Trpc* genes was targeted and the resulting mRNA and protein levels were subsequently monitored by quantitative RT-PCR and Western blotting. Fig.1A shows that in NRK cells transfected with shRNA against *Trpc1* gene (dTRPC1 cells) the mRNA level of *Trpc1* was reduced to 37.6 ± 5.8 % (n=4), when compared to control cells that were transfected with control shRNA, while no effect on *Trpc1* expression was observed in cells transfected with shRNA against *Trpc6* (dTRPC6 cells). On the other hand, *Trpc6* expression was reduced to 39.8 ± 2.6 % (n=4) in dTRPC6 cells, while no reduction was observed in dTRPC1 cells (Fig. 1B). Western blot analysis showed a significant reduction in expression of Trpc1 protein in dTRPC1 cells, without affecting the protein level of Trpc6 (Fig.1C). Similarly, the protein level of Trpc6, but not of Trpc1, was reduced in dTRPC6 cells (Fig. 1D), when compared to the expression level of smooth muscle α- actin. These results indicate that expression of Trpc channels can be selectively repressed by an shRNA-mediated knockdown approach.

Effect of knockdown of Trpc1 and Trpc6 on store-operated Ca^{2+} entry (SOCE)

In order to study the role of specific Trpc channels on SOCE in quiescent NRK cells, single-cell Ca^{2+} imaging experiments were performed, in which BHQ-treated cells were changed from a nominal calcium-free medium to a medium containing 5 mM Ca^{2+}, and the resulting increase in Fura-2 fluorescence was quantified. Fig. 2A shows the obtained traces for control cells, dTRPC1 cells and dTRPC6 cells. Upon averaging (Fig. 2B) our data show that in quiescent NRK cells the increase in calcium uptake was significantly reduced in dTRPC1 cells (to 44.7 ± 9.2%; n=5) when compared to control cells, while no significant effect was observed in dTRPC6 cells. Also in density-arrested cells, in which expression of Trpc6 is upregulated six-fold (Dernison, Almirza et al. 2010), we observed no difference in SOCE between BHQ-treated control and dTRPC6 cells, which was -

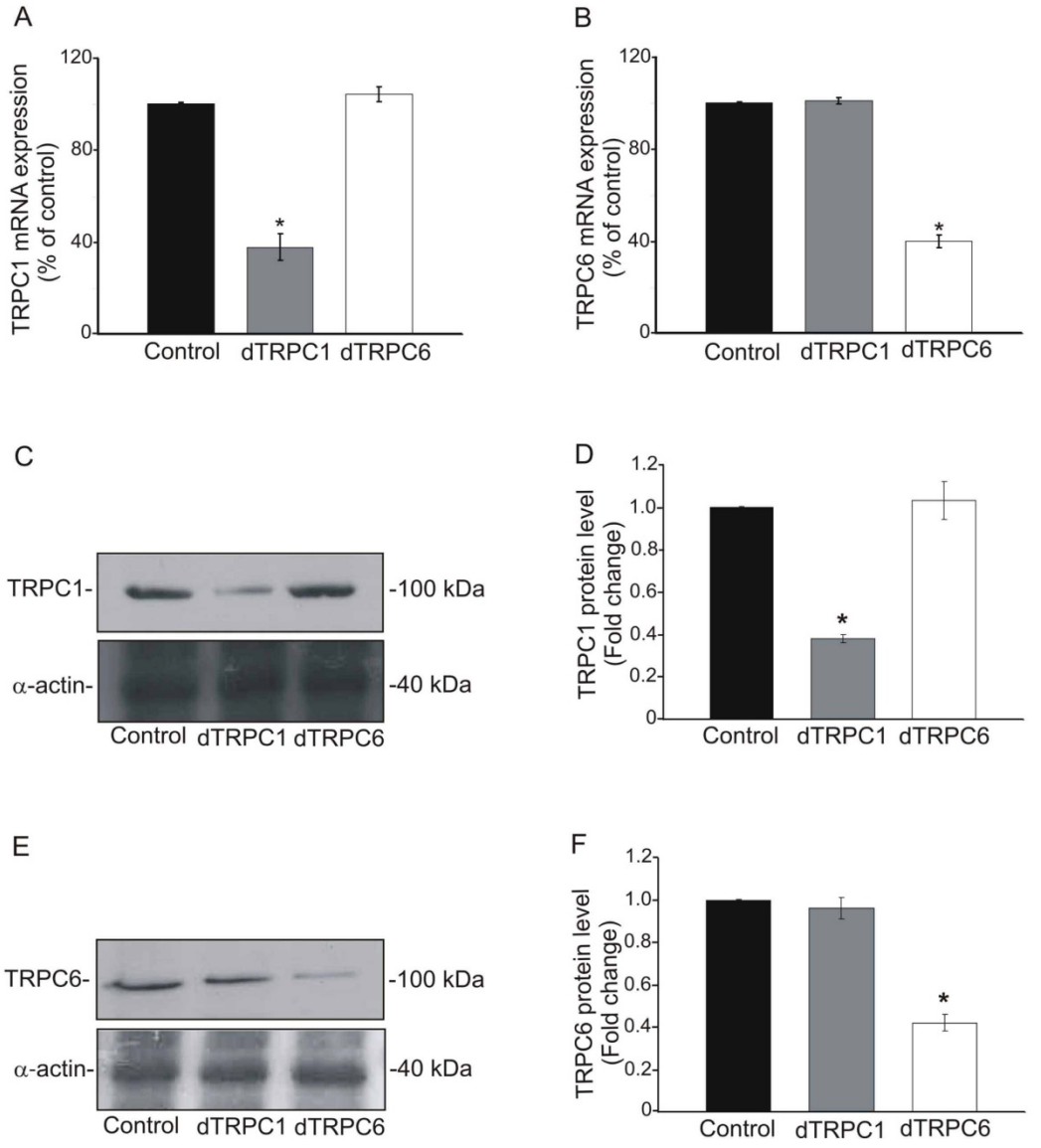

Fig. 1. Assessment of *Trpc1* and *Trpc6* expression in NRK cells stably expressing shRNA targeting specific Trpc genes. (A and B) NRK cells stably expressing shRNA constructs specific for *Trpc1* (dTRPC1 cells, dark grey), *Trpc6* (dTRPC6 cells, light grey) and control shRNA (control cells, black) were established. Quantitative PCR analysis of mRNA levels for *Trpc1* (A) and *Trpc6* (B) is shown for each of the three cell lines and expressed relative to control cells. Data represent mean and SEM of at least four independent experiments. Asterisk denotes a significant difference ($p<0.05$) compared to control cells. (C and D) Western blot analysis of Trpc1 and Trpc6 levels in whole cell lysates of three cell lines, as visualized by specific antibodies against rat Trpc1 (C) and Trpc6 (D). Staining with antibodies against rat α-actin was used as a loading control.

assayed in the presence of nifedipine to prevent spontaneous calcium action potentials (figure 2C and 2D).This observation argues against the possibility that expression levels of Trpc6 are too low to contribute significantly to SOCE.

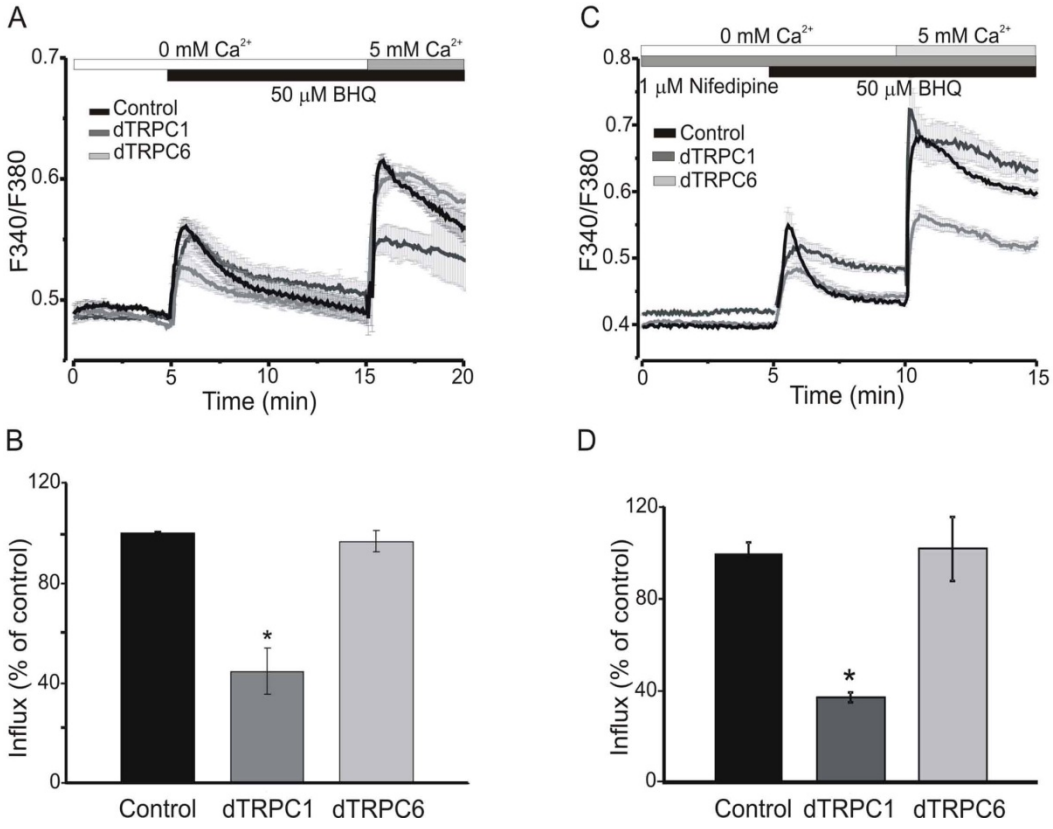

Fig. 2. Effect of knockdown of *Trpc1* and *Trpc6* on store-operated calcium entry in quiescent NRK cells. BHQ-induced store operated calcium entry in quiescent cells (A) and density-arrested cells (C) of control (black), dTRPC1 (dark gray) and dTRPC6 (light gray) cells. Cells were loaded with Fura 2-AM for 30 min and treated with BHQ (50 μM) in the absence of Ca^{2+}. After depletion of the calcium stores (first phase of calcium increase), 5 mM of extracellular Ca^{2+} were added and ion uptake was measured as a function of time (second phase of calcium increase). The traces are averages of 45 cells from a single experiment. All recordings in density-arrested cells were performed in presence of nifedipine to prevent entry of calcium through L-type calcium channels. The gray band around the traces represents the SEM-error bars for every data point. (B and D) Data summarized for the amplitude of the calcium influx (second phase), expressed as mean ± SEM for at least 5 independent experiments. Asterisk denotes a significant difference ($p<0.05$) compared to control cells.

Effect of knockdown of Trpc1 and Trpc6 on receptor-operated Ca^{2+} entry (ROCE)

We have recently shown that both quiescent and density-arrested NRK cells exhibit SOCE, while only density-arrested cells exhibit ROCE. In order to determine the role of Trpc1 and Trpc6 in ROCE of density-arrested NRK cells, the increase in intracellular calcium was measured following addition of OAG, a membrane permeable DAG analogue, to nifedipine-treated dTRPC1, dTRPC6 and control cells. Fig. 3A (traces) and 3B (statistics) show that in dTRPC6 cells OAG-induced calcium entry was significantly reduced (to 54.1% ± 8.9%; N=4) when compared to control cells, while no reduction was observed in dTRPC1 cells. These result show that Trpc6, but not Trpc1, is involved in ROCE in density-arrested NRK cells, which is in line with the observation that *Trpc6* expression is upregulated six-fold when quiescent NRK cells are grown to density-arrest.

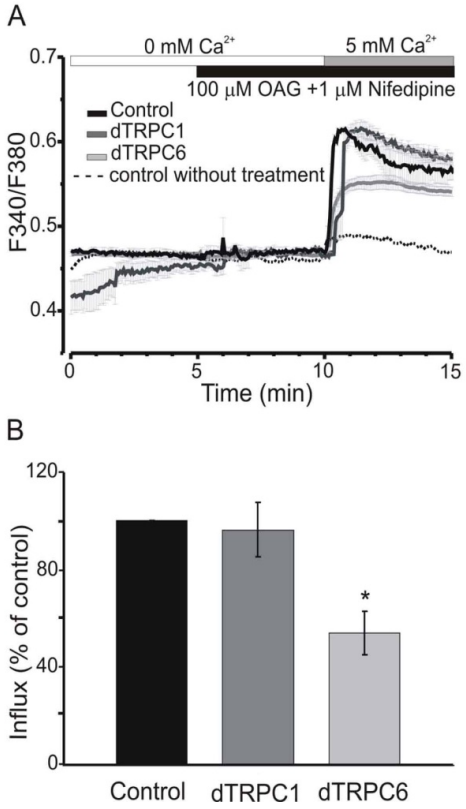

Fig. 3. **Effect of knockdown of *Trpc1* and *Trpc6* on receptor-operated calcium entry in density-arrested NRK cells.** (A) Density-arrested control (black), dTRPC1 (dark gray) and dTRPC6 (light gray) cells were loaded with Fura-2AM and treated with OAG (100 μM) and nifedipine (1 μM), after which the amplitude of the influx of Ca^{2+} was measured. The traces are averages of 45 cells from a single experiment, as representative for four independent experiments. (B) Data summarized for the amplitude of OAG-induced Ca^{2+}-entry upon addition of 5 mM-extracellular Ca^{2+} (peak-entry). Data represent mean ± SEM for at least 5 independent experiments, whereby the asterisk denotes a significant difference ($p<0.05$) compared to control cells.

Knockdown of Stim1 and Orai1in NRK fibroblasts

In order to determine the potential involvement of Stim1 and Orai1 in Ca^{2+} entry in NRK cells, we stably transfected these cells with an shRNA-expressing vector to target either of these genes. Figure 4A shows that in cells expressing *Stim1* shRNA (dSTIM1 cells) the *Stim1* mRNA level was reduced to 41.3 ± 5.3% (n=3) compared to control transfected cells, while Fig. 4B shows that in cells expressing *Orai1* shRNA (dORAI1 cells) the *Orai1* mRNA level was reduced to 49.2 ± 2.4% (n=3) compared to control transfected cells. Western blot analysis confirmed that a reduction in mRNA level resulted in a specific reduction of Orai1 and Stim1 protein levels in dSTIM1 and dORAI1 cells (Fig. 4C,D).

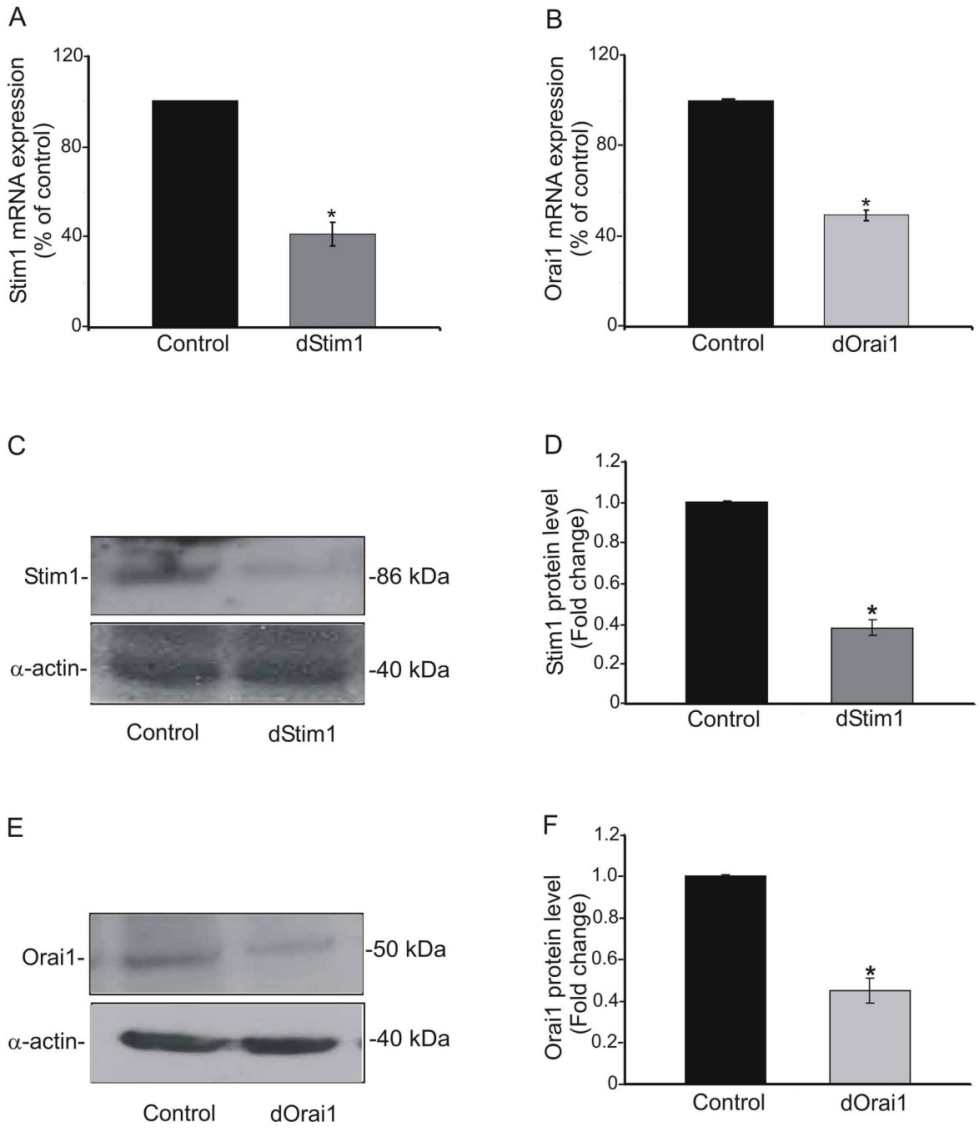

Fig. 4. Effect of knockdown of *Stim1* and *Orai1* on expression levels in NRK fibroblasts.

NRK cells were stably transfected with either shRNA against *Stim1* (dSTIM1 cells) or against *Orai1* (dORAI1 cells). (A) Quantitative PCR analysis of *Stim1* RNA levels in quiescent NRK control cells and

dSTIM1 cells. (B) Quantitative PCR analysis of *Orai1* RNA levels in quiescent NRK control cells and dORAI1 cells. Single PCR products were identified in NRK cells for *Stim1* (A) and *Orai1* (B) of the expected size. Data are representative of three independent experiments, carried out in duplicate. Asterisk denotes a significant difference ($p<0.05$) compared to control cells. (C) Western blot analysis of Stim1 in control cells and dSTIM cells, using antibodies against rat Stim1. (D) Western blot analysis of Orai1 in control cells and dORAI1 cells, using antibodies against rat Orai1. Antibodies against rat α-actin were used as a loading control.

Effect of knockdown of Stim1 and Orai1 on SOCE in NRK cells

Figure 5 shows that addition of 5 mM Ca^{2+} to BHQ-treated dSTIM1 and dORAI1 cells in the quiescent state resulted in a reduced Ca^{2+} uptake, when compared to control NRK cells. When averaging over 225 cells in 5 independent experiments, a reduction in calcium influx to 65.1 ± 6.4% was observed for dSTIM1 cells, and to 56.9 ± 4.1% for dORAI1 cells. These results show that *Orai1* or *Stim1* are both directly involved in store-operated Ca^{2+} entry in NRK cells.

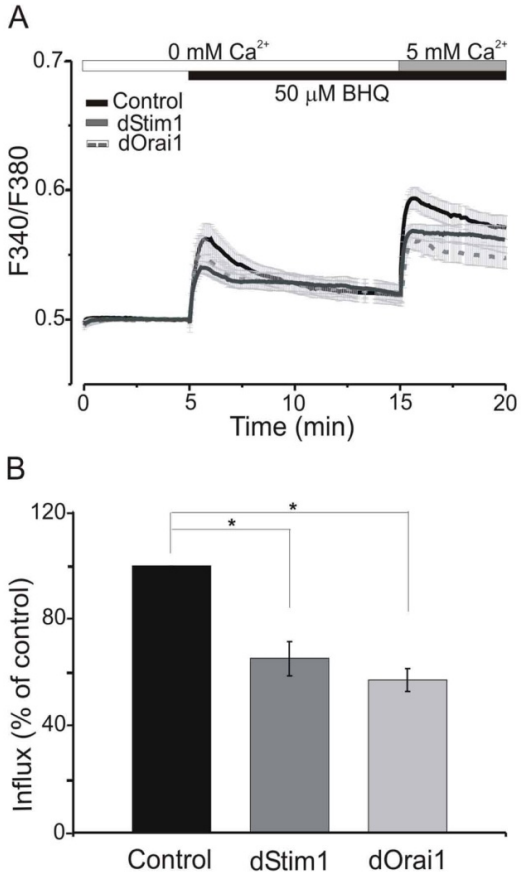

Fig. 5. Effect of knockdown of *Stim1* and *Orai1* on store-operated Ca^{2+} entry in NRK fibroblasts.

(A) Comparison of 5 mM Ca^{2+}-induced calcium entry in BHQ-treated NRK control, dSTIM1 and dORAI1 cells. Each trace is the average of 45 cells from a single experiment, which is representative for five distinct

experiments. (B) Data summarized for control cells, dSTIM1 and dORAI1 cells, whereby the peak values of Ca^{2+} entry were averaged over all 5 experiments (mean ± SEM). Asterisk denotes a significant difference ($p<0.05$) compared to control cells.

Effect of knockdown of Trpc1, Stim1, and Orai1 on PGF2α -induced Ca^{2+} oscillations

We have previously shown that addition of PGF2α to quiescent NRK cells induces calcium oscillations in more than 90% of the cells in the monolayer, with a frequency that is highly variable between individual cells. The initial calcium peak results from intracellular calcium release from IP_3-sensitive stores, whereas the subsequent calcium transients are mediated by interplay between IP_3-sensitive calcium stores and an influx of extracellular calcium (Harks, Scheenen et al. 2003). Since constitutive Ca^{2+} entry is needed for sustained Ca^{2+} oscillations and our above data show that Trpc1, Orai1 and Stim1 are all three involved in capacitative Ca^{2+} entry of NRK cells, we hypothesized that these proteins may play an important role in the maintenance of Ca^{2+} oscillations induced by PGF2α.

To investigate this hypothesis, we examined the effect of knockdown of *Trpc1*, *Trpc6, Orai1* and *Stim1* on the Ca^{2+} oscillations induced by 100 nM PGF2α in quiescent NRK monolayers. Figure 6A shows a typical example of PGF2α-induced Ca^{2+} oscillations in NRK control monolayers, whereby the oscillations in individual cells differ in their frequency, but show a sustained character as long as 1 mM Ca^{2+} is present in the extracellular medium. In dSTIM1, dORAI1 and dTRPC1 cells (Fig. 6B, 6C and 6D, respectively), the frequency of these oscillations was significantly reduced following PGF2α treatment, whereas no effect of Trpc6 knockdown was observed on the Ca2+ oscillation in dTRPC6 cells.

Because of the high variability of these oscillations, we analyzed 253 individual cells in 5 independent monolayer cultures. The PGF2α-induced calcium responses were divided into three categories, characterized as either: (i) no secondary transients after an initial calcium transient, (ii) less than five secondary transients after an initial calcium transient within a time frame of 15 min, (iii) five or more secondary calcium transients within a time frame of 15 min (Fig. 6E). The data show that in control populations the majority of cells (89.0 ± 9.2%) have a dominant response of 5 or more secondary transients within 15 min after stimulation with PGF2α. In contrast in dSTIM1, dORAI1 and dTRPC1 cultures, the cells predominantly showed less than 5 transients within 15 min: 82.5 % of the dSTIM1 cells, 75% of the dORAI1 cells and 55% of the dTRPC1 cells. In contrast, no significant

difference in oscillation frequency was observed between dTRPC6, in which 87.5% have a dominant response of 5 or more secondary transients within 15 min, and control cells after stimulation with $PGF_{2\alpha}$. . These data show that knockdown of either *Stim1*, *Orai1* or *Trpc1* results in a reduced frequency of Ca^{2+} oscillations induced by $PGF_{2\alpha}$. These results support previously published observations that constitutive calcium entry across the plasma membrane is required to maintain calcium oscillations (Harks, Scheenen et al. 2003), and further underline that Stim1, Orai1 and Trpc1 are all three involved in store-operated calcium entry in NRK cells.

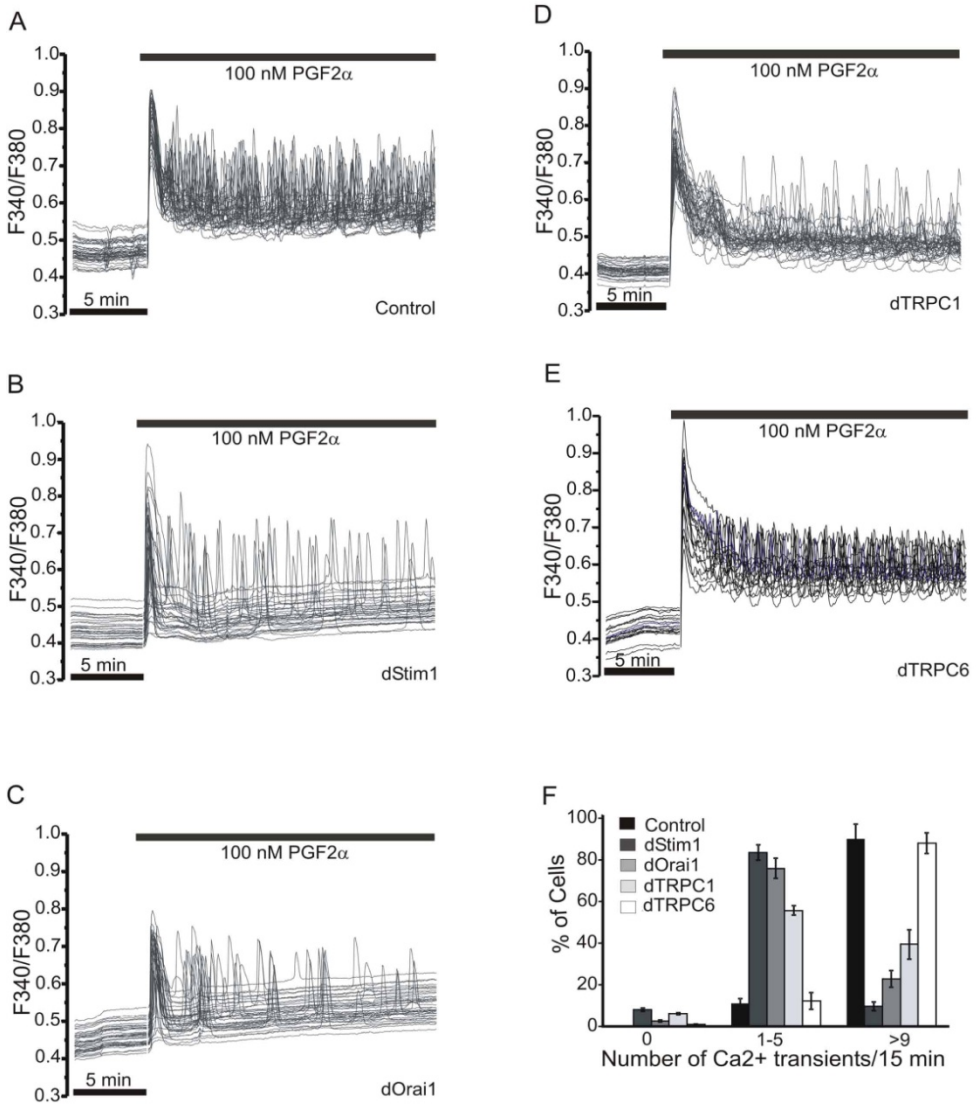

Fig. 6. **Effect of knockdown of *Stim1*, *Orai1* and *Trpc1* on $PGF_{2\alpha}$- induced calcium oscillations in NRK fibroblasts.** Single cell dynamic calcium video imaging measurements were carried out on Fura-2 AM loaded quiescent NRK control cells (A), dSTIM1 cells (B), dORAI1 cells (C), dTRPC1 (D) and dTRPC6 cells (E) after stimulation with 100 nM $PGF_2\alpha$ in the presence of 1 mM of extracellular Ca^{2+}. (F) For each individual cell, the oscillation frequency was determined by the number of Ca^{2+} spikes during a 15 min

interval after the initial peak induced by agonist treatment. Based on these data cells were divided into three categories: no oscillations; 1-5 oscillations; 6 or more oscillations. At least 40 to 50 traces were analyzed in each preparation of 5 independent experiments for each cell line and data are presented as the mean ± SEM.

Discussion

The aim of the present study was to investigate the molecular components that play a role in the influx of extracellular Ca^{2+} in NRK fibroblasts. Here we show that NRK cells express various members of the Trpc family of calcium transporters, as well as Stim1 and Orai1, which have both been involved in capacitive calcium entry. Using an shRNA approach against these various transporters, we have shown that Trpc1, Stim1 and Orai1 are particularly involved in store-operated calcium entry, while Trpc6 is mainly involved in receptor-operated calcium entry in these cells. Our data furthermore indicated that knockdown of either *Trpc1*, *Stim1* or *Orai1* results in a reduced frequency of $PGF_{2\alpha}$-induced Ca^{2+} oscillations in NRK cells, indicating that uptake of extracellular calcium is important for continuation of these oscillations. In combination, our data indicate that Trpc1, Stim1 and Orai1 interplay in regulating calcium uptake in NRK cells under conditions that intracellular calcium stores have become depleted.

Initially, we tested at least three different shRNA constructs for each gene to downregulate its expression, and chose the one which induced the highest reduction in mRNA level, as measured by quantitative PCR, and protein level, as measured by Western blotting. In none of the cases did stable transfection with an shRNA against one of these genes affect expression of any of the other transport genes. This was also true for the various *Trpc* genes, in spite of their sequence homology (see Fig. 1).

Our previous studies have indicated that density-arrested NRK cells produce and secrete low amounts of $PGF_{2\alpha}$ (Harks, Peters et al. 2005). This prostaglandin is able to activate a Gq-protein-coupled FP receptor, which results in PLC-dependent hydrolysis of PIP_2 into IP_3 and DAG. As a result density-arrested NRK cells can show an increased level of intracellular DAG, which is sufficient to activate ROCE. Our observation that density-arrested cells but not quiescent NRK cells exhibit ROCE, may be related to the six-fold increase in *Trpc6* expression which is observed when quiescent cells are grown to density-arrest (Dernison, Almirza et al. 2010). Our observation that Trpc6 is involved in ROCE is in agreement with the general hypothesis that members of the TRPC3/TRPC6/TRPC7 subfamily form receptor-operated and not store-operated calcium channels (Trebak, St et

al. 2003). However, several other studies have recently reported that TRPC6 may also be involved in SOCE (Brechard, Melchior et al. 2008; El Boustany, Bidaux et al. 2008; Redondo, Jardin et al. 2008). The other OAG-inducible channels, Trpc3 and Trpc7, are not detectable in NRK cells, but we have shown that in addition to Trpc1 and Trpc6, these cells also express Trpc5 (Dernison, Almirza et al. 2010). We were able to generate knockdown of *Trpc5* by a specific shRNA that resulted in 85% reduction of the *Trpc5* transcript (data not shown). However, we did not observe any effect on either the BHQ-induced calcium entry (SOCE) or on the OAG-induced calcium entry (ROCE) in NRK cells. The latter result may be explained by the observation that TRPC5 may become desensitized by PKC upon treatment of cells with the DAG analogue OAG (Zhu, Chae et al. 2005). Moreover, *TRPC5* overexpression studies in HEK293 and DT40 cells have shown that this channel is not activated upon depletion of intracellular calcium stores following addition of thapsigargin (Venkatachalam, Zheng et al. 2003).

We have previously shown that the mRNA level of Trpc6 was dramatically increased, but not that of Trpc1 in DA state (Dernison, Almirza et al. 2010). However, according to this study, knock down of Trpc1, but not TRPC6 was related to the oscillation frequency of DA cells, which indicates that Trpc1 seems not to be related with enhanced oscillation in DA cells. This contradictory result can be explained by the fact that the expression level of Trpc1 in quiescent and density-arrested NRK cells did not change comparing to Trpc6. In addition, Trpc1 expression level is much higher than Trpc6 level even after these growing to density-arrested stage. Therefore, it can be safely assumed that the contribution of the Trpc6 channels are additive or Trpc1 has the major effect on the Ca2+ entry and as consequence Ca^{2+} oscillation.

Further, in the present study, we showed that reduction of Trpc6 by shRNA did not have any effect on $PGF_{2\alpha}$-induced Ca^{2+} oscillation in NRK cells which is in contrast to previous report (Li, Zacharia et al. 2008) that shows that knockdown of TRPC6 by siRNA results in decreased oscillation by AVP and OAG in A7r5 cells. Again, this might be explained by the fact that Trpc1 functioned as a major route for Ca^{2+} entry in the presence of agonist, despite the upregulation of Trpc6 expression level and on the other hand, recent study in native vascular myocytes have shown that stimulation by angiotensin II resulted in inhibition of TRPC6 channels by TRPC1/C5 channel activity through a Ca^{2+}- and PKC-dependent mechanism (Shi, Ju et al. 2010). So this suggest that the function of Trpc channels is extremely cell-type dependent.

Finally, our results show that individual knockdown of *Trpc1*, *Orai1* or *Stim1* reduced SOCE in NRK cells to a similar extent. This may indicate that a complex of these three proteins mediates SOCE. Although TRPC6 and ORAI1 can clearly function independently of each other and have different channel properties when activated by STIM1 (Zeng, Yuan et al. 2008), abundant evidence supports the formation of heteromeric complexes of these proteins. First, overexpression of *ORAI1* into TRPC1 expressing cells induced enhanced SOCE, which suggests a functional association between ORAI1 and TRPC channels (Liao, Erxleben et al. 2007). Biochemically it has been shown that ORAI1 interacts with both the C- and N-terminal region of TRPC channels. Furthermore, it has been shown in human salivary gland cells that STIM1 assembles with the ORAI1/TRPC1 complex and that all three proteins are essential for generation of SOCE in these cells (Ong, Cheng et al. 2007). This important finding could indicate that in NRK cells Trpc6-mediated ROCE functions independently of Stim1 activity, while SOCE may require the assembly of a Trpc1-Stim1-Orai1 ternary complex. Verification of these hypotheses will require further research, as well as of the mechanism whereby DAG and IP_3 can activate the two modes of calcium entry upon FP receptor activation.

Acknowledgement

This research project was funded in part by the Netherlands Organization for Scientific Research (NWO; project 805.47.066).

References

Almirza, W. H., M. M. Dernison, et al. (2008). "Role of the prostanoid FP receptor in action potential generation and phenotypic transformation of NRK fibroblasts." Cellular signalling **20**(11): 2022-2029.

Bradford, M. M. (1976). "A rapid and sensitive method for the quantitation of microgram quantities of protein utilizing the principle of protein-dye binding." Analytical biochemistry **72**: 248-254.

Brechard, S., C. Melchior, et al. (2008). "Store-operated Ca2+ channels formed by TRPC1, TRPC6 and Orai1 and non-store-operated channels formed by TRPC3 are involved in the regulation of NADPH oxidase in HL-60 granulocytes." Cell Calcium **44**(5): 492-506.

Chen, C. and H. Okayama (1987). "High-efficiency transformation of mammalian cells by plasmid DNA." Molecular and cellular biology **7**(8): 2745-2752.

Cornelisse, L. N., R. Deumens, et al. (2002). "Sauvagine regulates Ca2+ oscillations and electrical membrane activity of melanotrope cells of Xenopus laevis." J Neuroendocrinol **14**(10): 778-787.

Dernison, M. M., W. H. Almirza, et al. (2010). "Growth-dependent modulation of capacitative calcium entry in normal rat kidney fibroblasts." Cellular signalling **22**(7): 1044-1053.

El Boustany, C., G. Bidaux, et al. (2008). "Capacitative calcium entry and transient receptor potential canonical 6 expression control human hepatoma cell proliferation." Hepatology **47**(6): 2068-2077.

Fasolato, C., M. Hoth, et al. (1993). "Ca2+ and Mn2+ influx through receptor-mediated activation of nonspecific cation channels in mast cells." Proceedings of the National Academy of Sciences of the United States of America **90**(7): 3068-3072.

Feske, S., Y. Gwack, et al. (2006). "A mutation in Orai1 causes immune deficiency by abrogating CRAC channel function." Nature **441**(7090): 179-185.

Franzius, D., M. Hoth, et al. (1994). "Non-specific effects of calcium entry antagonists in mast cells." Pflugers Archiv : European journal of physiology **428**(5-6): 433-438.

Hardie, R. C. and B. Minke (1993). "Novel Ca2+ channels underlying transduction in Drosophila photoreceptors: implications for phosphoinositide-mediated Ca2+ mobilization." Trends in neurosciences **16**(9): 371-376.

Harks, E. G., P. H. Peters, et al. (2005). "Autocrine production of prostaglandin F2alpha enhances phenotypic transformation of normal rat kidney fibroblasts." American journal of physiology. Cell physiology **289**(1): C130-137.

Harks, E. G., W. J. Scheenen, et al. (2003). "Prostaglandin F2 alpha induces unsynchronized intracellular calcium oscillations in monolayers of gap junctionally coupled NRK fibroblasts." Pflugers Archiv : European journal of physiology **447**(1): 78-86.

Hoth, M. and R. Penner (1992). "Depletion of intracellular calcium stores activates a calcium current in mast cells." Nature **355**(6358): 353-356.

Inoue, R., T. Okada, et al. (2001). "The transient receptor potential protein homologue TRP6 is the essential component of vascular alpha(1)-adrenoceptor-activated Ca(2+)-permeable cation channel." Circulation research **88**(3): 325-332.

Kusters, J. M., M. M. Dernison, et al. (2005). "Stabilizing role of calcium store-dependent plasma membrane calcium channels in action-potential firing and intracellular calcium oscillations." Biophysical journal **89**(6): 3741-3756.

Lalioti, M. D., J. Zhang, et al. (2006). "Wnk4 controls blood pressure and potassium homeostasis via regulation of mass and activity of the distal convoluted tubule." Nature genetics **38**(10): 1124-1132.

Lee, K. P., J. P. Yuan, et al. (2010). "An endoplasmic reticulum/plasma membrane junction: STIM1/Orai1/TRPCs." FEBS letters **584**(10): 2022-2027.

Li, M., J. Zacharia, et al. (2008). "Effects of siRNA knock-down of TRPC6 and InsP(3)R1 in vasopressin-induced Ca(2+) oscillations of A7r5 vascular smooth muscle cells." Pharmacological research : the official journal of the Italian Pharmacological Society **58**(5-6): 308-315.

Liao, Y., C. Erxleben, et al. (2008). "Functional interactions among Orai1, TRPCs, and STIM1 suggest a STIM-regulated heteromeric Orai/TRPC model for SOCE/Icrac channels." Proceedings of the National Academy of Sciences of the United States of America **105**(8): 2895-2900.

Liao, Y., C. Erxleben, et al. (2007). "Orai proteins interact with TRPC channels and confer responsiveness to store depletion." Proceedings of the National Academy of Sciences of the United States of America **104**(11): 4682-4687.

Liou, J., M. L. Kim, et al. (2005). "STIM is a Ca2+ sensor essential for Ca2+-store-depletion-triggered Ca2+ influx." Current biology : CB **15**(13): 1235-1241.

Mercer, J. C., W. I. Dehaven, et al. (2006). "Large store-operated calcium selective currents due to co-expression of Orai1 or Orai2 with the intracellular calcium sensor, Stim1." The Journal of biological chemistry **281**(34): 24979-24990.
Ong, H. L., K. T. Cheng, et al. (2007). "Dynamic assembly of TRPC1-STIM1-Orai1 ternary complex is involved in store-operated calcium influx. Evidence for similarities in store-operated and calcium release-activated calcium channel components." The Journal of biological chemistry **282**(12): 9105-9116.
Parekh, A. B. and J. W. Putney, Jr. (2005). "Store-operated calcium channels." Physiological reviews **85**(2): 757-810.
Peinelt, C., M. Vig, et al. (2006). "Amplification of CRAC current by STIM1 and CRACM1 (Orai1)." Nature cell biology **8**(7): 771-773.
Prakriya, M., S. Feske, et al. (2006). "Orai1 is an essential pore subunit of the CRAC channel." Nature **443**(7108): 230-233.
Putney, J. W., Jr. (1986). "A model for receptor-regulated calcium entry." Cell Calcium **7**(1): 1-12.
Putney, J. W., Jr. (1990). "Capacitative calcium entry revisited." Cell Calcium **11**(10): 611-624.
Redondo, P. C., I. Jardin, et al. (2008). "Intracellular Ca2+ store depletion induces the formation of macromolecular complexes involving hTRPC1, hTRPC6, the type II IP3 receptor and SERCA3 in human platelets." Biochimica et biophysica acta **1783**(6): 1163-1176.
Roos, J., P. J. DiGregorio, et al. (2005). "STIM1, an essential and conserved component of store-operated Ca2+ channel function." The Journal of cell biology **169**(3): 435-445.
Salido, G. M., S. O. Sage, et al. (2009). "TRPC channels and store-operated Ca(2+) entry." Biochimica et biophysica acta **1793**(2): 223-230.
Selinger, Z., Y. N. Doza, et al. (1993). "Mechanisms and genetics of photoreceptors desensitization in Drosophila flies." Biochimica et biophysica acta **1179**(3): 283-299.
Shi, J., M. Ju, et al. (2010). "TRPC6 channels stimulated by angiotensin II are inhibited by TRPC1/C5 channel activity through a Ca2+- and PKC-dependent mechanism in native vascular myocytes." The Journal of physiology **588**(Pt 19): 3671-3682.
Spassova, M. A., J. Soboloff, et al. (2006). "STIM1 has a plasma membrane role in the activation of store-operated Ca(2+) channels." Proceedings of the National Academy of Sciences of the United States of America **103**(11): 4040-4045.
Takemura, H., A. R. Hughes, et al. (1989). "Activation of calcium entry by the tumor promoter thapsigargin in parotid acinar cells. Evidence that an intracellular calcium pool and not an inositol phosphate regulates calcium fluxes at the plasma membrane." The J Biol Chem **264**(21): 12266-12271.
Thastrup, O., A. P. Dawson, et al. (1989). "Thapsigargin, a novel molecular probe for studying intracellular calcium release and storage." Agents and actions **27**(1-2): 17-23.
Trebak, M., J. B. G. St, et al. (2003). "Signaling mechanism for receptor-activated canonical transient receptor potential 3 (TRPC3) channels." The Journal of biological chemistry **278**(18): 16244-16252.
van Zoelen, E. J. (1991). "Phenotypic transformation of normal rat kidney cells: a model for studying cellular alterations in oncogenesis." Critical reviews in oncogenesis **2**(4): 311-333.
Venkatachalam, K., F. Zheng, et al. (2003). "Regulation of canonical transient receptor potential (TRPC) channel function by diacylglycerol and protein kinase C." The Journal of biological chemistry **278**(31): 29031-29040.
Vig, M., A. Beck, et al. (2006). "CRACM1 multimers form the ion-selective pore of the CRAC channel." Current biology : CB **16**(20): 2073-2079.
Vig, M., C. Peinelt, et al. (2006). "CRACM1 is a plasma membrane protein essential for store-operated Ca2+ entry." Science **312**(5777): 1220-1223.
Wigler, M., S. Silverstein, et al. (1977). "Transfer of purified herpes virus thymidine kinase gene to cultured mouse cells." Cell **11**(1): 223-232.
Williams, R. T., P. V. Senior, et al. (2002). "Stromal interaction molecule 1 (STIM1), a transmembrane protein with growth suppressor activity, contains an extracellular SAM domain modified by N-linked glycosylation." Biochimica et biophysica acta **1596**(1): 131-137.
Yeromin, A. V., S. L. Zhang, et al. (2006). "Molecular identification of the CRAC channel by altered ion selectivity in a mutant of Orai." Nature **443**(7108): 226-229.
Zeng, W., J. P. Yuan, et al. (2008). "STIM1 gates TRPC channels, but not Orai1, by electrostatic interaction." Molecular cell **32**(3): 439-448.
Zhang, S. L., A. V. Yeromin, et al. (2006). "Genome-wide RNAi screen of Ca(2+) influx identifies genes that regulate Ca(2+) release-activated Ca(2+) channel activity." Proceedings of the National Academy of Sciences of the United States of America **103**(24): 9357-9362.

Zhang, S. L., Y. Yu, et al. (2005). "STIM1 is a Ca2+ sensor that activates CRAC channels and migrates from the Ca2+ store to the plasma membrane." Nature **437**(7060): 902-905.
Zhu, M. H., M. Chae, et al. (2005). "Desensitization of canonical transient receptor potential channel 5 by protein kinase C." American journal of physiology. Cell physiology **289**(3): C591-600.

CHAPTER 6

General Discussion

General Discussion

The development of the RNA interference (RNAi) technique in the last decade has offered a powerful approach to determine the function of individual genes by blocking the translation of their specific mRNA (Fire, Xu et al. 1998). Due to the high efficiency and specificity of RNAi in suppressing gene expression, we used this technique as a selective, simple and cost-effective tool for studying the contribution of individual genes in the growth regulation and phenotypic transformation of NRK fibroblasts.

NRK fibroblasts provide an interesting model system for studying the mechanism of density-dependent growth inhibition and phenotypic transformation. These cells are able to acquire different growth stages depending on the addition of specific combinations of growth factors, which either results in density-dependent growth inhibition or phenotypic transformation (van Zoelen 1991). Previous studies have shown that a specific membrane potential characterizes each of these growth stages. These differences in membrane potential have been associated with the increased secretion of the cyclooxygenase (COX) product $PGF_{2\alpha}$ by NRK fibroblasts in their culture medium (Harks, Peters et al. 2005).

The aim of the present study was to investigate the role of the membrane potential in growth regulation and phenotypic transformation of NRK fibroblasts by use of the RNAi approach. Emphasis was laid on three aspects of the phenotypic transformation process, i.e. the depolarization of the plasma membrane to –20 mV, the loss of density-dependent growth and the induction of anchorage-independent proliferation. In addition, we have investigated the molecular mechanism of calcium dynamics and membrane excitability required for pacemaking activity of density-arrested NRK fibroblasts.

Our studies provided the first direct evidence for an exclusive role of the $PGF_{2\alpha}$-specific FP receptor in modulating the membrane potential of NRK fibroblasts during their different growth stages, but also led to the conclusion that membrane depolarization is not a prerequisite for the acquisition of a transformed phenotype. Moreover, our data provided the first direct evidence that the activity of $PGF_{2\alpha}$ secreted by putative pacemaker cells may underlie the generation of calcium action potentials in density-arrested NRK fibroblasts. Furthermore, by knockdown of individual IP_3-receptor encoding *Itpr* genes we provided the first direct evidence that the frequency of IP_3-dependent calcium oscillations determines the periodicity of action potential firing in density-arrested NRK fibroblasts.

Moreover, we showed that calcium store-dependent calcium entry is differentially regulated through store-operated channels (SOCs) and receptor-operated channels (ROCs) in quiescent and density-arrested NRK fibroblasts. Furthermore, by selective gene knockdown we demonstrated a role for Trpc1, Stim1 and Orai1 in store-operated calcium entry, whereas Trpc6 is specifically involved in receptor-operated calcium entry. Finally, our data show that Stim1, Orai1 and Trpc1, but not Trpc6, are necessary for the $PGF_{2\alpha}$-induced Ca^{2+} oscillations in NRK cells.

Membrane potential and growth regulation

It has been suggested that modulation of the membrane potential plays a role in the regulation of density-dependent growth inhibition (DDGI) (Binggeli and Weinstein 1986; Marino, Iliev et al. 1994). In the present study we have investigated whether depolarization of NRK cells is required for loss of DDGI and induction of phenotypic transformation. This study was initiated by the observation that phenotypically transformed NRK cells have a more depolarized membrane potential than density-arrested cells (-20 mV vs. -70 mV). We have previously shown that this depolarization results from the secretion of $PGF_{2\alpha}$ by transformed NRK cells in their culture medium and the subsequent activation of its FP receptor. Externally added $PGF_{2\alpha}$ is also able to depolarize quiescent cells but, when tested in the additional presence of EGF, it is only a poor inducer of phenotypic transformation in these cells. Our present studies show that knockdown of the FP receptor fully prevents membrane depolarization induced by externally added or autocrine produced $PGF_{2\alpha}$, but does not prevent retinoic acid-mediated phenotypic transformation (chapter 2). From these results it is concluded that the depolarization observed in phenotypically transformed cells indeed results from activation of the FP receptor, but on the other hand that activation of this receptor and concomitant depolarization is not essential for loss of DDGI.

This observation shows that the expression of functional FP receptors in NRK fibroblasts is responsible for modulation of membrane potential, but that this modulation is not essential for inducing phenotypic transformation in these cells. These findings appear consistent with previous studies in other cell types. It has been shown that membrane depolarization induced by changes in extracellular ion concentrations inhibits G_1/S progression of lymphocytes, astrocytes and Schwann cells, suggesting that

hyperpolarization is required for S-phase initiation (Canady, Ali-Osman et al. 1990; Freedman, Price et al. 1992; Wilson and Chiu 1993). In B-cell lymphocytes, inhibition of ion channels induces a reversible cell cycle arrest (Amigorena, Choquet et al. 1990) and similar results have been obtained in other cell types (Sundelacruz, Levin et al. 2008). Conversely, depolarization of the plasma membrane seems to be essential for the G_2/M transition. Current models outline a rhythmic oscillation of the membrane potential throughout the cell cycle, with a hyperpolarization spike immediately before DNA synthesis starts, followed by a prolonged period of depolarization necessary for mitosis (Santella, Ercolano et al. 2005). This appears to be a conserved mechanism, from the early cell divisions in embryos through the normal division of cells in differentiated tissues (Bregestovski, Medina et al. 1992; Sundelacruz, Levin et al. 2008). The required threshold could imply that these changes in the membrane potential may not be sufficient to induce loss of DDGI and phenotypic transformation, although it may be a necessary step for subsequent induction of proliferation. Further considerations on the role of the membrane potential in DDGI are presented in the next paragraph.

In addition we observed that cells, which lack expression of the FP receptor, are still able to undergo density-arrest, but do no longer show periodic firing of action potentials. Obviously such action potentials are not a requirement for NRK cells to undergo density-dependent growth inhibition. So although these data show that a functional FP receptor is essential for the generation of calcium action potentials, the biological role of these action potentials remains elusive. These observations are in line with our hypothesis that a limited number of cells in density-arrested NRK cultures act as pacemaker cells by local production of $PGF_{2\alpha}$. These considerations will be further discussed in this chapter.

Mechanisms underlying density-dependent growth inhibition and phenotypic transformation of NRK fibroblasts

One of the main characteristics of non-transformed cells is their ability to undergo density-dependent growth inhibition upon *in vitro* culturing. Increasing cell-cell contact in adherent cells eventually blocks the ability of polypeptide growth factors and integrins to induce such cells to proliferate. A variety of genes is upregulated when normal cells become density-arrested, including so-called GAS (growth arrest-specific) genes, various cyclin-dependent kinase inhibitors, caveolin, tyrosine phosphatases and protein kinase C-isoforms

(reviewed by (Nelson and Daniel 2002)). The inability of growth factors to stimulate density-arrested cells to proliferate has not only been associated with altered activity of the above intracellular signaling molecules, but also with a reduced expression of various growth factor receptors upon increasing cell density (Rizzino, Kazakoff et al. 1988). Due to oncogenic transformation normal cells lose their ability to undergo density-dependent growth inhibition, while in parallel they acquire the ability to proliferate under anchorage-independent conditions, suggesting that similar molecular mechanisms underlie these two processes. This observation is of particular relevance, since anchorage-independent growth of transformed cells is considered to be the best in vitro correlate of tumorigenicity in vivo (Shin, Freedman et al. 1975). In recent years it has become clear that only a small fraction of cells within a tumor has the ability to form a secondary tumor in nude mice. These so-called cancer stem cells show the intrinsic ability to grow under anchorage-independent conditions in vitro, indicating that for stem cells anchorage-independent growth may be unrelated to density-dependent growth control.

In the present study we have used NRK cells as a model system to study the molecular mechanisms underlying density-dependent growth control and induction of anchorage-independent proliferation. When cultured in the presence of EGF as the only growth stimulatory factor, these cells show a normal phenotype, characterized by density-dependent growth arrest and the inability to form colonies in soft agar. Ligand binding studies have shown that the EGF receptor density on the NRK surface decreases with increasing cell density (Rizzino, Kazakoff et al. 1990). In combination with the low expression levels of the EGF receptor in these cells (approximately 3000 receptors per cell), we have postulated that these cells become density-arrested as soon as, with increasing cell density, the number of EGF receptors drops below a threshold value, after which EGF becomes unable to generate sufficient growth stimulating signals in the cell (Rizzino, Kazakoff et al. 1990; van Zoelen 1991). This hypothesis is confirmed by the observation that EGF-induced density-arrest of NRK cells can be overcome by the addition of modulating agents, such as transforming growth factor-beta (TGFβ) and retinoic acid (RA). These modulators are not growth stimulatory by themselves, but they are able to enhance the expression of EGF receptors in NRK cells (Lahaye, Walboomers et al. 1999) and concomitantly to induce a transformed phenotype in these cells. This hypothesis is also confirmed by the observation that upon overexpression of the human EGF receptor gene

(*EGFR*) NRK cells show EGF-induced anchorage-independent growth, also in the absence TGFβ (Kizaka-Kondoh, Akiyama et al. 2000).

A general problem in studying the role of the EGF receptor in phenotypic transformation of NRK cells is its low expression level, which hampers studies on the dynamics of this receptor. In a previous study we have transfected NRK cells with a human *EGFR*-construct linked to the luciferase gene (Lahaye et al., 1999a). The results showed that culturing of NRK cells under anchorage-independent conditions induced a strong repression of *EGFR* promoter activity. Addition of TGFβ or RA resulted in an upregulation of *EGFR* promoter activity, to a similar level as observed in attached cells. Modern quantitative RT-PCR techniques have the sensitivity to measure modulation of *Egfr* mRNA levels during density-dependent growth inhibition and phenotypic transformation of NRK cells. Figure 1 shows that the *Egfr* mRNA level is reduced by approximately 50% when quiescent NRK cells are grown to density-arrest by the addition of EGF and insulin. EGF is known to upregulate the expression of its own receptor (Thompson and Rosner 1989), but the present data show that NRK cells are unable to do so when reaching confluence. Subsequent treatment of these density-arrested cells with RA or TGFβ enhances *Egfr* expression to a level above that of quiescent cells. Minor effects were observed upon addition of $PGF_{2\alpha}$, which is a growth-modulating agent that is secreted by transformed NRK cells. Proliferation studies have shown that density-arrested NRK cells are non-responsive, while quiescent cells and phenotypically transformed cells are responsive to growth stimulation by EGF. The present results therefore underline that subtle differences in EGF receptor expression levels are associated with the transition of NRK cells form a normal to a transformed phenotype.

Anchorage-independent growth can be studied by colony formation in soft agar, or by analyzing the ability of cells to form spheres on low attachment tissue culture plates. We have used the latter condition to study the effect of RA and TGFβ on *Egfr* mRNA levels in NRK cells. Figure 2 show that both RA and TGFβ induce a 2-3-fold up-regulation of *Egfr* expression under such anchorage-independent conditions. In the presence of EGF alone these non-adherent cells do not respond mitogenically to EGF, while in the additional presence of RA and TGFβ they do. This implies again that a relatively small increase in EGF receptor expression is sufficient to make these cells responsive again to EGF.

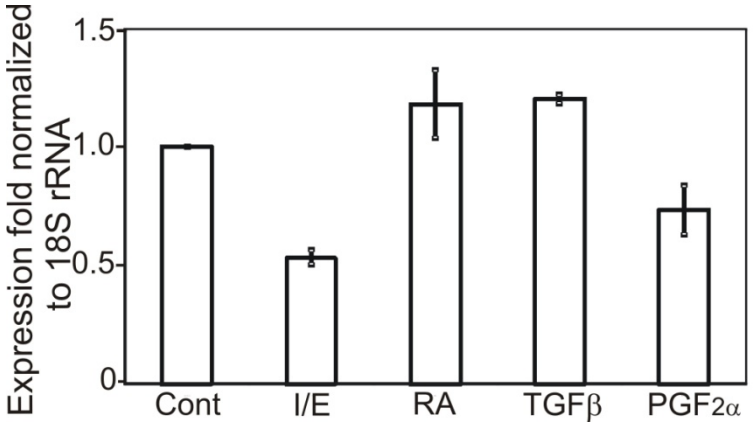

Fig. 1. Growth stage-dependent expression of *Egfr* mRNA levels in NRK fibroblasts.
Serum-deprived, quiescent NRK cells (Cont) were treated for 48 hours with 5 ng/ml EGF in the presence of 5 µg/ml insulin to reach density-dependent growth inhibition (I/E). These cells were subsequently restimulated to proliferate by the addition of 50 ng/ml RA, 1 ng/ml TGFβ or 1 µM $PGF_{2\alpha}$ for 48 hours. *Egfr* mRNA levels were measured by quantitative RT-PCR and plotted as fold expression relative to control cells. Indicated standard errors of the mean are based two independent experiments in duplicate.

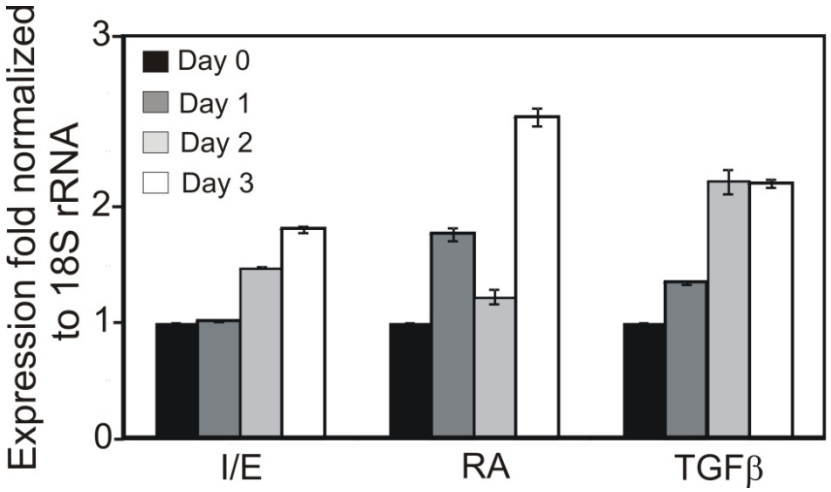

Fig. 2. Effect of anchorage-independent culturing of NRK cells and phenotypic transformation-inducing agents on *Egfr* mRNA expression levels. NRK cells were seeded on poly (HEMA)-coated dishes in the presence of 5 ng/ml EGF and 5 µg/ml insulin (I/E), or in the additional presence of 50 ng/ml RA (RA) or 1 ng/ml TGFβ (TGFβ). mRNA was isolated from spheres after the indicated time points and *Egfr* mRNA levels were measured by quantitative RT-PCR. Indicated standard errors of the mean are based on three independent experiments.

Previous studies have shown that in NRK cells, which overexpress human EGFR, addition of EGF is sufficient to induce anchorage-independent growth (Kizaka-Kondoh, Akiyama et al. 2000). We have constructed similar cells to study the effect of EGF receptors on density-dependent growth control of NRK cells. Scatchard analysis following ^{125}I-EGF binding studies showed that NRK cells transfected with *EGFR* (NER-1 cells) contained approximately 23,500 EGF binding sites per cell, compared to 3,000 on wild-type NRK cells (data not shown). Figure 3A confirms that wild-type NRK cells are unable to grow in soft agar, both in the presence and absence of EGF, while NER-1 cells readily form colonies when treated with EGF. Figure 3B shows that wild-type NRK cells become density-arrested when treated with EGF alone, but continue to undergo S-fase progression in the additional presence of RA or -to a lesser extent $PGF_{2\alpha}$. Under similar experimental conditions confluent NER-1 cells continued to proliferate when treated with EGF, irrespective of the presence of RA or $PGF_{2\alpha}$. These data show that NRK cells do not undergo density-dependent growth arrest when EGF can activate sufficiently high levels of EGF receptors.

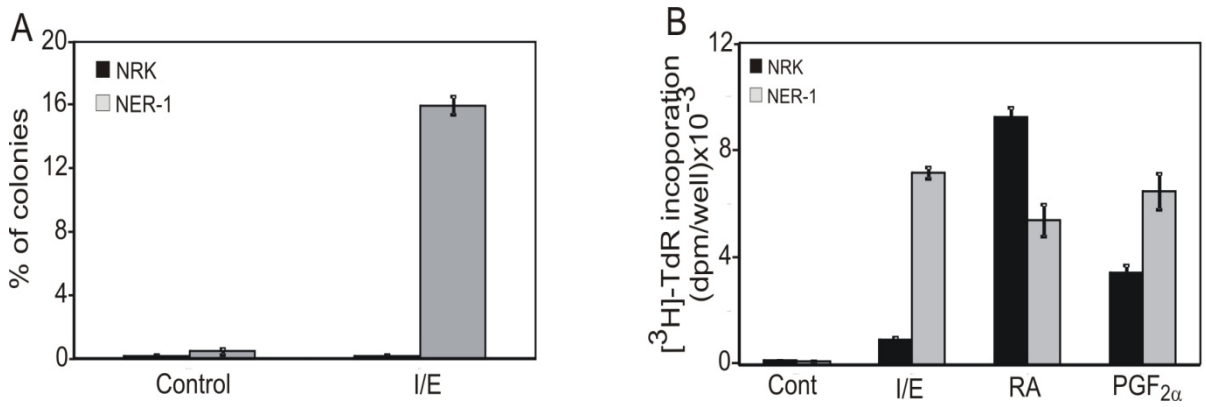

Fig. 3. Effect of EGF receptors on density-dependent growth control of NRK cells.

(A) Quantitative analysis of soft agar colonies of wild-type NRK (Control) and NER-1 cells (NER), cultured in the absence and presence of 10 ng/ml EGF. Data are expressed as the number of colonies relative to the number of inoculated cells, based on the average of two replicate cultures. (B) [^{3}H]-Thymidine incorporation in wild-type NRK cells (black bar) and NER1 cells (gray bar). The cells were grown to density-arrest in the presence of 5 ng/ml EGF (I/E), and were thereafter restimulated to proliferate by the addition of RA (50 ng/ml) or $PGF_{2\alpha}$ (100 nM). Cumulative incorporation of [3H]-thymidine was measured between 24 and 48 hours after the addition of serum-free medium, which contained in addition to EGF also the transformation-inducing agents. The control (Cont) represents [^{3}H]-thymidine incorporation values of the cells in the absence of EGF and transformation-inducing agents. Values are represented as the mean ± SEM (n=3), whereby n indicates the number of independent experiments.

Taken together, our results confirm the central role of the EGF receptor density in control of density-dependent growth inhibition and phenotypic transformation of NRK cells. It remains unclear, however, how NRK cells sense their density and what intracellular processes are involved in the density-dependent expression of the *Egfr* gene. The above results agree with our model that NRK cells grown to high density can no longer proliferate because the EGF receptor density has dropped below a threshold value. It remains to be established, however, to what extent density-dependent growth arrest of NRK cells results from intense intercellular contact, which is a prerequisite for so-called contact inhibition. Density-arrested NRK cells can no longer be stimulated by EGF, but are still responsive to PDGF (Van Zoelen, Van Rotterdam et al. 1993). Obviously, the density of PDGF receptors (Pdgfra and Pdgfrb) in density-arrested NRK cells is not below a critical threshold. This suggests that EGF-induced density-arrest of NRK cells is not the consequence of intense intercellular contact.

Mechanism of pacemaker activity

We have previously hypothesized that the action potentials in density-arrested NRK monolayers are induced by localized pacemaker cells and subsequently transmitted to the remaining cells which act as followers and participate in the propagation of these action potentials (Harks 2003). However, the exact mechanism for generation of such pacemaker centers has not been identified. In this study we have shown that activation of the FP receptors by $PGF_{2\alpha}$ is essential for the generation of action potentials in density-arrested NRK fibroblasts. Following knockdown of the FP receptor gene, NRK cells that had been grown to density-arrest in the presence of EGF, did no longer show spontaneous firing of periodic calcium action potentials (Chapter 2).

In a previous study, we have shown that $PGF_{2\alpha}$ can induce IP_3-mediated calcium oscillations and membrane depolarization of NRK cells (Harks, Scheenen et al. 2003). This is most likely explained by the observation that secretion of $PGF_{2\alpha}$ and the subsequent activation of its receptor in an autocrine manner result in activation of Ca^{2+}-dependent chloride channels, which depolarize the membrane. This membrane depolarization will be transduced via gap junctions to non-$PGF_{2\alpha}$ producing cells, which can thus act as follower cells. This conclusion is supported by an elegant study in which a ring was placed on top of a quiescent monolayer of NRK cells and $PGF_{2\alpha}$ was added locally inside the ring. This addition resulted in calcium oscillations within the cells inside the ring, but induced the

generation of calcium action potentials in the non-treated cells outside the ring. These data indicate that density-arrested monolayers of NRK cells may contain clusters of $PGF_{2\alpha}$ producing pacemaker cells that are electrically coupled to non- $PGF_{2\alpha}$ producing cells that propagate the action potentials as follower cells. The stimulated cells supply the required IP_3 for calcium oscillations, while the non-stimulated cells provide the required membrane potential for opening of the L-type calcium channel (Dernison, Kusters et al. 2008). In other systems where calcium action potentials have been studied, pacemaker and follower cells are distinct cell types. For example, the interstitial cells of Cajal (ICC cells) spontaneously generate active pacemaker currents that may be recorded as plateau and slow potentials. These pacemaker currents drive the spontaneous electrical and mechanical activities of smooth muscle cells of the gastrointestinal and urinary tract, as well as of the fallopian tubes (Komuro 2006; McHale, Hollywood et al. 2006). Also in those systems pacemaking activity requires an initial depolarization process followed by activation of voltage-dependent calcium channels. In the sinoatrial node, intracellular calcium oscillations within the pacemaker cells activate Na^+/Ca^{2+}-exchange, which results in sodium influx and subsequent depolarization (Maltsev, Vinogradova et al. 2006; Imtiaz, von der Weid et al. 2010), while in smooth muscle cells activation of a calcium-activated chloride current mediates cell depolarization (Wang, Hogg et al. 1992; Hirst, Bramich et al. 2002).

Mechanism of calcium entry in NRK fibroblasts

In a number of studies we have provided a detailed characterization of the calcium homeostasis in NRK fibroblasts as a function of their growth status. A characteristic feature of NRK growth regulation is an alteration in intracellular Ca^{2+} handling, which may play a role in the growth regulation process itself (Harks, Scheenen et al. 2003; Harks, Peters et al. 2005). Despite extensive research little is still known about the mechanism of intracellular Ca^{2+} signaling during growth regulation of NRK fibroblasts. We were able to show that SOCE is activated by depletion of IP_3-sensitive stores in both quiescent and the density-arrested NRK cells. Furthermore we demonstrated for the first time that proliferation of these cells from the quiescent to density-arrested state is accompanied by an increase in ROCE, which was measured as an influx of extracellular Ca^{2+} upon treatment with the cell permeable diacylglycerol analog OAG (chapter 4). These results indicate that proliferation of NRK cells from the quiescent to the density-arrested stage

requires an enhanced supply of Ca^{2+} to refill the intracellular Ca^{2+}-stores, which is provided by an activation of different Ca^{2+} entry pathways. This differentially regulated activation of calcium entry pathways provides NRK fibroblasts with an elegant mechanism to meet their calcium requirements under the different growth conditions. Moreover, it has already been shown previously (Kusters, Dernison et al. 2005) that a store-dependent regulation of calcium entry is required to couple membrane excitability with calcium dynamics, in order to maintain proper calcium homeostasis in NRK fibroblasts.

In support to our finding, we investigated the molecular identity of the channels that are involved in the mechanism of Ca^{2+} entry in NRK cells. In spite of the fact that NRK fibroblasts express the genes encoding Trpc1, Trpc5 and Trpc6, which all three show expression levels that are dependent upon the growth stage of the cells, only Trpc1 and Trpc6 appear to be involved in Ca^{2+} entry in NRK cells. Our data indicate a specific role for Trpc1 in the activation of SOCE, whereas Trpc6 appears to be involved in ROCE (chapter 5). The majority of functional TRPC channels *in vivo* are heterotetrameric complexes of different TRPC subunits (Ay, Prakash et al. 2004; Albert, Saleh et al. 2007). TRPC1 associates with TRPC4 and TRPC5, whereas TRPC6 can associate with TRPC3 and TRPC7 (Goel, Sinkins et al. 2002; Hofmann, Schaefer et al. 2002). When one of the TRPC subunits is suppressed, compensatory up-regulation of other subunits can be observed (Dietrich, Mederos et al. 2005). We found that two potential partners involved in SOCE (Trpc1 and Trpc5) and one in ROCE (Trpc6) are expressed in quiescent NRK cells, but only Trpc5 and Trpc6 show upregulation when cells become density-arrested. However, knockdown of neither *Trpc5* nor *Trpc6* by specific shRNAs appeared to have any effect on SOCE in NRK cells, whereas knockdown of only *Trpc6* was found to attenuate ROCE in these cells significantly. These findings indicate that heterotetrameric complex formation of TRPC channel subtypes does probably not occur in NRK cells. On the other hand, we have observed that quiescent NRK cells readily express the Ca^{2+}-channel protein subunit Orai1 and found that this Ca^{2+}-channel subunit is upregulated when proliferating NRK cells reach density-arrest. This finding suggests that Orai1 might be critically involved in Ca^{2+} entry associated with growth modulation of NRK cells (chapter 5). The above findings further indicate that dynamic complexes of this novel Ca^{2+}-channel protein subunit with either Trpc1 or Trpc6 may represent the composition of SOCs and ROCs in NRK cells, respectively.

Recently an essential role of STIM1, the Ca^{2+} sensor in the ER, in SOCE was identified in a variety of cell types (Takahashi, Watanabe et al. 2007; Peel, Liu et al. 2008), including NRK cells (chapter 5). It has been shown that after store depletion, STIM1 relocalizes and accumulates within "junctional" ER structures, located 10–25 nm from the plasma membrane (Wu, Buchanan et al. 2006). Notably, TRPC channels are also confined to plasma membrane micro-domains adjacent to the underlying "junctional" ER (Golovina 2005). Still, the molecular interactions involved in activation of SOCs by STIM1 remain poorly understood.

In NRK fibroblasts, suppression of Stim1 expression with shRNA greatly reduced BHQ-activated SOCE (chapter 5) and EGF-induced proliferation of the cells, as measured by thymidine incorporation studies (data not shown). STIM1 has been characterized as a potential tumor suppressor gene, giving rise to a protein product with growth-inhibitory activity (Sabbioni, Barbanti-Brodano et al. 1997; Sabbioni, Veronese et al. 1999). In agreement with these observations it has been shown previously that down regulation of STIM1 suppresses phosphorylation of the cAMP-responsive element binding protein (CREB) and concomitantly the growth of vascular smooth muscle cells in tissue culture (Takahashi, Watanabe et al. 2007). The exact mechanism by which STIM1 and ORAI1 regulate SOCE and ROCE, both in the presence and absence of TRPC proteins, is however still largely unknown. Our current findings in NRK fibroblasts support the recent model that the stoichiometry of STIM1, ORAI1 and TRPCs in protein complexes determines their function as either SOCs or ROCs (see for review,(Lee, Yuan et al. 2010; Cheng, Liu et al. 2011)).

Coupling between calcium oscillations and periodic action potential firing

The data presented in this study support the hypothesis that activation of the FP receptor by $PGF_{2\alpha}$ produced by putative pacemaker cells underlies the generation of calcium action potentials in density-arrested NRK fibroblasts (chapter 2). Furthermore they form the first experimental support for the hypothesis that IP_3-receptor mediated Ca^{2+}-oscillations provide NRK cells with a timing mechanism for periodic action potential firing in the density-arrested stage of growth (chapter 3). Also other studies have demonstrated an interaction between calcium oscillations and action potentials in a variety of cell types that exhibit pacemaking activity (Imtiaz, von der Weid et al. 2010). Ca^{2+}-store-based pacemaking, such as in NRK fibroblasts, has a role in a range of tissues where cells are

electrically connected by gap junctions such as intestinal cells of Cajal (Hirst and Ward 2003), urethral cells (Hashitani 2006; Imtiaz, von der Weid et al. 2010) and sinoatrial nodal pacemaker cells in the heart (Lakatta, Maltsev et al. (2010); Joung, Chen et al. 2011). The key for a functional pacemaker mechanism in such cellular syncytia is that oscillatory Ca^{2+} release from intracellular stores generates periodically inward currents and resultant depolarisations in the pacemaking cells, which become readily conducted through the cellular network. The conducted depolarisations in turn lead to activation of other Ca^{2+} stores in the cellular syncytium. This latter step could be mediated by depolarisation-induced Ca^{2+} entry (Kusters, van Meerwijk et al. 2008) and / or production of IP_3 (Imtiaz, Smith et al. 2002).

In this study we have shown for the first time that the periodicity of action potential firing in NRK fibroblasts is dependent on the frequency of oscillatory Ca^{2+} release from intracellular IP_3-dependent stores. A striking correlation has been found between the frequency of $PGF_{2\alpha}$-induced Ca^{2+} oscillations and the frequency of firing of action potentials by the cells, both of which depend on the relative expression levels of the IP_3R subtypes (chapter 3). This correlation could be further substantiated when cells in which a specific IP_3R subtype is knocked down, would be used in the earlier described ring assay. By applying such an experimental approach in combination with patch clamp electrophysiology and vital calcium imaging techniques (Dernison, Kusters et al. 2008), the interrelationship between the frequency of the $PGF_{2\alpha}$-induced Ca^{2+} oscillations in pacemaker cells and that of propagated action potential firing in the follower cells could be further examined. In addition, studying the role of other Ca^{2+} stores, e.g. mitochondria, and their effect on the Ca^{2+} oscillations in these pacemaker cells will be an interesting subject for future research.

Although we have elucidated the mechanism of action potential firing in cultured fibroblasts, we can only speculate about the *in vivo* function of these action potentials. Since fibroblasts can form cellular communication networks *in vivo* (Langevin 2006) which expand throughout entire organs, their excitability in combination with electrical coupling may provide them with an efficient tool for fast and long-distance signaling. In this way, agonist-induced depolarization evoked in a few cells, for example by $PGF_{2\alpha}$ (chapter 1), may be transduced to non-stimulated neighboring cells, thereby recruiting a larger population of cells to respond in unison to local stimuli. So, fibroblasts may serve as

an excitable and conductive pathway by which signals generated on one side of a tissue or organ can be transduced to the other side.

Because fibroblasts can be coupled to other cell types including epithelial cells (Hunter and Pitts 1981), myocytes (Gaudesius, Miragoli et al. 2003) and cells from immune system (Oliani, Girol et al. 1995), while in addition action potentials can be transduced through heterocellular gap junctions (De Roos 1997), fibroblasts may also affect the physiological function of other cells types *in vivo*. It remains to be established whether the excitability and action potential propagation in NRK cells is a more general feature of fibroblasts. In this respect, it is interesting to mention that voltage-activated ion channels have been reported in several other fibroblastic cell lines including Balb/c 3T3 fibroblasts (Lovisolo, Alloatti et al. 1988), NIH/3T3 fibroblasts (Chen, Corbley et al. 1988), Swiss 3T3 fibroblasts (Peres, Sturani et al. 1988) and HF fibroblasts (Baumgarten, Toscas et al. 1992).

Future perspectives

In NRK fibroblasts several mechanisms have been proposed to play a role in DDGI. However, a density-dependent modulation of EGF-receptor levels is currently the most appropriate model to describe growth arrest of EGF-treated NRK cells. In this model, EGF receptor levels decrease with increasing cell density, such that below a critical density the cells become unresponsive to stimulating activity of EGF, resulting in DDGI. The cell can undergo phenotypic transformation by an increase of EGF receptor numbers, as induced by factors such as retinoic acid and TGF_{β}, thus enhancing the growth-stimulating signals of EGF, or alternatively by the activation of parallel growth-stimulating pathways by factors such as platelet-derived growth factor PDGF. Nevertheless, it remains to be established to what extent density-dependent growth arrest of NRK cells results from intense intercellular contact, which is a prerequisite for so-called contact inhibition. Still our results indicate that with respect to their Ca^{2+} signaling characteristics density-arrested NRK monolayers behave clearly different from quiescent monolayers.

Within our long-term interest in NRK cells as a model system for studying the Ca^{2+} signaling in density-arrested NRK fibroblasts, we have gained a wide knowledge about the mechanisms that are involved in pacemaking activity in NRK cell monolayers. In particular we have identified most of the steps involved in the generation and propagation of calcium action potentials, including the specific ionic conductances involved and their

molecular entities. Based on these data we have determined the exact sequence of events that are involved in producing periodic pacemaker activity and gained insight in the important role of $PGF_{2\alpha}$ as a trigger to initiate these events. Despite these lines of evidence for a prominent role of the FP receptor in the pacemaking activity of NRK fibroblasts, the pacemaker cells themselves have not been identified yet in NRK cultures due to a lack of specific markers. In addition, it is also not clear if density-arrested NRK cultures contain a stable or a dynamic population of pacemaker cells. Theoretical studies have indicated that for pacemaking activity to occur in a monolayer of NRK cells, a group of at least 50-80 $PGF_{2\alpha}$-induced pacemaker cells are required. It would be interesting to investigate whether, upon expression of the enhanced green fluorescent protein (eGFP) gene under transcriptional control of the COX2 or the FP receptor promoter, groups of pacemaking NRK cells could be identified in a density-arrested monolayer based on their fluorescent properties.

References

Albert, A. P., S. N. Saleh, et al. (2007). "Multiple activation mechanisms of store-operated TRPC channels in smooth muscle cells." J Physiol **583**(Pt 1): 25-36.

Amigorena, S., D. Choquet, et al. (1990). "Ion channel blockers inhibit B cell activation at a precise stage of the G1 phase of the cell cycle. Possible involvement of K+ channels." J Immunol **144**(6): 2038-2045.

Ay, B., Y. S. Prakash, et al. (2004). "Store-operated Ca2+ entry in porcine airway smooth muscle." Am J Physiol Lung Cell Mol Physiol **286**(5): L909-917.

Baumgarten, L. B., K. Toscas, et al. (1992). "Dihydropyridine-sensitive L-type Ca2+ channels in human foreskin fibroblast cells. Characterization of activation with the growth factor Lys-bradykinin." The Journal of biological chemistry **267**(15): 10524-10530.

Binggeli, R. and R. C. Weinstein (1986). "Membrane potentials and sodium channels: hypotheses for growth regulation and cancer formation based on changes in sodium channels and gap junctions." J Theor Biol **123**(4): 377-401.

Bregestovski, P., I. Medina, et al. (1992). "Regulation of potassium conductance in the cellular membrane at early embryogenesis." J Physiol Paris **86**(1-3): 109-115.

Canady, K. S., F. Ali-Osman, et al. (1990). "Extracellular potassium influences DNA and protein syntheses and glial fibrillary acidic protein expression in cultured glial cells." Glia **3**(5): 368-374.

Chen, C. F., M. J. Corbley, et al. (1988). "Voltage-sensitive calcium channels in normal and transformed 3T3 fibroblasts." Science **239**(4843): 1024-1026.

Cheng, K. T., X. Liu, et al. (2011). "Local Ca(2)+ entry via Orai1 regulates plasma membrane recruitment of TRPC1 and controls cytosolic Ca(2)+ signals required for specific cell functions." PLoS biology **9**(3): e1001025.

De Roos, A. D. (1997). Electrophysiological Aspects of Growth Factor Signaling in NRK Fibroblasts University of Nijmegen, The Netherlands.

.

Dernison, M. M., J. M. Kusters, et al. (2008). "Local induction of pacemaking activity in a monolayer of electrically coupled quiescent NRK fibroblasts." Cell Calcium **44**(5): 429-440.

Dietrich, A., Y. S. M. Mederos, et al. (2005). "Increased vascular smooth muscle contractility in TRPC6-/- mice." Mol Cell Biol **25**(16): 6980-6989.

Fire, A., S. Xu, et al. (1998). "Potent and specific genetic interference by double-stranded RNA in Caenorhabditis elegans." Nature **391**(6669): 806-811.

Freedman, B. D., M. A. Price, et al. (1992). "Evidence for voltage modulation of IL-2 production in mitogen-stimulated human peripheral blood lymphocytes." J Immunol **149**(12): 3784-3794.
Gaudesius, G., M. Miragoli, et al. (2003). "Coupling of cardiac electrical activity over extended distances by fibroblasts of cardiac origin." Circ Res **93**(5): 421-428.
Goel, M., W. G. Sinkins, et al. (2002). "Selective association of TRPC channel subunits in rat brain synaptosomes." J Biol Chem **277**(50): 48303-48310.
Golovina, V. A. (2005). "Visualization of localized store-operated calcium entry in mouse astrocytes. Close proximity to the endoplasmic reticulum." J Physiol **564**(Pt 3): 737-749.
Harks, E. G. (2003). Excitable Fibroblasts University of Nijmegen.
Harks, E. G., P. H. Peters, et al. (2005). "Autocrine production of prostaglandin F2alpha enhances phenotypic transformation of normal rat kidney fibroblasts." Am J Physiol Cell Physiol **289**(1): C130-137.
Harks, E. G., W. J. Scheenen, et al. (2003). "Prostaglandin F2 alpha induces unsynchronized intracellular calcium oscillations in monolayers of gap junctionally coupled NRK fibroblasts." Pflugers Arch **447**(1): 78-86.
Hashitani, H. (2006). "Interaction between interstitial cells and smooth muscles in the lower urinary tract and penis." J Physiol **576**(Pt 3): 707-714.
Hirst, G. D., N. J. Bramich, et al. (2002). "Regenerative component of slow waves in the guinea-pig gastric antrum involves a delayed increase in [Ca(2+)](i) and Cl(-) channels." J Physiol **540**(Pt 3): 907-919.
Hirst, G. D. and S. M. Ward (2003). "Interstitial cells: involvement in rhythmicity and neural control of gut smooth muscle." J Physiol **550**(Pt 2): 337-346.
Hofmann, T., M. Schaefer, et al. (2002). "Subunit composition of mammalian transient receptor potential channels in living cells." Proc Natl Acad Sci U S A **99**(11): 7461-7466.
Hunter, G. K. and J. D. Pitts (1981). "Non-selective junctional communication between some different mammalian cell types in primary culture." J Cell Sci **49**: 163-175.
Imtiaz, M. S., D. W. Smith, et al. (2002). "A theoretical model of slow wave regulation using voltage-dependent synthesis of inositol 1,4,5-trisphosphate." Biophys J **83**(4): 1877-1890.
Imtiaz, M. S., P. Y. von der Weid, et al. (2010). "SR Ca2+ store refill--a key factor in cardiac pacemaking." J Mol Cell Cardiol **49**(3): 412-426.
Imtiaz, M. S., P. Y. von der Weid, et al. (2010). "Synchronization of Ca2+ oscillations: a coupled oscillator-based mechanism in smooth muscle." The FEBS journal **277**(2): 278-285.
Joung, B., P. S. Chen, et al. (2011). "The role of the calcium and the voltage clocks in sinoatrial node dysfunction." Yonsei medical journal **52**(2): 211-219.
Kizaka-Kondoh, S., N. Akiyama, et al. (2000). "Role of TGF-beta in EGF-induced transformation of NRK cells is sustaining high-level EGF-signaling." FEBS Lett **466**(1): 160-164.
Komuro, T. (2006). "Structure and organization of interstitial cells of Cajal in the gastrointestinal tract." J Physiol **576**(Pt 3): 653-658.
Kusters, J. M., M. M. Dernison, et al. (2005). "Stabilizing role of calcium store-dependent plasma membrane calcium channels in action-potential firing and intracellular calcium oscillations." Biophys J **89**(6): 3741-3756.
Kusters, J. M., W. P. van Meerwijk, et al. (2008). "Fast calcium wave propagation mediated by electrically conducted excitation and boosted by CICR." Am J Physiol Cell Physiol **294**(4): C917-930.
Lahaye, D. H., F. Walboomers, et al. (1999). "Phenotypic transformation of normal rat kidney fibroblasts by endothelin-1. Different mode of action from lysophosphatidic acid, bradykinin, and prostaglandin f2alpha." Biochim Biophys Acta **1449**(2): 107-118.
Lakatta, E. G., V. A. Maltsev, et al. (2010) " A coupled SYSTEM of intracellular Ca2+ clocks and surface membrane voltage clocks controls the timekeeping mechanism of the heart's pacemaker." Circ Res **106**(4): 659-673.
Langevin, H. M. (2006). "Connective tissue: a body-wide signaling network?" Med Hypotheses **66**(6): 1074-1077.
Lee, K. P., J. P. Yuan, et al. (2010) "An endoplasmic reticulum/plasma membrane junction: STIM1/Orai1/TRPCs." FEBS Lett **584**(10): 2022-2027.
Lovisolo, D., G. Alloatti, et al. (1988). "Potassium and calcium currents and action potentials in mouse Balb/c 3T3 fibroblasts." Pflugers Archiv : European journal of physiology **412**(5): 530-534.
Maltsev, V. A., T. M. Vinogradova, et al. (2006). "The emergence of a general theory of the initiation and strength of the heartbeat." J Pharmacol Sci **100**(5): 338-369.
Marino, A. A., I. G. Iliev, et al. (1994). "Association between cell membrane potential and breast cancer." Tumour Biol **15**(2): 82-89.

McHale, N. G., M. A. Hollywood, et al. (2006). "Organization and function of ICC in the urinary tract." J Physiol **576**(Pt 3): 689-694.
Nelson, P. J. and T. O. Daniel (2002). "Emerging targets: molecular mechanisms of cell contact-mediated growth control." Kidney Int **61**(1 Suppl): S99-105.
Oliani, S. M., A. P. Girol, et al. (1995). "Gap junctions between mast cells and fibroblasts in the developing avian eye." Acta Anat (Basel) **154**(4): 267-271.
Peel, S. E., B. Liu, et al. (2008). "ORAI and store-operated calcium influx in human airway smooth muscle cells." Am J Respir Cell Mol Biol **38**(6): 744-749.
Peres, A., E. Sturani, et al. (1988). "Properties of the voltage-dependent calcium channel of mouse Swiss 3T3 fibroblasts." The Journal of physiology **401**: 639-655.
Rizzino, A., P. Kazakoff, et al. (1990). "Density-induced down regulation of epidermal growth factor receptors." In Vitro Cell Dev Biol **26**(5): 537-542.
Rizzino, A., P. Kazakoff, et al. (1988). "Regulatory effects of cell density on the binding of transforming growth factor beta, epidermal growth factor, platelet-derived growth factor, and fibroblast growth factor." Cancer Res **48**(15): 4266-4271.
Sabbioni, S., G. Barbanti-Brodano, et al. (1997). "GOK: a gene at 11p15 involved in rhabdomyosarcoma and rhabdoid tumor development." Cancer Res **57**(20): 4493-4497.
Sabbioni, S., A. Veronese, et al. (1999). "Exon structure and promoter identification of STIM1 (alias GOK), a human gene causing growth arrest of the human tumor cell lines G401 and RD." Cytogenet Cell Genet **86**(3-4): 214-218.
Santella, L., E. Ercolano, et al. (2005). "The cell cycle: a new entry in the field of Ca2+ signaling." Cellular and molecular life sciences : CMLS **62**(21): 2405-2413.
Shin, S. I., V. H. Freedman, et al. (1975). "Tumorigenicity of virus-transformed cells in nude mice is correlated specifically with anchorage independent growth in vitro." Proc Natl Acad Sci U S A **72**(11): 4435-4439.
Sundelacruz, S., M. Levin, et al. (2008). "Membrane potential controls adipogenic and osteogenic differentiation of mesenchymal stem cells." PLoS One **3**(11): e3737.
Takahashi, Y., H. Watanabe, et al. (2007). "Functional role of stromal interaction molecule 1 (STIM1) in vascular smooth muscle cells." Biochem Biophys Res Commun **361**(4): 934-940.
Thompson, K. L. and M. R. Rosner (1989). "Regulation of epidermal growth factor receptor gene expression by retinoic acid and epidermal growth factor." J Biol Chem **264**(6): 3230-3234.
van Zoelen, E. J. (1991). "Phenotypic transformation of normal rat kidney cells: a model for studying cellular alterations in oncogenesis." Crit Rev Oncog **2**(4): 311-333.
Van Zoelen, E. J., W. Van Rotterdam, et al. (1993). "Differential effects of PDGF isoforms on proliferation of normal rat kidney cells." Growth Factors **9**(4): 329-339.
Wang, Q., R. C. Hogg, et al. (1992). "Properties of spontaneous inward currents recorded in smooth muscle cells isolated from the rabbit portal vein." J Physiol **451**: 525-537.
Wilson, G. F. and S. Y. Chiu (1993). "Mitogenic factors regulate ion channels in Schwann cells cultured from newborn rat sciatic nerve." J Physiol **470**: 501-520.
Wu, M. M., J. Buchanan, et al. (2006). "Ca2+ store depletion causes STIM1 to accumulate in ER regions closely associated with the plasma membrane." J Cell Biol **174**(6): 803-813.

Summary

Not only during development but also in the adult organism, cellular growth is strictly regulated by various control mechanisms, which ensure that cells start and stop dividing at the proper time and place. Dysfunction of these regulatory mechanisms results in uncontrolled proliferation of cells and can be the basis for a large diversity of pathological conditions including cancer. Therefore, insight into the elementary mechanisms that control normal cell growth is essential for understanding pathological growth abnormalities.

Under non-pathological conditions cells undergo density-dependent growth inhibition at high cell densities. This protection mechanism, also known as contact inhibition, aims at preventing excessive cell growth. In the present study, we have used NRK fibroblasts as a model system to study the role of the membrane potential in growth regulation and phenotypic transformation. These cells are able to acquire different growth stages depending on the addition of specific combinations of growth factors, which results in either density-dependent growth inhibition or phenotypic transformation. The membrane potential of NRK cells strongly depends on the growth stage of these cells. Quiescent cultures of NRK cells show a stable membrane potential of −70 mV, while cells that have become density-arrested show spontaneous calcium action potentials. Upon subsequent addition of retinoic acid (RA) or transforming growth factor beta (TGFβ) these density-arrested cells become phenotypically transformed, which is accompanied by a depolarization of the plasma membrane to −20 mV. These differences in membrane potential have been associated with increased secretion of the cyclooxygenase (COX) product $PGF_{2\alpha}$ by NRK fibroblasts in the culture medium. In this thesis we used an RNAi approach to unveil the exact mechanism by which secretion of $PGF_{2\alpha}$ contributes to the transformation of NRK fibroblasts in conjunction with membrane depolarization, loss of density-dependent growth arrest and the induction of anchorage-independent proliferation. Furthermore, we investigated the molecular mechanism of calcium dynamics and membrane excitability required for pacemaking activity of NRK fibroblasts.

In **Chapter 2** we studied the role of the prostanoid FP receptor in action potential generation and phenotypic transformation of NRK fibroblasts by knocking down the expression of its encoding *Ptgfr* gene. Our results demonstrate that the membrane depolarization of phenotypically transformed NRK cells is a consequence of FP receptor activation, thus indicating that in these cells $PGF_{2\alpha}$ acts in an autocrine manner. However,

activation of the FP receptor does not appear to be essential for cellular transformation induced by RA of TGFβ. Furthermore we showed that knockdown of *Ptgfr* prevents the firing of action potentials in density-arrested cells, which provides direct evidence that activity of $PGF_{2\alpha}$ by putative pacemaker cells underlies the generation of calcium action potentials in NRK fibroblasts.

In **Chapter 3** we examined the involvement of IP_3 receptor subtypes in $PGF_{2\alpha}$-induced calcium oscillations and pacemaking activity of NRK fibroblasts. Our results show that the reduced frequency of $PGF_{2\alpha}$-induced calcium oscillations in density-arrested cells, when compared to quiescent cells, results from differences in the expression ratio between the IP_3R1 and the IP_3R3 receptor. Moreover, by knockdown of individual *Itpr* genes we observed that the IP_3-receptor subtypes expressed in NRK cells have a different role in shaping the Ca^{2+} signal induced by $PGF_{2\alpha}$. We show that a low expression level of IP_3R1 results in reduction or even disappearance of Ca^{2+} oscillations, whereas lowering of IP_3R3 expression is associated with an increase in the Ca^{2+} oscillations with high amplitude. These data provide the first direct evidence that the frequency of IP_3-dependent calcium oscillations determines the periodicity of action potential firing in density-arrested NRK fibroblasts.

In **Chapter 4** we investigated the mechanims whereby calcium is taken up by NRK cells, as a requirement to maintain periodic calcium oscillations. Our data show that store-operated and receptor-operated calcium channels in quiescent and density-arrested cells differentially regulate calcium entry.

In **Chapter 5** we identified the molecular components that are involved in store-operated calcium entry and $PGF_{2\alpha}$-induced calcium oscillations in NRK fibroblasts. Results of selective knock down of the genes encoding Trpc1, Trpc6, Orai1 and Stim1 suggest that specific dynamic complexes of these proteins are involved in store-operated and receptor-operated calcium entry. Moreover, our data indicate that Stim1, Orai1 and Trpc1, but not Trpc6, are involved in the $PGF_{2\alpha}$-induced Ca^{2+} oscillations in NRK cells.

In **Chapter** 6 our results are discussed in terms of the role of the EGF receptor in density-arrest and phenotypic transformation of NRK cells, as well as on the role of autocrine $PGF_{2\alpha}$ production in pacemaker activity and generation of calcium action potentials in density-arrested NRK monolayers.

Samenvatting

Niet alleen tijdens de ontwikkeling, maar ook in het volwassen organisme wordt cellulaire groei nauwkeurig gereguleerd door een aantal controle-mechanismen, die er voor zorgen dat cellen op de juiste tijd en plaats starten en stoppen met delen. Ontregeling van deze regulerende mechanismen leidt tot ongecontroleerde proliferatie van cellen en kan de basis vormen voor een grote verscheidenheid aan ziekten waaronder kanker. Daarom is inzicht in de elementaire mechanismen die de normale celgroei reguleren essentieel voor het begrijpen van pathologische groei-afwijkingen.

Onder normale omstandigheden ondergaan cellen een dichtheidsafhankelijke remming van de groei bij hoge celdichtheden. Dit bescherming-mechanisme, ook wel *dichtheidsafhankelijke groeiremming* genoemd, is gericht op het voorkomen van buitensporige celgroei. In de huidige studie hebben wij gebruik gemaakt van NRK fibroblasten als in vitro modelsysteem om de rol van de membraan-potentiaal in dichtheidsafhankelijke groeiregulatie te bestuderen. Deze cellen vertonen, afhankelijk van de toevoeging van specifieke combinaties van groeifactoren, dichtheidsafhankelijke groeiremming of juist fenotypische transformatie waarbij, net als in tumorcellen het mechanisme van groeiremming verloren is gegaan. De membraan-potentiaal van NRK cellen is sterk afhankelijk van het groeistadium van deze cellen. Rustende NRK cellen hebben een stabiele membraanpotentiaal van -70 mV, terwijl de cellen die dichtheidsafhankelijke groeiremming vertonen spontane calcium actiepotentialen vuren. NRK cellen die door toevoeging van retinoic acid (RA) of transforming growth factor beta (TGFβ) fenotypisch zijn getransformeerd, zijn gedepolariseerd tot een membraanpotentiaal van -20 mV. Deze verschillen in membraanpotentiaal hebben wij kunnen associëren met een verhoogde uitscheiding van het cyclooxygenase (COX) product $PGF_{2\alpha}$ door NRK fibroblasten in het kweekmedium. In dit proefschrift hebben wij gebruik gemaakt van de RNA interference (RNAi) techniek om te onderzoeken op welke wijze de secretie van $PGF_{2\alpha}$ bijdraagt aan de depolarisatie, het verlies van dichtheidsafhankelijke groeiremming en de inductie van verankering-onafhankelijke groei tijdens fenotypische transformatie van NRK cellen. Verder hebben wij het moleculaire mechanisme onderzocht van de calcium dynamiek en membraan exciteerbaarheid die nodig zijn voor pacemaking activiteit van NRK fibroblasten.

In hoofdstuk 2 hebben wij de rol van de prostanoid FP-receptor bij de inductie van actiepotentialen en fenotypische transformatie van NRK fibroblasten onderzocht door de

expressie van de *Ptgfr* gen met shRNA te onderdrukken. Onze resultaten tonen aan dat de membraan-depolarisatie van fenotypisch getransformeerde NRK cellen het gevolg is van FP-receptor activering, waaruit geconcludeerd kan worden dat in deze cellen $PGF_{2\alpha}$ op een autocriene manier werkzaam is. Activering van de FP-receptor blijkt echter niet essentieel te zijn voor fenotypische transformatie van de cellen geïnduceerd door RA of TGFβ. Verder blijkt dat het onderdrukken van *Ptgfr* expressie voorkomt dat dichtheid geïnhibeerde NRK cellen calcium actiepotentialen vuren, hetgeen een direct bewijs is dat een secretie van $PGF_{2\alpha}$ door veronderstelde pacemaker cellen ten grondslag ligt aan het opwekken van dergelijke calcium actiepotentialen.

In hoofdstuk 3 hebben wij de betrokkenheid van de IP3 receptor subtypen onderzocht in $PGF_{2\alpha}$-geïnduceerde calcium oscillaties en pacemaker activiteit van NRK fibroblasten. Onze resultaten tonen aan dat de verlaagde frequentie van $PGF_{2\alpha}$-geïnduceerde calcium oscillaties in dichtheid geïnhibeerde NRK cellen, vergeleken met rustende cellen, het gevolg is van een andere verhouding in expressie tussen de IP_3R1 en de IP_3R3 receptor. Bovendien, hebben wij door de expressie van individuele *Itpr* genen te onderdrukken, geconstateerd dat de verschillende IP_3-receptor subtypen in NRK-cellen een specifieke rol hebben in de vormgeving van het door de $PGF_{2\alpha}$ Ca^{2+} signaal. Onze resultaten tonen aan dat een laag expressie-niveau van IP_3R1 resulteert in een afname of zelfs verdwijning van Ca^{2+} oscillaties, terwijl verlaging van IP_3R3 expressie geassocieerd is met een hogere frequentie en amplitude van de Ca^{2+} oscillaties. Deze gegevens zijn het eerste experimentele bewijs dat de frequentie van IP_3-afhankelijke calcium oscillaties bepaalt met welke periodiciteit de actiepotentialen worden gevuurd in dichtheid geïnhibeerde NRK cellen.

In hoofdstuk 4 hebben wij het mechanisme onderzocht waarmee extracellulair calcium wordt opgenomen door NRK cellen, hetgeen noodzakelijk is om periodieke calcium-oscillaties te kunnen genereren. Onze gegevens tonen aan dat calcium-opname in rustende cellen wordt verzorgd door zowel store-operated (SOC) als receptor-operated (ROC) calcium kanalen, terwijl in dichtheid geïnhibeerde cellen met name ROC kanalen actief zijn.

In hoofdstuk 5 hebben wij de moleculaire componenten geïdentificeerd die betrokken zijn bij de SOC kanalen en daarmee van belang zijn voor $PGF_{2\alpha}$-geïnduceerde calciumoscillaties in NRK fibroblasten. Door selectief de expressie van de genen die coderen voor Trpc1, Trpc6, Orai1 en Stim1 te onderdrukken, hebben wij aanwijzingen

gekregen dat specifieke dynamische complexen van deze eiwitten betrokken zijn in de SOC en ROC gemedieerde opname van calcium. Bovendien blijkt uit onze gegevens dat Stim1, Orai1 en Trpc1, maar niet Trpc6, betrokken zijn bij de $PGF_{2\alpha}$-geïnduceerde Ca^{2+} oscillaties in NRK cellen.

In hoofdstuk 6 zijn onze resultaten besproken in relatie tot de rol van de EGF-receptor bij dichtheidsafhankelijke groeiïnhibitie en fenotypische transformatie van NRK cellen. Daarnaast is de rol van autocriene $PGF_{2\alpha}$ productie bediscussieerd in relatie tot pacemaker-activiteit en het opwekken van calcium actiepotentialen in dichtheid geïnhibeerde NRK monolagen.

Dankwoord

Op deze plaats wil ik graag iedereen bedanken die een bijdrage heeft geleverd aan het tot stand komen van mijn proefschrift. Een aantal van hen wil ik vanwege hun bijzondere bijdrage met name noemen.

Allereerst Dr. Lex Theuvenet en Prof. Joop van Zoelen, mijn dank voor de mogelijkheid die jullie geboden hebben om mijn onderzoek uit te voeren, voor jullie nuttige commentaar op mijn manuscripten en voor het vertrouwen in een goede afronding van dit meer-jaren project. Verder denk ik met plezier terug aan de gezellige sfeer tijdens de dagjes-uit, speurtochten en etentjes die jullie voor de afdeling organiseerden. Deze vormden een welkome afwisseling op het werk. Mijn speciale dank gaat uit naar Prof. Dick Ypey. Dick door je uitgebreide kennis op het gebied van elektrofysiologie en je aanstekelijke enthousiasme was je inbreng nuttig voor het onderzoek. Dr. Wilbert van Meerwijk, jou wil ik bedanken voor je nuttige discussies gedurende die jaren en vooral je humor.

Peter Peters wil ik bedanken voor de technische ondersteuning en met name de patch-clamp metingen. Walter van Rotterdam, jou wil ik bedanken voor je technische ondersteuning en mijn speciale dank ook voor de gezellige rook-pauzes. Mijn collega Marc, bedankt voor alle gezelligheid en steun. Hetzelfde geldt voor al mijn collega's op het afdeling. Onze secretaresse Janny, bedankt voor alle hulp bij het regelen van congressen e.d. en voor de gezellige praatjes die er altijd even tussendoor konden. Verder wil ik mijn studenten Denise en Harriette bedanken voor hun bijdrage.

Mijn familie en vrienden wil ik bedanken voor alle interesse en steun. Jullie zorgden voor de nodige afleiding tijdens het onderzoek en tijdens het schrijven van het proefschrift.

Curriculum vitae

Wadia Hassan Almirza werd geboren op 6 december 1970 te Basra, Irak. Sinds 1998 woont hij in Nederland, waar hij in 2004 de studie Biochemie voltooide aan de Rijksuniversiteit Groningen. In het kader van deze opleiding volgde hij een onderzoekstage op de afdeling Celbiologie en Elektronenmicroscopie van de Medische Faculteit (onder begeleiding van Dr. Han van der Want) en een onderzoekstage op de afdeling Celbiochemie (onder begeleiding van Dr. Dauwe Veltman) van de Faculteit Wiskunde en Natuurwetenschappen van deze universiteit. In de periode van september 2004 tot september 2008 werkte hij als AIO op de afdeling Celbiologie van de Faculteit Natuurwetenschappen, Wiskunde en Informatica van de Radboud Universiteit Nijmegen (onder begeleiding van Dr. A.P.R. Theuvenet) in welke periode hij het in dit proefschrift verwerkte onderzoek verrichtte. Sinds 2009 is hij werkzaam als post-doc op de afdeling Neurowetenschappen en Farmacologie van het Rudolf Magnus Instituut, Universitair Medisch Centrum Utrecht.

Publications

1- Role of the prostanoid FP receptor in action potential generation and phenotypic transformation of NRK fibroblasts. W.H. Almirza, M.M. Dernison, P.H.J. Peters, E.J.J. van Zoelen, A.P.R. Theuvenet. *Cellular Signalling* **20** (2008) 2022-2029.

2- Different role of the subtype 1 inositol 1,4,5-trisphosphate receptor in prostaglandin $F_{2\alpha}$-induced calcium oscillations and pacemaking activity of NKR fibroblasts. W.H. Almirza, P.H.J. Peters, E.J.J. van Zoelen, A.P.R. Theuvenet. *Cell Calcium* **47** (2010) 544-53.

3- Role of Trpcs, Stim1 and Orai1 Proteins in $PGF_{2\alpha}$-induced Calcium signaling in NRK Fibroblasts. W.H.M. Almirza, P. Peters, E.J.J. van Zoelen & A.P.R. Theuvenet. (Resubmitted to Cell Calcium)

4- Growth State-dependent Modulation of Capacitative Calcium Entry in Normal Rat Kidney Fibroblasts. M.M. Dernison, W.H.M.A. Almirza, W.P.M. van Meerwijk, E.J.J. van Zoelen, A.P.R. Theuvenet. *Cellular signalling* **22** (2010) 1044-1053.

5- Retinoic acid-dependent and –independent downstream pathways of Pitx3 in mesodiencepalic dopamine neurons. M.J. Jacobs, J. van Veenvliet, W.H. Almirza, E. Hoekstra, L. von Oerthel, P. Burbach and M.P. Smidt. (Resubmitted to Development)